

FEDERAL UNIVERSITY OF SANTA MARIA  
CENTER OF TECHNOLOGY  
GRADUATE PROGRAM IN ENVIRONMENTAL ENGINEERING

Robson Leo Pachaly

**ASSESSMENT OF SWMM APPROACHES TO SIMULATE DYNAMIC  
CONDITIONS IN STORMWATER SYSTEMS**

Santa Maria, RS  
2019

**Robson Leo Pachaly**

**ASSESSMENT OF SWMM APPROACHES TO SIMULATE DYNAMIC CONDITIONS  
IN STORMWATER SYSTEMS**

Thesis submitted to the Graduate Program  
in Environmental Engineering at Federal  
University of Santa Maria (UFSM, RS), as  
a partial requirement to obtain the degree  
of **Master in Environmental Engineering**.

Advisor: Prof. Dr. Daniel Gustavo Allasia Picilli

Co-advisor: Prof. Dr. Jose G. Vasconcelos

Santa Maria, RS  
2019

Pachaly, Robson Leo

Assessment of SWMM approaches to simulate dynamic conditions in stormwater systems / Robson Leo Pachaly.- 2019.

129 p.; 30 cm

Orientador: Daniel Gustavo Allasia Piccilli

Coorientador: Jose G. Vasconcelos

Dissertação (mestrado) - Universidade Federal de Santa Maria, Centro de Tecnologia, Programa de Pós-Graduação em Engenharia Ambiental, RS, 2019

1. Storm Water Management Model 2. Hydraulic Modeling  
3. Saint Venant Equations 4. Rapid Inflow 5. Hydraulic Transients I. Allasia Piccilli, Daniel Gustavo II. Vasconcelos, Jose G. III. Título.

Sistema de geração automática de ficha catalográfica da UFSM. Dados fornecidos pelo autor(a). Sob supervisão da Direção da Divisão de Processos Técnicos da Biblioteca Central. Bibliotecária responsável Paula Schoenfeldt Patta CRB 10/1728.

---

©2019

All rights reserved to Robson Leo Pachaly. Reproduction of parts or all of this work can only be done by citation of the source.

Phone +55 55 991166620; Eletronic Address.: robsonleopachaly@yahoo.com.br

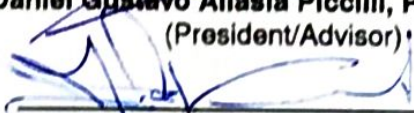
**Robson Leo Pachaly**

**ASSESSMENT OF SWMM APPROACHES TO SIMULATE DYNAMIC CONDITIONS  
IN STORMWATER SYSTEMS**

Thesis submitted to the Graduate Program  
in Environmental Engineering at Federal  
University of Santa Maria (UFSM, RS), as  
a partial requirement to obtain the degree  
of **Master in Environmental Engineering**.

**Approved on June 26, 2019:**

  
\_\_\_\_\_  
**Daniel Gustavo Allasia Piccilli, Ph.D. (UFSM)**  
(President/Advisor)

  
\_\_\_\_\_  
**Jose G. Vasconcelos, Ph.D. (Auburn University)**  
(Co-advisor)

  
\_\_\_\_\_  
**Ben R. Hodges, Ph.D. (University of Texas at Austin)**

  
\_\_\_\_\_  
**Leandro C. Pinto, Ph.D. (UFSM)**

Santa Maria, RS  
2019

*"Utopia lies at the horizon.  
When I draw nearer by two steps,  
it retreats two steps.  
If I proceed ten steps forward,  
it swiftly slips ten steps ahead.  
No matter how far I go,  
I can never reach it.  
What, then, is the purpose of utopia?  
It is to cause us to advance."*

*(Eduardo Galeano)*

## ABSTRACT

### ASSESSMENT OF SWMM APPROACHES TO SIMULATE DYNAMIC CONDITIONS IN STORMWATER SYSTEMS

Author: Robson Leo Pachaly

Advisor: Prof. Dr. Daniel Gustavo Allasia Piccilli

Co-advisor: Prof. Dr. Jose G. Vasconcelos

The representation of physical phenomena by mathematical and computational models have evolved in recent years due to technological and computational advances. Hydraulic modeling has been used for engineers and decision-makers to provide reliable solutions for many engineering problems. The Storm Water Management Model (SWMM) is one of the most used and established models worldwide. This model has been used extensively since the mid-1970 for many engineering applications such as the representation of the hydrology and hydraulics of urban stormwater systems. However, modeling complex hydraulic processes such as rapid inflow in collection systems, mixed flows or transients can produce many types of instabilities that SWMM does not properly simulate. These instabilities can be reduced by selecting a proper routing time-step and shortening the conduits length. Also, the last SWMM version released (5.1.013) implemented the Preismann Slot (SLOT) as pressurization algorithm and this new feature introduced new possibilities of modeling such phenomena. Therefore, this work aims to improve SWMM hydraulic modeling by adopting artificial spatial discretization and verifying the best surcharge method and routing time-step to simulate dynamic situations. The results showed that the SWMM hydraulic modeling capacity was significantly improved and able to simulate extreme hydraulic phenomena such as rapid inflows and slow and fast transients when artificial spatial discretization is adopted along proper selection of routing time-step and surcharge method. As a result of this work, a software called ReSWMM that reads SWMM input files, adds the artificial discretization and estimates appropriate routing time-steps was developed.

**Keywords:** Storm Water Management Model. Hydraulic Modeling. Saint Venant Equations. Rapid Inflow. Hydraulic Transients.

## RESUMO

### ASSESSMENT OF SWMM APPROACHES TO SIMULATE DYNAMIC CONDITIONS IN STORMWATER SYSTEMS

Autor: Robson Leo Pachaly

Orientador: Prof. Dr. Daniel Gustavo Allasia Piccilli

Coorientador: Prof. Dr. Jose G. Vasconcelos

A representação de fenômenos físicos por modelos matemáticos e computacionais evoluiu consideravelmente nos últimos anos devido a avanços tecnológicos e computacionais. Modelagem hidráulica tem sido utilizada por engenheiros e gestores para prover soluções confiáveis para muitos problemas de engenharia. O Storm Water Management Model (SWMM) é um dos modelos mais utilizados e consagrados mundialmente. Este modelo tem sido amplamente utilizado desde a década de setenta para diversas aplicações na engenharia como a representação hidrológica e hidráulica de sistemas de drenagem. Entretanto, a modelagem hidráulica de processos complexos, como o enchimento rápido de canais de drenagem, escoamento misto ou transientes podem vir a gerar muitos tipos de instabilidades que o SWMM não simula adequadamente. Essas instabilidades podem ser reduzidas selecionando um passo de tempo adequado e reduzindo o comprimento dos condutos. Ainda, a última versão disponibilizada (5.1.013) implementou a fenda de Preissmann (SLOT) como algoritmo de pressurização e esta nova implementação introduziu novas possibilidades para modelar tais fenômenos. Portanto, esse trabalho visa melhorar a modelagem hidráulica do SWMM adotando discretização espacial artificial e verificando o melhor método de sobretaxa e passo de tempo para simular situações dinâmicas. Os resultados mostraram que a modelagem hidráulica do SWMM foi significativamente melhorada e capaz de simular fenômenos hidráulicos extremos como enchimentos rápidos e transientes lentos e rápidos quando discretização espacial artificial é adotada juntamente com seleção adequada de passo de tempo e método de sobretaxa. Como resultado desse trabalho, um software chamado ReSWMM que lê os arquivos de entrada do SWMM, adiciona a discretização artificial e estima passos de tempo apropriados foi desenvolvido.

**Palavras-chave:** Storm Water Management Model. Modelagem Hidráulica. Equações de Saint Venant. Enchimento rápido. Transientes Hidráulicos.

## LIST OF FIGURES

<b>ARTICLE 1</b> .....	<b>14</b>
Figure 3.1 – Collection system layout. ....	17
Figure 3.2 – Traditional SWMM link-node configuration. ....	20
Figure 3.3 – Alternative layout: regular interval (10 dummy junctions). ....	21
Figure 3.4 – Alternative layout: fixed interval (1 m-3 m). ....	22
Figure 3.5 – Alternative layout: diameter based (10x) .....	23
Figure 3.6 – Field measurement results for (a) event 1 and (b) event 2. ....	25
Figure 3.7 – Results for (a) event 1 and (b) event 2 using the traditional network layout. ....	26
Figure 3.8 – Results for (a) event 1 and (b) event 2 using regular interval for 10 dummy junctions. ....	27
Figure 3.9 – Results for (a) event 1 and (b) event 2 using fixed interval. ....	28
Figure 3.10 – Results for (a) event 1 and (b) event 2 using the diameter based approach. ....	30
Figure 3.11 – Flow profile of the traditional approach. ....	34
Figure 3.12 – Flow profile of the regular Interval approach. ....	34
<b>ARTICLE 2</b> .....	<b>39</b>
Figure 4.1 – Test cases samples. ....	48
Figure 4.2 – Example 3 SWMM results showing delayed flow arrivals and recession of traditional (i.e. link-node) approaches, compared to discretized modeling .....	52
Figure 4.3 – Selected SWMM results for Example 6 for all modeling conditions tested. ....	53
Figure 4.4 – Example 6 link 8061 results showing numerical instabilities when Eq.4.7 is used to estimate the routing time-step for both traditional and discretized approaches. ....	54
Figure 4.5 – Selected SWMM results for Example 10 indicating numerical oscillations in traditional modeling approaches. ....	55
Figure 4.6 – Detail of the predicted flows between nodes 3 and 4 in Example 10. ...	56
Figure 4.7 – Example 11 results. ....	57
Figure 4.8 – Example 11 - Fig. 4.7 (A) in detail. ....	58
Figure 4.9 – Example 12 results showing instabilities using the non-discretized model with the SLOT pressurization algorithm. ....	59
Figure 4.10 – Example 13 results using the original head convergence tolerance (A) and the improvements achieved in terms of numerical stability when reducing the head convergence tolerance (B). ....	60
Figure 4.11 – Example 14 results. ....	62
Figure 4.12 – Example 15 adjusting the head convergence tolerance. ....	63
<b>ARTICLE 3</b> .....	<b>70</b>
Figure 5.1 – Surge tank. ....	73
Figure 5.2 – Pipeline flow startup. ....	74
Figure 5.3 – Instantaneous valve closure. ....	76
Figure 5.4 – Surge tank graphical results. ....	85
Figure 5.5 – Surge tank simulation using the non-discretized model and setting the slot width based on $c = 1000$ m/s. ....	87
Figure 5.6 – Pipeline flow startup graphical results. ....	91



Figure 5.7 – Instantaneous valve closure transient graphical results. ....	97
<b>APPENDIX A - RESWMM (V 0.1) .....</b>	<b>120</b>
Figure A.1 – ReSWMM interface.....	121
Figure A.2 – SWMM interface.....	122
Figure A.3 – SWMM tool options.....	122
Figure A.4 – SWMM add-on configuration.....	123
Figure A.5 – ReSWMM open input file. ....	124
Figure A.6 – ReSWMM select input file. ....	124
Figure A.7 – ReSWMM analyze input file.....	125
Figure A.8 – ReSWMM select discretization technique. ....	126
Figure A.9 – ReSWMM regular interval. ....	126
Figure A.10 – ReSWMM fixed interval. ....	127
Figure A.11 – ReSWMM diameter-based. ....	127
Figure A.12 – ReSWMM discretization successful.....	128
Figure A.13 – Link-node approach. ....	129
Figure A.14 – Diameter-based discretization. ....	129

## LIST OF TABLES

<b>ARTICLE 1</b> .....	<b>14</b>
Table 3.1 – Traditional layout simulation summary .....	26
Table 3.2 – Alternative layout: regular interval simulation summary. ....	28
Table 3.3 – Alternative layout: fixed intervals simulation summary.....	29
Table 3.4 – Alternative layout: diameter based simulation summary.....	30
Table 3.5 – Model performance for event 1 .....	31
Table 3.6 – Model performance for event 2. ....	32
Table 3.7 – Model performance for event 1 with timing adjustment. ....	32
Table 3.8 – Model performance for event 2 with timing adjustment. ....	33
<b>ARTICLE 2</b> .....	<b>39</b>
Table 4.1 – QA report test cases summary. ....	47
Table 4.2 – Flow continuity error summary.....	50
Table 4.3 – Computational time spent summary. ....	64
<b>ARTICLE 3</b> .....	<b>70</b>
Table 5.1 – Simulations summary.....	82
Table 5.2 – Surge tank routing time-steps (s) summary.....	83
Table 5.3 – Surge tank maximum upsurge results (m). ....	84
Table 5.4 – $L^2$ norm results for surge tank analysis.....	87
Table 5.5 – Pipeline flow startup routing time-steps (s) summary.....	89
Table 5.6 – Pipeline startup flow (m <sup>3</sup> /s) results. ....	90
Table 5.7 – $L^2$ norm results for pipeline flow startup analysis. ....	92
Table 5.8 – Instantaneous valve closure transient routing time-steps (s) summary..	94
Table 5.9 – Instantaneous valve closure transient maximum upsurge results (m)...	95
Table 5.10 – Instantaneous valve closure transient wave period results (s).....	98
Table 5.11 – $L^2$ norm results for instantaneous valve closure transient analysis....	99

## SUMMARY

<b>1</b>	<b>INTRODUCTION</b>	<b>10</b>
<b>2</b>	<b>OBJECTIVES</b>	<b>13</b>
2.1	MAIN OBJECTIVE	13
2.2	SPECIFIC OBJECTIVES	13
<b>3</b>	<b>ARTICLE 1 - FIELD EVALUATION OF DISCRETIZED MODEL SETUPS FOR THE STORM WATER MANAGEMENT MODEL</b>	<b>14</b>
3.1	INTRODUCTION	14
3.2	METHODOLOGY	16
<b>3.2.1</b>	<b>Field investigation</b>	<b>16</b>
<b>3.2.2</b>	<b>Numerical investigation</b>	<b>18</b>
3.2.2.1	<i>General simulation options</i>	18
3.2.2.2	<i>Traditional layout</i>	20
3.2.2.3	<i>Alternative layout: regular interval (10 dummy junctions) discretization</i>	21
3.2.2.4	<i>Alternative layout: fixed interval (1 m-3 m) discretization</i>	22
3.2.2.5	<i>Alternative layout: diameter-based (10x) discretization</i>	22
3.2.2.6	<i>Model performance evaluation</i>	23
3.3	RESULTS AND DISCUSSION	24
<b>3.3.1</b>	<b>Field measurements</b>	<b>24</b>
<b>3.3.2</b>	<b>Comparison of field measurements and modeling results</b>	<b>25</b>
3.3.2.1	<i>Traditional approach</i>	25
3.3.2.2	<i>Alternative layout: regular interval (10 dummy junctions) discretization</i>	27
3.3.2.3	<i>Alternative layout: fixed interval (1 m-3 m) discretization</i>	28
3.3.2.4	<i>Alternative layout: diameter based (10x) discretization</i>	29
3.3.2.5	<i>Statistical analysis</i>	31
<b>3.3.3</b>	<b>Evaluation of flow profiles</b>	<b>33</b>
3.4	CONCLUSIONS	35
<b>4</b>	<b>ARTICLE 2 - COMPARING SWMM 5.1 CALCULATION ALTERNATIVES TO REPRESENT UNSTEADY STORMWATER SEWER FLOWS</b>	<b>39</b>
4.1	INTRODUCTION AND OBJECTIVE	39
4.2	METHODS	42
<b>4.2.1</b>	<b>SWMM formulation</b>	<b>42</b>
4.2.1.1	<i>Routing time-step and artificial discretization</i>	43
<b>4.2.2</b>	<b>Quality assurance examples</b>	<b>45</b>
<b>4.2.3</b>	<b>Criteria for evaluation of numerical solutions</b>	<b>48</b>
4.3	RESULTS AND DISCUSSION	49
<b>4.3.1</b>	<b>Evaluation of flow continuity errors</b>	<b>49</b>
<b>4.3.2</b>	<b>Evaluation of numerical stability</b>	<b>51</b>
<b>4.3.3</b>	<b>Computational time</b>	<b>63</b>
4.4	CONCLUSIONS	65
<b>5</b>	<b>ARTICLE 3 - EVALUATING SWMM CAPABILITIES TO SIMULATE SLOW AND FAST TRANSIENTS OF STORMWATER SYSTEMS</b>	<b>70</b>
5.1	INTRODUCTION	70
5.2	METHODS	72
<b>5.2.1</b>	<b>Analytical solutions</b>	<b>72</b>
5.2.1.1	<i>Case 1: Surge tank</i>	72

5.2.1.2	<i>Case 2: Pipeline flow startup</i> .....	74
5.2.1.3	<i>Case 3: Instantaneous valve closure transient</i> .....	75
<b>5.2.2</b>	<b>SWMM formulation</b> .....	<b>77</b>
5.2.2.1	<i>Spatial discretization</i> .....	79
5.2.2.2	<i>Temporal discretization</i> .....	80
<b>5.2.3</b>	<b>Model performance evaluation</b> .....	<b>81</b>
5.3	RESULTS AND DISCUSSION .....	81
<b>5.3.1</b>	<b>Simulations Summary</b> .....	<b>81</b>
<b>5.3.2</b>	<b>Case 1: Surge tank</b> .....	<b>82</b>
<b>5.3.3</b>	<b>Case 2: Pipeline flow startup</b> .....	<b>88</b>
<b>5.3.4</b>	<b>Case 3: Instantaneous valve closure transient</b> .....	<b>93</b>
5.4	CONCLUSIONS AND RECOMMENDATIONS .....	100
<b>6</b>	<b>DISCUSSION</b> .....	<b>107</b>
<b>7</b>	<b>CONCLUSIONS</b> .....	<b>110</b>
	<b>APPENDIX A – RESWMM (V 0.1)</b> .....	<b>120</b>
A.1	SWMM ADD-ON .....	121
A.2	STANDALONE APPLICATION .....	123

## 1 INTRODUCTION

The design of water systems has been transformed in the past centuries by advances in technology and computing. This transformation along the necessity of design and plan structures more economically and quickly as possible led to the development of many hydraulic models and software (CUNGE et al., 1980; POPESCU, 2014). In general, a model can be defined as a simplified, schematic representation of the real world. They are conceived to help engineers, scientists and decision-makers to understand what is happening in the present and create scenarios of what may happen in the future (POPESCU, 2014). Modern computational and mathematical techniques allowed hydraulic modeling to have more precise and faster solutions for many types of hydraulic structures (CUNGE et al., 1980; STURM, 2001; ZOPPOU, 2001; MAYS, 2001; BATES et al., 2005; NOVAK et al., 2010; CHAUDHRY, 2013; MAIR et al., 2014). The mathematical modeling of flow can be considered nowadays an important engineering tool and it has its origins in the 19th century work of Saint-Venant and Boussinesq (CUNGE et al., 1980; POPESCU, 2014).

The Saint-Venant equations, a set of two partial differential equations (continuity and momentum) which describes the behavior of a variable over time and space, are often used to describe open-channel flows. Some hypotheses or simplifications are assumed in its formulation, but they are often sufficient to represent the most important aspects of open-channel flows (CUNGE et al., 1980; STURM, 2001; CHAUDHRY, 2007; POPESCU, 2014). A closed-form solution for these equations is not available because they have the presence of non-linear terms. Therefore, many hydraulic engineers use numerical solutions for an approximate numerical result (BATES et al., 2005; CHAUDHRY, 2007, 2013). It is important to highlight that only using considerable simplifications for these equations that analytical solutions are available (CUNGE et al., 1980; STURM, 2001; CHAUDHRY, 2007). However, these simplifications limit the applicability of these solutions for specific situations.

Many numerical methods such as the Method of Characteristics, Method of Finite Differences, and others are extensively used by these hydraulic models and software (STURM, 2001). According to Bates et al. (2005), these methods convert the differential equations into a set of algebraic equations that can be manipulated by a computer. The use of digital computers to numerically solve these equations has been an alternative to physical modeling in many areas of fluid dynamics. Consequently, advancements in computational hydraulics emerged along improvements in computers. Today, it is possible to run large and complex simulations on a typical personal computer (BATES et al., 2005; POPESCU, 2014). However, the numerical solutions may have varying accuracy when solving these equations due to its capacity of representing discontinuities or complex boundary conditions (CUNGE

et al., 1980; STURM, 2001; CHAUDHRY, 2007; POPESCU, 2014).

A challenging application to be modeled is the flow in stormwater sewers and tunnels, or in combined sewer systems. Many situations occurring in these systems can lead to countless instabilities problems (YEN, 1986). Because of that, each characteristic presented in a drainage system demands special requirements to be accurately modeled by hydraulic models and software (CUNGE et al., 1980; YEN, 1986). The flow regime transition from open-channel to pressurized flow (HAMAM et al., 1982; YEN, 1986; GUO, Q. et al., 1991; LI et al., 1999; TRAJKOVIC et al., 1999; LI et al., 2001; WRIGHT; VASCONCELOS; RIDGWAY, 2003; VASCONCELOS; WRIGHT, 2004; VASCONCELOS; WRIGHT; ROE, 2006b,a; POLITANO et al., 2007; WRIGHT; VASCONCELOS; CREECH et al., 2008) is a subject that has been extensively studied over the last years. Such transitions may lead to significant variations in pressure, flow depth, velocity and expulsion and entry of air in collection systems, resulting in infrastructure collapses, blowing off manholes, geysering and other operational issues (BOUSSO et al., 2013).

One of the most worldwide used and established modeling tools is the Storm Water Management Model (SWMM) (ROSSMAN, 2015), result of a multi-decade development that included many researchers, users and collaborators (HUBER et al., 2012). This model is a dynamic hydrological-hydraulic model that can be used to transport runoff through collection systems such as storm water, sewers, combined sewers, and others. SWMM 5 calculation module, EXTRAN, solves the Saint-Venant equations employing a link-node approach (i.e. no spatial discretization in-between nodes) (ROESNER et al., 1988; ROSSMAN, 2015). In these calculations, some numerical instabilities may occur but often these can be mitigated by altering the time step and the conduits length (ROESNER et al., 1988; ROSSMAN, 2015). It is important to notice that SWMM does not automatically identify when such conditions exist, so it is up to the user to verify the numerical stability of the model and to determine if the simulation results are valid for the modeling objectives. From time to time, inexperienced users face severe inflows scenarios and/or challenging geometries that may lead to these instabilities. As a consequence, the SWMM results could be misinterpreted by the user and do not represent the process in analysis.

The SWMM-EXTRAN original pressurization algorithm handles the transition from open-channel to pressurized flows using an alternative continuity condition at the nodes (ROSSMAN, 2017). This adaptation represents well the unsteady flows usually present in stormwater systems but its capability to simulate highly dynamic situations, such as transient flows, is unknown. In SWMM most recent version (5.1.013), the Preissmann Slot (SLOT) (PREISSMANN, 1961; USEPA, 2018) was implemented as pressurization algorithm, allowing the user to select how the transition from open-channel to pressurized flow will be handled by SWMM. This implementation introduced

new possibilities of modeling dynamic flows in SWMM. To date, no studies were found analyzing the potential benefits of modeling highly dynamic conditions along the Preissmann Slot in SWMM. Furthermore, since SWMM is an open-source software, many users are trying to expand its applications for situations where it was not originally conceived, such as intermittent water distribution systems (CAMPISANO; GULLOTTA et al., 2019), mixed flows (VASCONCELOS; ELDAYIH et al., 2018), or force main transients (RIDGWAY, 2008). In some cases, altering the source-code is required (CHO et al., 2007) but often times changing the conventional model setup brings improvements. It is considered here that coupling these two approaches may result in significant improvements in SWMM hydraulic modeling.

In this light, the present work aims to improve SWMM hydraulic modeling by facilitating the use of artificial spatial discretization and verifying which algorithm to handle flow regime transition yields better results in highly dynamic conditions. The results of this Master Thesis are presented in a series of three papers. First, a field experiment in which predetermined volumes of water were suddenly released into a physical stormwater collection system was performed to gather data of a rapid inflow. These data were compared with SWMM modeling to verify the potential benefits of implementing artificial spatial discretization. Second, well-known SWMM models, presented in Rossman (2006), were spatially discretized and compared to its original results considering varying flow regime transition algorithms available in SWMM. Finally, the SWMM source-code was adapted to assess if the model can simulate slow and fast transients with a narrower slot width. For this study, classic flow conditions that have analytical solutions were selected for this assessment. As a result of this work, an application named ReSWMM was developed to help in creating artificial spatial discretization in SWMM by placing intermediate nodes between actual nodes and suggesting a routing time-step.

## 2 OBJECTIVES

### 2.1 MAIN OBJECTIVE

The main objective of this work is to assess SWMM approaches to simulate dynamic flows in stormwater systems, considering variations in temporal and spatial discretization along different pressurization algorithms.

### 2.2 SPECIFIC OBJECTIVES

- Identify the best SWMM approach to simulate dynamic inflow conditions and/or challenging geometries in stormwater systems;
- Evaluate improvements in terms of flow continuity errors and numerical stability when artificial spatial discretization is adopted;
- Verify whether SWMM is capable of simulate accurately slow and fast transients;
- Assess the impact of extra computational effort introduced by additional spatial discretization;
- Develop a software for SWMM that introduces artificial spatial discretization of conduits.



### 3 ARTICLE 1 - FIELD EVALUATION OF DISCRETIZED MODEL SETUPS FOR THE STORM WATER MANAGEMENT MODEL<sup>1</sup>

#### Abstract

The Stormwater Management Model (SWMM) is a hydrologic–hydraulic model often used to simulate water flows in urban drainage systems and changes in water quality. The unsteady flow hydraulic solver in SWMM solves mass and momentum conservation equations for the entire conduit length, and mass is conserved at each junction. This link–node approach used by SWMM does not allow for discretization (i.e. intermediate calculation points) between consecutive junctions, which is adequate in gradual filling scenarios with appropriate calibration and suitable selection of routing time steps. However, because there are more rapid filling scenarios that are associated with intense rain events, the link–node solution approach will affect the accuracy of the hydraulic calculations. This work presents the results of a field investigation in which predetermined volumes of water were suddenly released into a physical stormwater collection system. Level loggers were installed to measure flow depth and outflow rates in these tests. The results were compared with SWMM modeling results obtained by the link–node approach using alternative SWMM model setups which included additional intermediate discretization. The goal was to assess the potential benefits of SWMM discretization in the context of rapidly filling collection systems.

#### 3.1 INTRODUCTION

The Storm Water Management Model (SWMM) is a dynamic hydrologic–hydraulic model often used in the context of urban drainage (ROSSMAN, 2015). It can be used to simulate runoff quantity and quality for single event or continuous hydrologic modeling (TSIHRINTZIS et al., 1998; CAMORANI et al., 2005; TEMPRANO et al., 2006; CHOW et al., 2012; QIN et al., 2013). The model calculates the runoff generated by subcatchments, routes it through the collection system and computes variables such as flow rate, flow depth and water quality parameters. SWMM is a model widely used worldwide (OBROPTA et al., 2007; NIAZI et al., 2017) and its applications include planning, analysis, design and diagnosis of stormwater drainage systems and combined and sanitary sewers systems (ROSSMAN, 2015).

SWMM allows flows to be routed through a wide variety of conduits, including pipes, channels, storage and treatment devices, pumps, and regulators. The model represents collections of system components using various types of nodes (e.g. junctions, storage units and outlets) and various types of conduits, referred to as links. SWMM's unsteady flow hydraulic solver is used to resolve the flow conditions

---

<sup>1</sup>Article published in **Journal of Water Management and Modeling**.

in the network of links and nodes through one-dimensional equations. Saint-Venant equations are used to solve unsteady flows, both in subcritical and supercritical modes, whereas pressurized unsteady flows are solved with a set of mass and momentum equations (ROSSMAN, 2017).

The Saint-Venant equations are a system of partial differential equations that represent the conservation of mass and linear momentum in conduits (STURM, 2001) and apply mass conservation and energy equations to resolve flows in each junction. Alternatively, SWMM can introduce some simplifications in the solution of the mass and momentum equations to solve flows using the zero-inertia wave or kinematic wave approaches (ROSSMAN, 2017). The first simplification neglects local or convective acceleration terms in the momentum equation and is applicable when backwater effects are dominant and hydraulic jumps or bores are absent. The kinematic wave solution is even simpler but more restrictive and is only recommended for flow conditions involving steeper slopes and rough beds (STURM, 2001).

Intense rain events leading to rapid filling conditions of collection systems have the potential to cause problems such as pressurization of conduits, entrapment of air pockets within the pipes, pressure surges and even water hammer (ZHOU et al., 2002; GUIZANI et al., 2006) independent of the system geometry. In such cases, the use of complete Saint-Venant equations is often necessary. However, the link–node solution method in SWMM does not use spatial discretization in conduits between two adjacent nodes and, because of that, the model does not represent highly dynamical changes well, particularly transitions to pressurized flow conditions (RIDGWAY; KUMPULA, 2007; VASCONCELOS; ELDAYIH et al., 2018). High values of flow continuity error, the presence of numerical spikes or oscillations and other could be yielded by SWMM solution when such situations occur. Reducing or allowing a variable time step, lengthening short conduits, dampening or ignoring the inertial terms of the Saint-Venant equations, or reducing the head convergence tolerance are approaches to deal with those unrealistic results (ROSSMAN, 2015), although the accuracy could be impaired.

According to Popescu (2014), using small temporal and spatial discretizations when solving the Saint-Venant equations can lead to improvements in accuracy since the approximation error is small. Therefore, through careful selection of time step and artificial discretization of conduits, simulation results can be significantly improved in SWMM (RIDGWAY; KUMPULA, 2007; VASCONCELOS; ELDAYIH et al., 2018). However, the artificial spatial discretization in SWMM was only investigated in reduced scale experiments (VASCONCELOS; ELDAYIH et al., 2018) or compared with other models (RIDGWAY; KUMPULA, 2007), never in an existent and on service stormwater collection system.

Nowadays, there are many hydraulic models that rely on discretization in their

formulations, including the Transient Analysis Program (TAP) by Applied Science (RIDGWAY; KUMPULA, 2007), Model for Urban Sewers (MOUSE) by the Danish Hydraulic Institute (DHI, 2017), among others. In these hydraulic models, the spatial discretization can be set automatically by the model when solving the flow in a network. However, in some, such as MOUSE (DHI, 2017), the number of grid points can be specified by the user. Moreover, a modified version of the Saint-Venant equations can be used to handle both pressurized and free surface flows. Therefore, it is hypothesized that SWMM results can be improved through spatial discretization modeling.

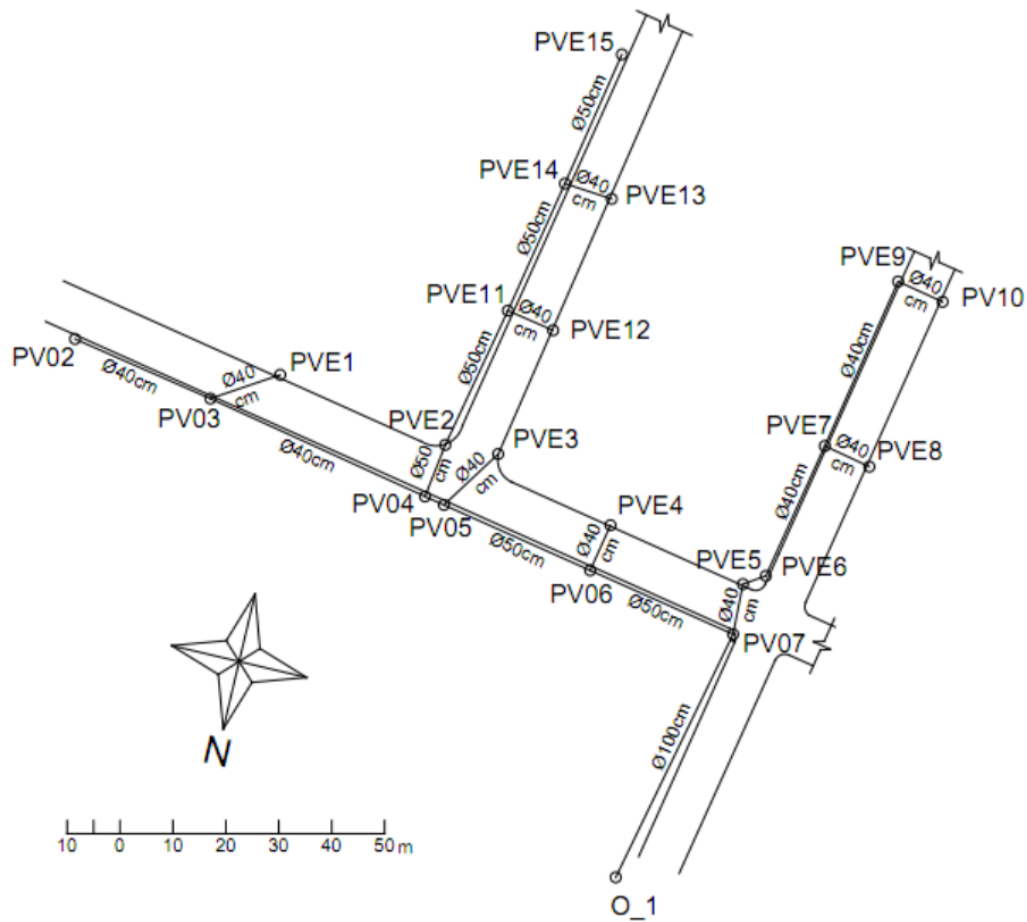
The goal of this work is to assess the potential benefits of SWMM discretization, as well as different discretization strategies, in the context of rapid inflows into collection systems. To achieve this goal, field tests were conducted in which a predetermined water volume was suddenly released into a collection system, resulting in changes in riser water levels that were monitored by sensors. Different SWMM models were created to describe this filling process and modeling results were compared with field pressure head measurements.

## 3.2 METHODOLOGY

### 3.2.1 Field investigation

The stormwater collection system used in this field investigation is located at the Federal University of Santa Maria (UFSM) in the city of Santa Maria, Rio Grande do Sul, Brazil. This system consists of 15 risers and 14 circular conduits, 6 of which are in the direct path of sudden inflow. The system design is shown in Figure 3.1.

Figure 3.1 – Collection system layout.



Source: The Author.

This collection system drains to an intermittent stream located at the northwest limit of the university campus which in turn discharges into the Lagoao do Ouro Creek. Prior to the field experiments the collection system was dry. The conditions of the system were not thoroughly inspected but it is safe to assume that its components are poorly maintained.

At the upstream riser, an artificial reservoir containing approximately  $10 \text{ m}^3$  water was created. At the system inlet (PV02), a 400 mm concrete conduit was blocked using a thick plastic mat secured with cables. Sudden removal of the cables led to the quick release of water, producing rapid inflow in the system.

During the system filling, the water levels at PV02 and PV07, 136 m apart, were monitored using HC-SR04 ultrasonic sensors built using the Arduino prototyping platform with accuracy of 3 mm, range 2 cm–4 m, and sampling frequency 1 Hz (ARDUINO, 2018). The measurements of water levels obtained during the system filling were used to determine if the alternative modeling setup produced more reliable results when compared to the standard link–node approach.

### 3.2.2 Numerical investigation

#### 3.2.2.1 General simulation options

SWMM (release 5.1.012) dynamic wave routing was used to perform the simulations because it solves the complete Saint-Venant equations and yields more precise results than alternative solvers. However, a small time step was chosen to maintain the numerical stability and consequently large computational effort was required, mainly in the case of the discretized layouts. The routing time step selected was 0.001 s. Smaller time steps did not improve the results significantly. When we used the time step recommended in SWMM-EXTRAN documentation (ROESNER et al., 1988), given in Equation 1, continuity errors were large:

$$\Delta T = \frac{L}{\sqrt{gD}} \quad (3.1)$$

where:

$\Delta T$  = time step,

$L$  = conduit length,

$g$  = gravity acceleration, and

$D$  = conduit diameter.

In dynamic wave modeling options, we decided to maintain the inertial terms at their full values under all conditions; the normal flow criteria chosen was the recommended slope and Froude number, and the main equation selected to compute friction losses during pressurized flow was the Hazen–Williams equation. The internally computed variable time step was disabled, so that the selected routing time step was maintained throughout the calculations.

When there are free surface flows, SWMM solves the Saint-Venant equations (Equations 3.2 and 3.3):

$$\frac{\partial A}{\partial t} + \frac{\partial Q}{\partial x} = 0 \quad (3.2)$$

$$\frac{\partial Q}{\partial t} + \frac{\partial(Q^2/A)}{\partial x} + gA \frac{\partial H}{\partial x} + gA(S_f + h_L) = 0 \quad (3.3)$$

Different equations (Equations 3.4 and 3.5) are used to solve flows in conduits in pressurized mode, in which a lumped inertia approach (WYLIE et al., 1993) is used:

$$Q = A_f V \quad (3.4)$$

$$\frac{\partial Q}{\partial t} = -\left(\frac{gA}{L}\right) \left( \frac{\Delta H}{1 + \Delta Q_{friction} + \Delta Q_{losses}} \right) \quad (3.5)$$

where:

$A$  = cross-sectional area of the flow,

$Q$  = flow rate,

$H$  = hydraulic head of water in the conduit (elevation head plus any possible pressure head),

$S_f$  = friction slope,

$h_L$  = local energy loss per unit length of conduit,

$g$  = gravity acceleration,

$A_f$  = full pipe flow,

$\Delta t$  = routing time step size,

$L$  = conduit length,

$V$  = average pipe flow velocity in full pipe conditions ( $Q/A_f$ ),

$\Delta Q_{friction}$  = a nondimensional term that increases with the friction losses along the conduit, and

$\Delta Q_{losses}$  = a nondimensional term that increases with the local losses along the conduit.

The simulation parameter Minimum Nodal Surface Area (MNSA), which represents the minimum plan area that is provided by a node, was changed to a small value of 0.01 m<sup>2</sup>. The default value for MNSA in SWMM is 1.167 m<sup>2</sup>, which corresponds to the plan area of 1.167 m<sup>2</sup> (12.566 ft<sup>2</sup>) of a typical 1.2 m (4 ft) diameter riser. Modifying the MNSA value changes the storage provided by every node in SWMM, which has an impact on calculations particularly when using dummy nodes to create artificial discretization. Since the artificial nodes are not supposed to create extra storage in the modeling efforts, the intention was to keep this model parameter small.

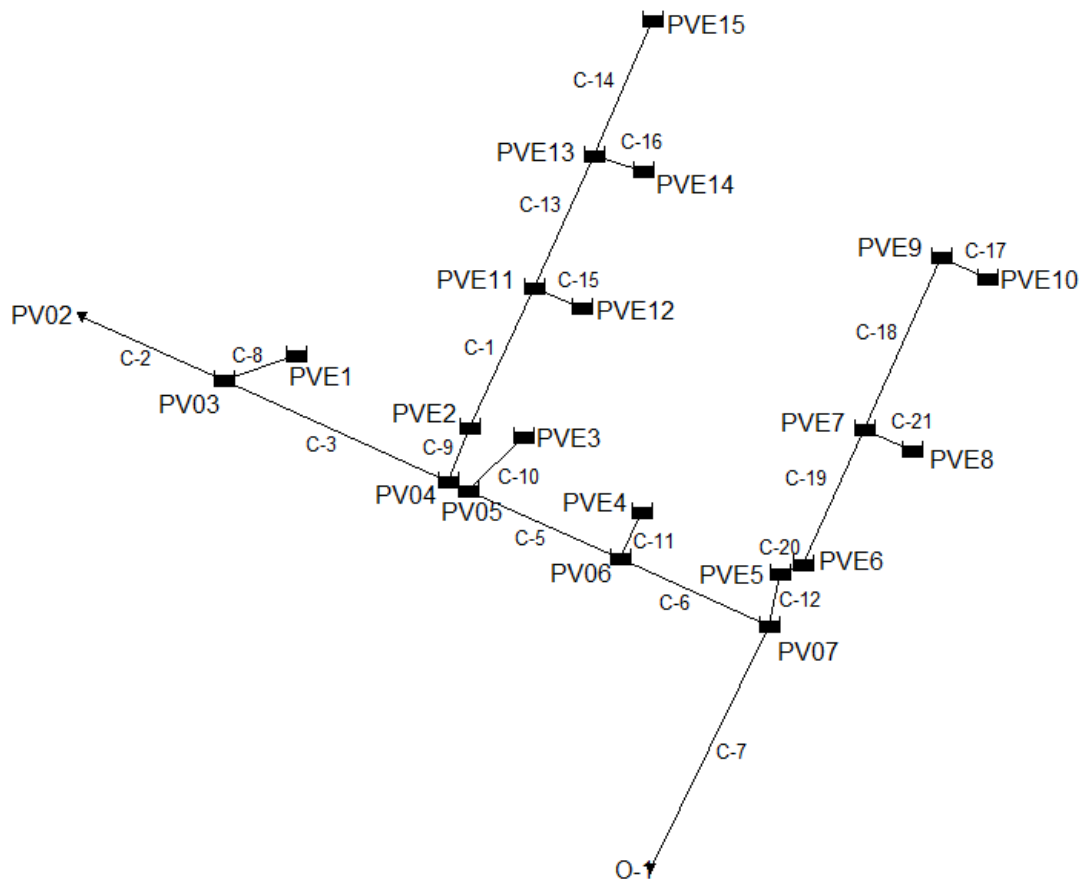
The conduit modeling parameters were set to represent the physical collection system characteristics. The conduit shape was set up as circular having a Manning roughness of 0.017 (monolithic concrete with rough form). The entry and exit losses were computed only for conduits entering and exiting the physical risers, with a value of 0.5.

As the observed field data were water levels, the system inflow should also be a water level to ensure more accurate modeling. To ensure this, the upstream junction (PV02) was converted to an outfall with no inflow with time series as the boundary condition. The invert elevation of PV02 was added to the water level measured at PV02 to create the water level time series. This water level time series was used as the boundary condition at PV02.

### 3.2.2.2 Traditional layout

SWMM (EPA 2017), currently in version 5.1, has an unsteady flow equation solver based on the EXTRAN algorithm described by Roesner et al. (1988) and Rossman (2006), which uses a link-node discretization. The traditional SWMM system layout which represents the physical configuration is shown in Figure 3.2.

Figure 3.2 – Traditional SWMM link-node configuration.



Source: The Author.

The drainage system in this study is relatively small, so riser storage should be included in the simulation for better results. Thus, storage units with areas matching the physical risers were used instead of junctions. In all simulated conditions the maximum depth of physical (or dummy) junctions was set to match the physical terrain elevation.

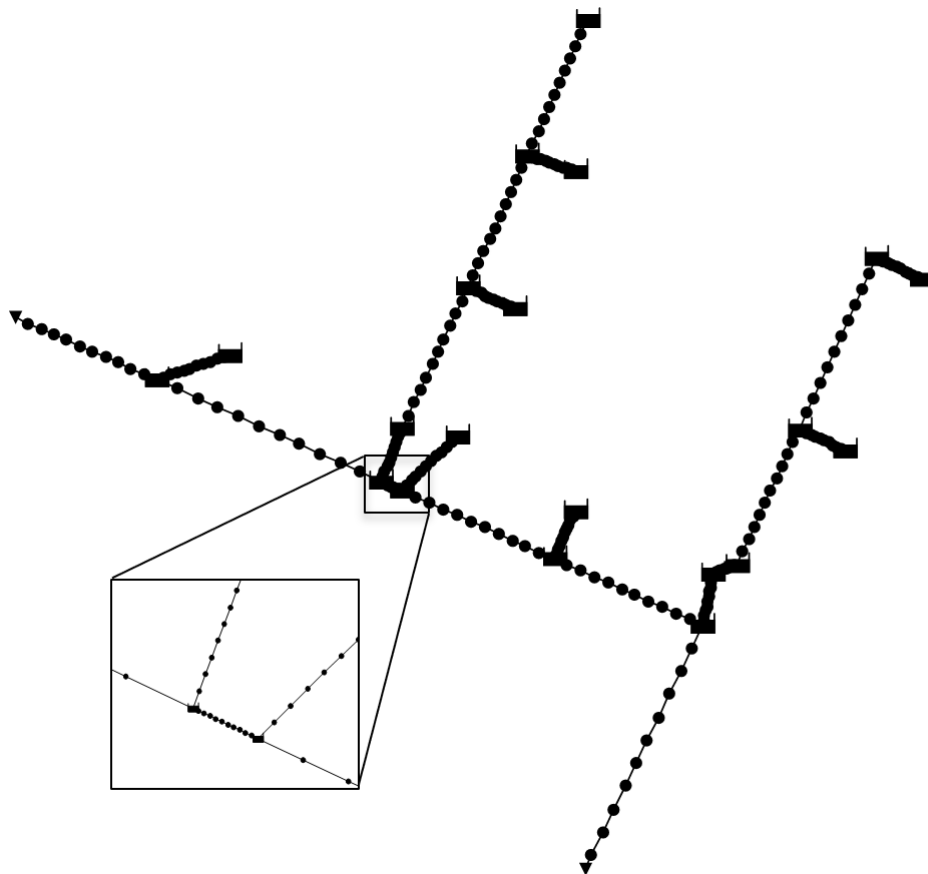
The flow routing algorithm used by SWMM does not use intra-conduit discretization between two adjacent nodes, which would be typical of more contemporary unsteady flow solvers. On the one hand the absence of intra-link discretization solutions significantly reduces computational effort, but on the other hand it can affect the ability of the model to accurately solve highly dynamic flow conditions associated with rapid fillings. Therefore, it is expected that adding artificial

spatial discretization in links could improve SWMM accuracy to model highly dynamic conditions.

### 3.2.2.3 Alternative layout: regular interval (10 dummy junctions) discretization

This alternative setup was conceived to create an artificial spatial discretization in the network by placing 10 intermediate dummy junctions between two consecutive storage units, as originally shown in the first (traditional) approach, independent of the link length. The minimum distance between each dummy junction is 0.32 m (PV04-PV05) and the maximum distance is 4.63 m (PV07-O\_1). This alternative SWMM layout, including a magnification in the PV04-PV03 stretch, is shown in Figure 3.3.

Figure 3.3 – Alternative layout: regular interval (10 dummy junctions).



Source: The Author.

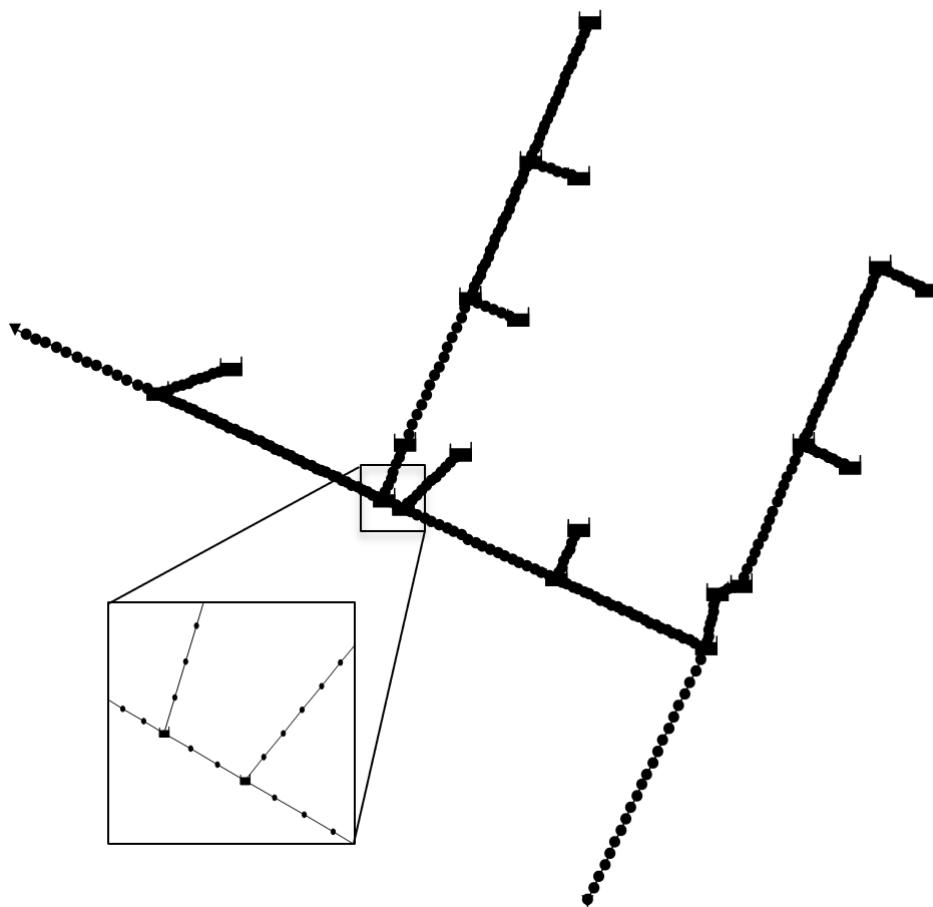
It is important to note that when artificial discretization is used the links generated by the new arrangement of dummy nodes maintain the same characteristics of the original link. In other words, the new links will inherit the original link roughness and the entry and exit losses will be accounted only in the first and last links connected to the physical risers.



### 3.2.2.4 Alternative layout: fixed interval (1 m-3 m) discretization

The second alternative layout was created by limiting the artificial spatial discretization between physical risers to a minimum distance of 1 m and a maximum of 3 m. This procedure resulted in the minimum discretization length 1.01 m (PV03-PV04) and maximum 2.22 m (PV07-O\_1) in order to obtain the required number of discretization intervals. The layout of this discretization and the magnification in the same location as the previous layout are shown in Figure 3.4.

Figure 3.4 – Alternative layout: fixed interval (1 m-3 m).



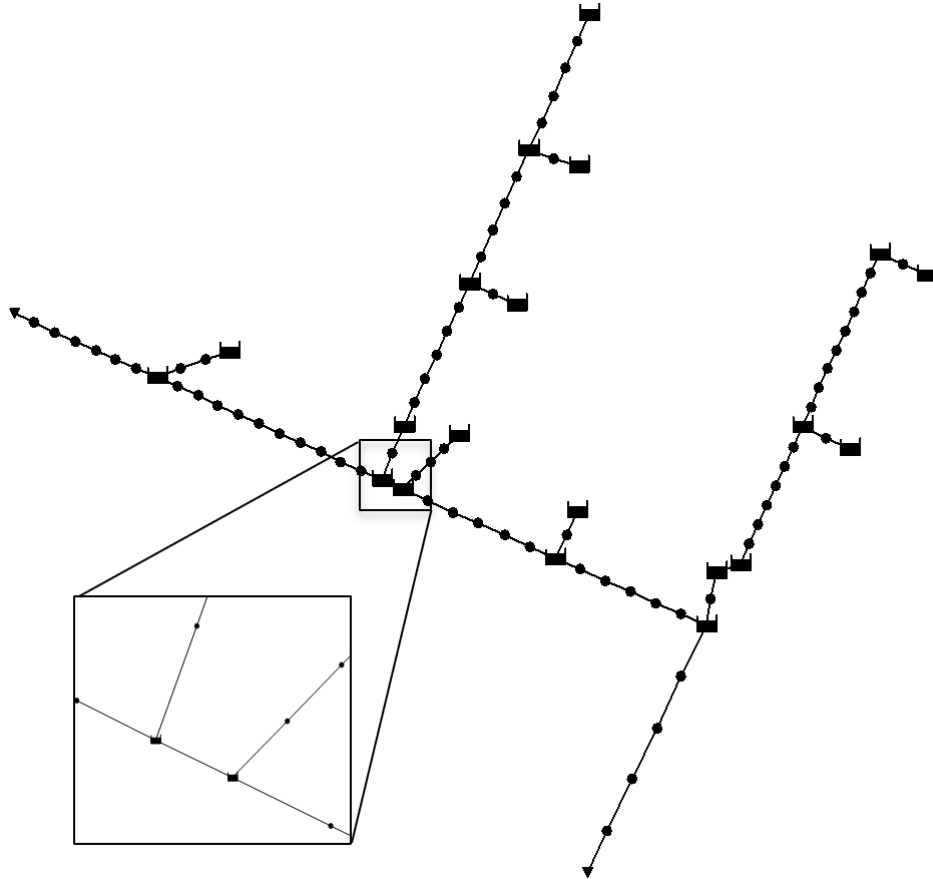
Source: The Author.

### 3.2.2.5 Alternative layout: diameter-based (10x) discretization

The last alternative layout was based on the link diameter. In other words, each link present in the system was divided by 10 times its own diameter. If necessary, the division was rounded to an integer to get an exact number of discretization nodes. This approach resulted in a minimum distance between each dummy junction of 3.51 m

(PVE3-PV05) and maximum 10.20 m (PV07-O\_1). The layout of this system and the magnification are shown in Figure 3.5.

Figure 3.5 – Alternative layout: diameter based (10x)



Source: The Author.

### 3.2.2.6 Model performance evaluation

The first model performance evaluation was a graphical analysis between observed and simulated data. According to ASCE (1993), a graphical analysis is necessary as a first step to evaluate the performance of a model since it provides a general overview of the performance and an overall feeling for model capabilities. The timing of water arrival at PV07, water oscillations, water rise and decline, peak value, and curve fitting to observed data were some of the key aspects analyzed for each approach. ASCE (1993) recommends these features as the main objectives of evaluating graphically single-events simulations.

The statistical analysis was performed using two metrics. The first one was the coefficient of determination ( $r^2$ ). This metric is the square of the Pearson product–moment correlation coefficient and it describes the proportion of the total

variance in measured data explained by the model, ranging from 0 to 1, with higher values indicating better agreement (LEGATES et al., 1999). The coefficient of determination is given by Equation 3.6:

$$r^2 = \left( \frac{\sum (y_{obs}^i - \overline{y_{obs}})(y_{comp}^i - \overline{y_{comp}})}{\sqrt{\sum (y_{obs}^i - \overline{y_{obs}})^2 \sum (y_{comp}^i - \overline{y_{comp}})^2}} \right)^2 \quad (3.6)$$

where:

$\overline{y_{comp}}$  = the mean of computed values,

$y_{obs}^i$  = the observed value for the *i*th observation,

$y_{comp}^i$  = the computed value for the *i*th observation,

$\overline{y_{obs}}$  = the mean of observed values.

Nash–Sutcliffe efficiency (NSE) (NASH et al., 1970) was also selected because it represents an improvement over the coefficient of determination since it is sensitive to differences in the observed and simulated means and variances (LEGATES et al., 1999). Also, this metric is widely used by hydrologists and engineers worldwide. The NSE is defined by Equation 3.7:

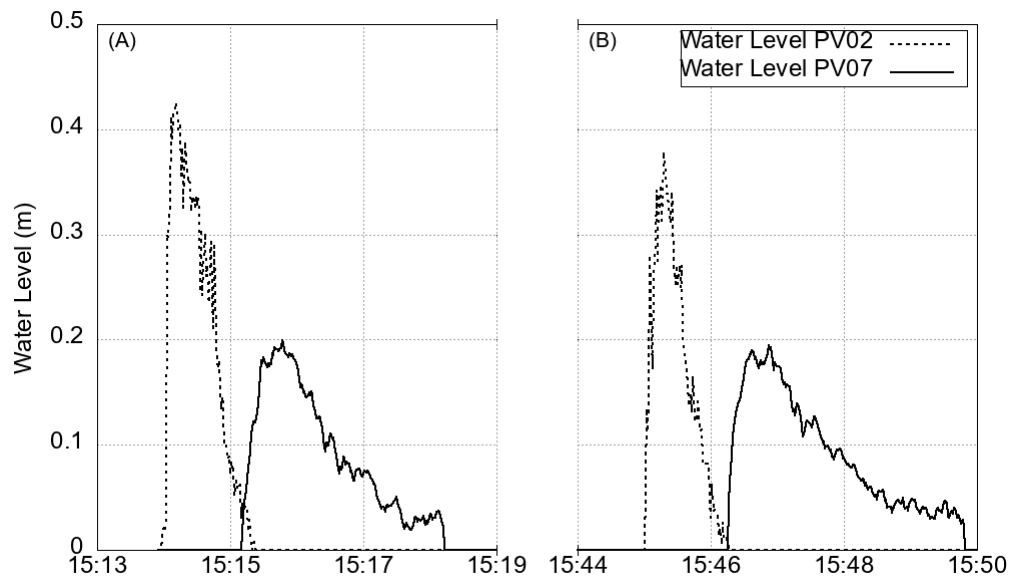
$$NSE = 1 - \left[ \frac{\sum_{i=1}^n (Y_i^{obs} - Y_i^{sim})^2}{\sum_{i=1}^n (Y_i^{obs} - \overline{Y_i^{obs}})^2} \right] \quad (3.7)$$

### 3.3 RESULTS AND DISCUSSION

#### 3.3.1 Field measurements

The upstream reservoir in the collection system was filled with water, and subsequently quickly released, for two separate experiments. The results generated from the first rapid filling event are referred to as event 1 results while the second release results are referred to as event 2 results. The measurements obtained at PV02 and PV07 for both events are shown in Figure 3.6.

Figure 3.6 – Field measurement results for (a) event 1 and (b) event 2.



Source: The Author.

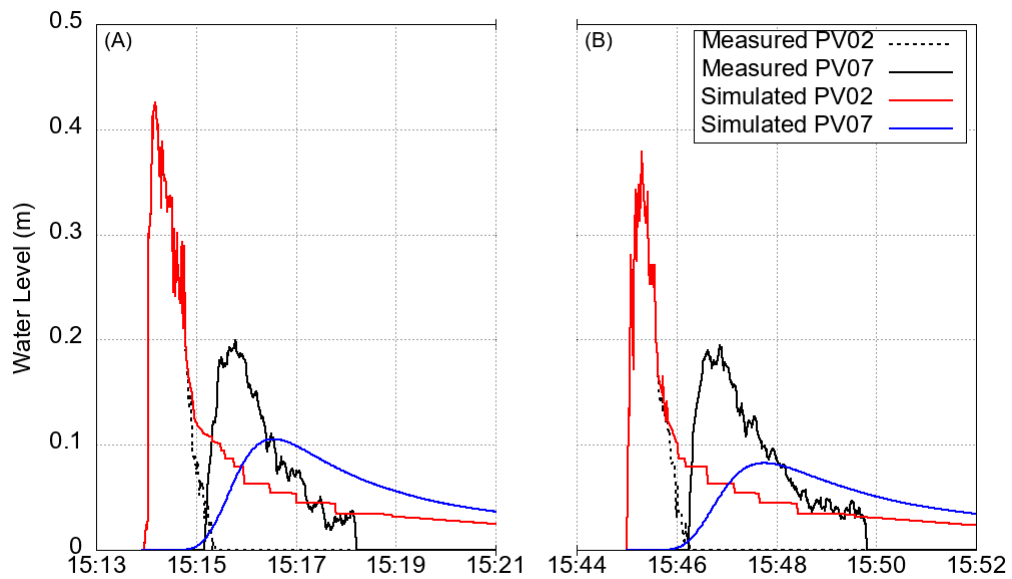
The results show that the general pattern of water level variation is similar for both events.

### 3.3.2 Comparison of field measurements and modeling results

#### 3.3.2.1 Traditional approach

Running the simulation using the traditional approach generated the results for the two events shown in Figure 3.7.

Figure 3.7 – Results for (a) event 1 and (b) event 2 using the traditional network layout.



Source: The Author.

The simulated results using the traditional layout for both events did not accurately represent the field data. The water level simulated at PV02 showed a recession curve that is not observed in the measured data. This layout gave an inaccurate time for the simulated water arrival at PV07 but the time when the simulated water level was more significant ( $>0.01$  m) is very similar to the observed time of that occurrence. However, the model did not capture the oscillations in water level, the modeled water level rise and decrease are diffuse, and the peak is underestimated.

Table 3.1 compares the measured times of water level arrival and peak depth values with the simulated results for both events at PV07. The table also shows the continuity error and total elapsed time for this simulation.

Table 3.1 – Traditional layout simulation summary

	Measured		Simulated			
	Peak Depth	Water Arrival Time	Peak Depth	Water Arrival Time	Continuity Error	Comp. Time
Event 1	0.20 m	15:15:11	0.10 m	15:14:31	-4.57%	21 s
Event 2	0.19 m	15:46:16	0.08 m	15:45:33	13.1%	24 s

Source: The Author.

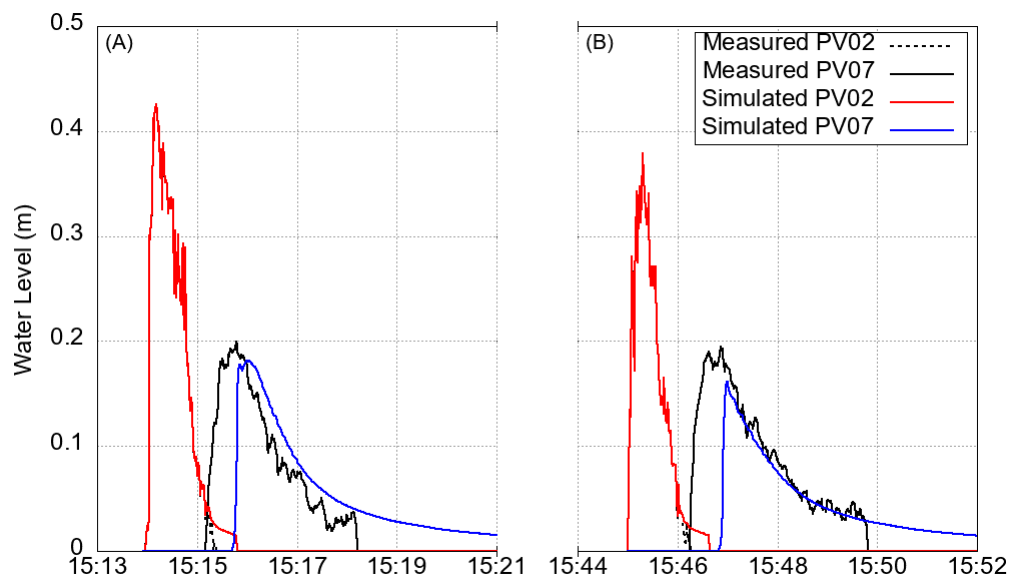
The maximum peak depth difference between observed and simulated values is 0.10 m for event 1 and 0.11 m for event 2. The simulated time of water arrival at PV07

is earlier by 40 s for event 1 and by 43 s for event 2. However, as stated above, for the arrival time when the water level is significant (i.e.  $>0.01$  m) these differences are reduced to 1 s for both events. The continuity errors for both events show that the sum of the all outflow from the network divided by the sum of all of the inflow to the network is not in balance. The time for the computation was in the order of just a few seconds.

### 3.3.2.2 Alternative layout: regular interval (10 dummy junctions) discretization

Running the simulation with 10 dummy junctions at regular intervals generated the results for the two events shown in 3.8.

Figure 3.8 – Results for (a) event 1 and (b) event 2 using regular interval for 10 dummy junctions.



Source: The Author.

This layout showed better results for the simulation at PV02. Compared to the traditional layout, this alternative layout showed a small difference between measured and simulated values at the recession of the inflow data. The simulations using this approach captured and the water level oscillations at PV07 and represented them better than the traditional approach. A sharper rise in water level at PV07 was also captured using this layout. However, the timing of water arrival is still

Table 3.2 compares the measured times of water level arrival and peak depth values with the simulated results for both events at PV07 and gives the continuity error and total elapsed time for this layout.

Table 3.2 – Alternative layout: regular interval simulation summary.

	Measured		Simulated			
	Peak Depth	Water Arrival Time	Peak Depth	Water Arrival Time	Continuity Error	Comp. Time
Event 1	0.20 m	15:15:11	0.18 m	15:15:38	0%	190 s
Event 2	0.19 m	15:46:16	0.16 m	15:46:45	0%	205 s

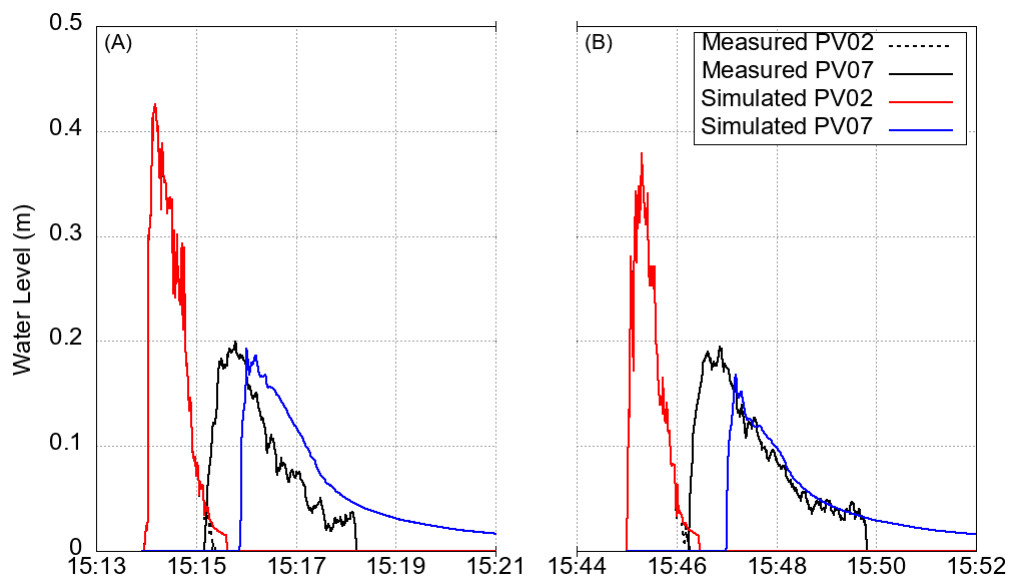
Source: The Author.

The simulation underestimated the peak depth by 0.02 m for event 1 and 0.03 m for event 2. The simulated time of water arrival at PV07 was later by 27 s for event 1 and by 29 s for event 2. The sum of all outflow from the network divided by the sum of all inflow to the network is in balance because the simulation returned a 0% continuity error. However, the computation time for the simulation was much longer than for the traditional layout.

### 3.3.2.3 Alternative layout: fixed interval (1 m–3 m) discretization

The next simulation used the fixed intervals. The results for both events are shown in Figure 3.9.

Figure 3.9 – Results for (a) event 1 and (b) event 2 using fixed interval.



Source: The Author.

As did the previous approach, this alternative layout showed improved results

compared to the traditional layout for the water rise and decrease and peak values at PV07. At PV02, a slight reduction of the inflow recession was seen compared to the previous approach. However, water oscillations at the peak region were more evident than in the previous regular intervals approach.

Table 3.3 compares the measured times of water level arrival and peak depth values with the simulated results for both events at PV07 and shows the continuity error and total elapsed time for this approach.

Table 3.3 – Alternative layout: fixed intervals simulation summary.

	Measured		Simulated			
	Peak Depth	Water Arrival Time	Peak Depth	Water Arrival Time	Continuity Error	Comp. Time
Event 1	0.20 m	15:15:11	0.19 m	15:15:51	0%	267 s
Event 2	0.19 m	15:46:16	0.17 m	15:46:58	0%	288 s

Source: The Author.

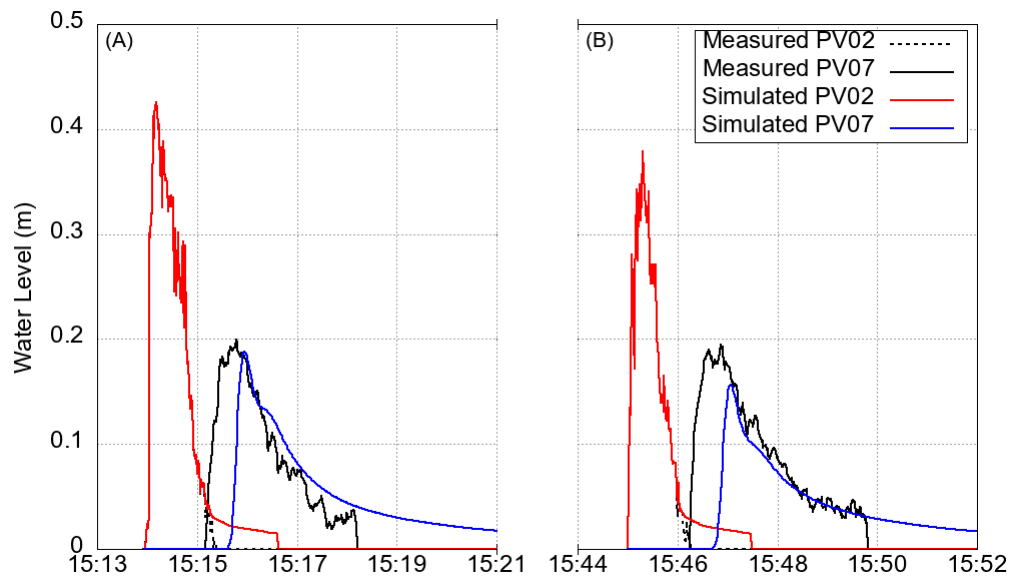
This approach decreased the difference between observed and simulated peak values. For event 1 the difference is 0.01 m and for event 2 the difference is 0.02 m. The timing of water arrival is less precise when compared to the traditional and the previous layouts. It is later by 40 s for event 1 and 42 s for event 2. The continuity error is also 0% but the computation time for this simulation is greater than for the other layouts.

#### 3.3.2.4 Alternative layout: diameter based (10×) discretization

The last alternative layout proposed in this work was that based on conduit diameter. Simulation results for this approach are shown in 3.10.



Figure 3.10 – Results for (a) event 1 and (b) event 2 using the diameter based approach.



Source: The Author.

The results obtained by this approach were similar to those obtained for the regular interval simulation, with slight differences in the peak regions and recession curves. Similar to the previous alternative layouts proposed in this work, the results were better than the traditional layout when analysing the water rise and decrease, peak values at PV07 and the recession curve of the inflow at PV02.

Table 3.4 compares the measured times of water level arrival and peak depth values with the simulated results for both events at PV07 and the continuity error and total elapsed time for this approach.

Table 3.4 – Alternative layout: diameter based simulation summary.

	Measured		Simulated			
	Peak Depth	Water Arrival Time	Peak Depth	Water Arrival Time	Continuity Error	Comp. Time
Event 1	0.20 m	15:15:11	0.19 m	15:15:28	0%	74 s
Event 2	0.19 m	15:46:16	0.16 m	15:46:33	0%	92 s

Source: The Author.

The results generated by this approach showed a difference in measured and simulated peak values of 0.01 m for event 1 and 0.03 m for event 2. The time of water arrival was later by 17 s for both events. As for all alternative layouts, the continuity

error was 0%. However, the computation time for this layout was smaller than for the other alternative layouts.

### 3.3.2.5 Statistical analysis

The metrics used to evaluate the model performance for event 1 are shown in Table 3.5.

Table 3.5 – Model performance for event 1.

<b>Traditional</b>		<b>Regular Interval</b>		<b>Fixed Interval</b>		<b>Diameter Based</b>	
<b>PV02</b>	<b>PV07</b>	<b>PV02</b>	<b>PV07</b>	<b>PV02</b>	<b>PV07</b>	<b>PV02</b>	<b>PV07</b>
Coefficient of determination ( $r^2$ )							
0.96	0.18	1.00	0.32	1.00	0.15	0.99	0.34
Nash Sutcliffe Efficiency (NSE)							
0.81	0.16	1.00	0.21	1.00	-0.15	0.99	0.28

Source: The Author.

Analysing the statistical results for PV02, the coefficient of determination was very close to 1 for each approach, showing good agreement between observed and simulated data. However, a smaller value of the coefficient of determination (0.96) is found when using the SWMM traditional approach. NSE accentuated the indication of disagreement between the observed and simulated data at PV02, with an NSE value of 0.81 for the Traditional approach. The alternative approaches were very close to 1, showing a very good agreement in this metric.

For PV07, the Fixed Interval had the lowest value of coefficient of determination (0.15). The Regular Interval (0.32) and Diameter Based (0.34) approaches showed improvements when compared to the Traditional approach (0.18). NSE values were similar to the coefficient of determination, having a value 0.16 for the Traditional, 0.21 for the Regular Interval, -0.15 for the Fixed Interval, and 0.28 for the Diameter Based. Considering both the coefficient of determination and NSE, the model did not generate good results. The reason for this is the incorrect timing of simulated water arrival at PV07, impairing in the metrics results.

The statistics used to evaluate the model performance for event 2 are shown in the Table 3.6.

Table 3.6 – Model performance for event 2.

<b>Traditional</b>		<b>Regular Interval</b>		<b>Fixed Interval</b>		<b>Diameter Based</b>	
<b>PV02</b>	<b>PV07</b>	<b>PV02</b>	<b>PV07</b>	<b>PV02</b>	<b>PV07</b>	<b>PV02</b>	<b>PV07</b>
Coefficient of determination ( $r^2$ )							
0.96	0.19	1.00	0.26	1.00	0.13	0.99	0.29
Nash Sutcliffe Efficiency (NSE)							
0.77	0.10	1.00	0.07	1.00	-0.14	0.99	0.13

Source: The Author.

For event 2 the statistical results at PV02 were similar to event 1, with the smaller value of coefficient of determination for the Traditional approach (0.96) and the alternative approaches showing values very close to 1. Similar to event 1, the NSE results for event 2 emphasized these results.

At PV07, the Fixed Interval also showed the smaller value (0.13) when the others, including the Traditional Approach, showed higher values of the coefficient of determination. Analysis of NSE shows that only the Diameter Based approach had the NSE value (0.13) greater than the Traditional approach (0.10).

We think that these poor statistical results are related to the timing of water arrival at PV07. Since the collection system used in this field investigation is aged and poorly maintained, some unaccounted storage, detritus, or illegal connections may not be perfectly represented by the SWMM simulation. To verify this, we adjusted the simulation results at PV07 to match the exact timing of measured water arrival at PV07. This generated the following statistics (Table 3.7) for event 1.

Table 3.7 – Model performance for event 1 with timing adjustment.

<b>Traditional</b>		<b>Regular Interval</b>		<b>Fixed Interval</b>		<b>Diameter Based</b>	
<b>PV02</b>	<b>PV07</b>	<b>PV02</b>	<b>PV07</b>	<b>PV02</b>	<b>PV07</b>	<b>PV02</b>	<b>PV07</b>
Coefficient of determination ( $r^2$ )							
0.96	0.02	1.00	0.91	1.00	0.92	0.99	0.77
Nash Sutcliffe Efficiency (NSE)							
0.81	-0.65	1.00	0.90	1.00	0.92	0.99	0.76

Source: The Author.

The results obtained were significantly improved. Analysing the coefficient of determination shows that the results are  $>0.90$  for all alternative approaches except the Diameter Based at PV07 (0.77). The Traditional approach at PV07 had the least value of 0.02. The NSE results were also good for the majority of alternative approaches,

having its least value for the Diameter Based approach at PV07 (0.76). The Traditional approach at PV07 also had the least value (-0.65) for the simulations.

Table 3.8 shows the results for event 2 adjusting the timing. It is possible to assert that the results were improved, showing very good coefficient of determination for PV02 (>0.95) for all approaches and good results for PV07 using the alternative approaches. As in the great majority of cases, PV02 simulated using the Traditional approach showed the least value (0.01) of the coefficient of determination. In all cases, the NSE emphasised the results obtained by the coefficient of determination.

Table 3.8 – Model performance for event 2 with timing adjustment.

<b>Traditional</b>		<b>Regular Interval</b>		<b>Fixed Interval</b>		<b>Diameter Based</b>	
<b>PV02</b>	<b>PV07</b>	<b>PV02</b>	<b>PV07</b>	<b>PV02</b>	<b>PV07</b>	<b>PV02</b>	<b>PV07</b>
Coefficient of determination ( $r^2$ )							
0.96	0.01	1.00	0.88	1.00	0.94	0.99	0.68
Nash Sutcliffe Efficiency (NSE)							
0.77	-0.60	1.00	0.71	1.00	0.80	0.99	0.53

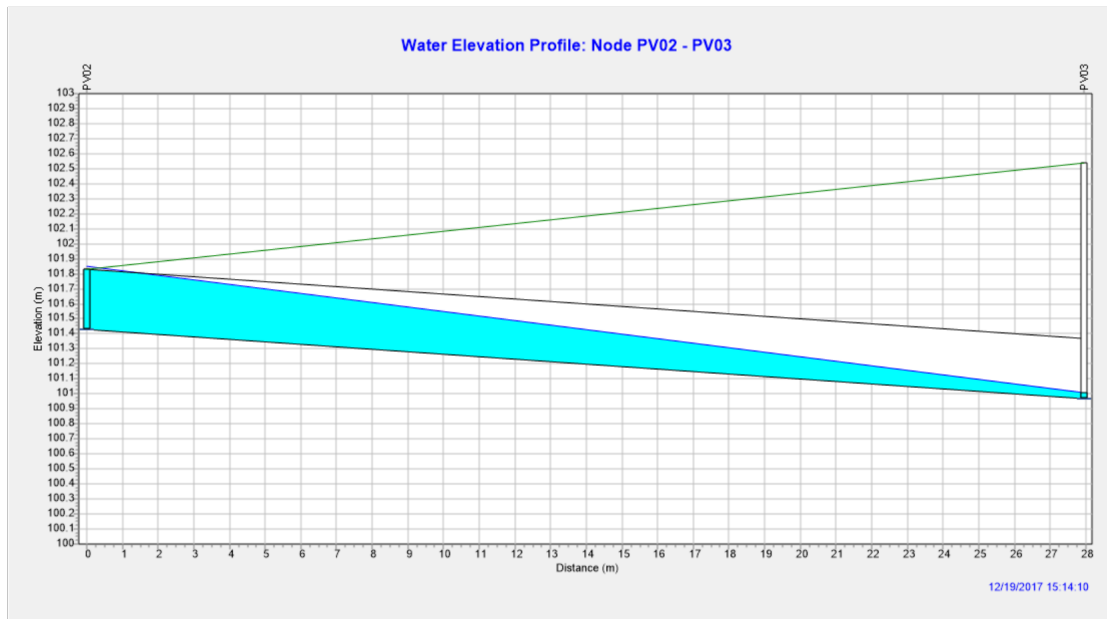
Source: The Author.

As for event 1, the results for event 2 were improved, showing very good coefficient of determination for PV02 (>0.95) for all approaches and good results for PV07 using the alternative approaches. As in the great majority of cases, PV02 simulated using the Traditional approach showed the least value (0.01) of the coefficient of determination. In all cases, the NSE emphasized the results obtained by the coefficient of determination.

### 3.3.3 Evaluation of flow profiles

A visual analysis of the SWMM flow profile behaviour was performed for both events. The results shown in this section are for event 1 at time 15:14:10 in the conduit between PV02 and PV03. When analysing the traditional layout behaviour (Figure 3.11), details of the wave generated by the rapid filling were not captured, and a simple flow wedge is shown due to the lack of spatial discretization.

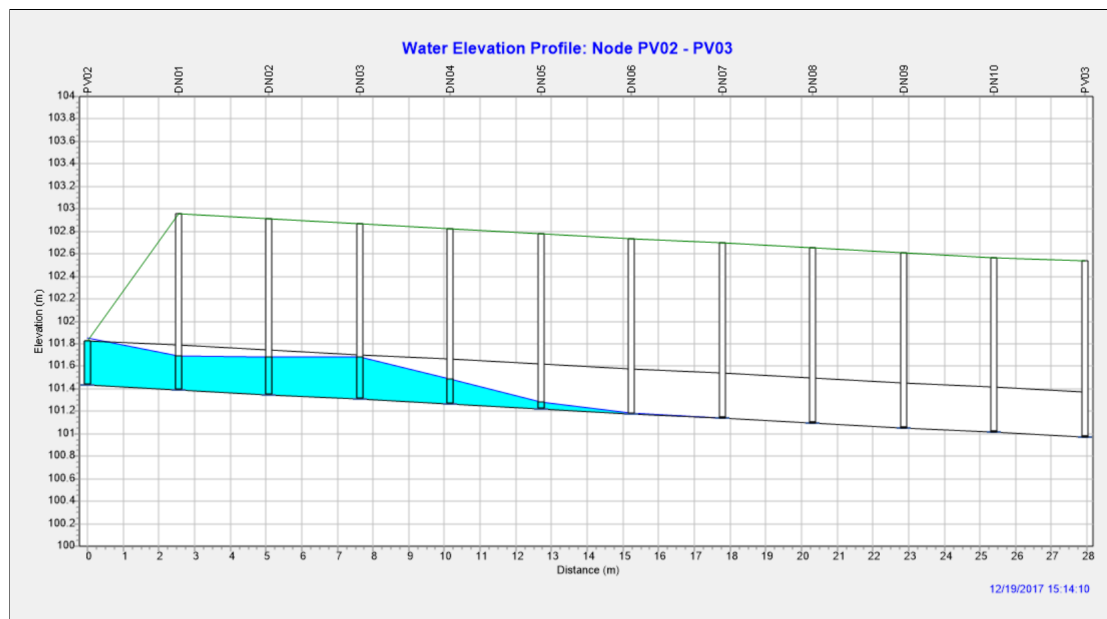
Figure 3.11 – Flow profile of the traditional approach.



Source: The Author.

Analysis of the behavior of the Regular Intervals alternative layout (Figure 3.12) shows that the wave formed by the rapid inflow into the system was more accurately represented. However, occasional instabilities in the flow profile were detected at the dummy junctions when the water level reached the conduit crown.

Figure 3.12 – Flow profile of the regular Interval approach.



Source: The Author.

The behavior of the other alternative approaches was very similar to the Regular Intervals, showing occasional instabilities at the dummy junctions and identifying the wave generated by the rapid inflow. Since the general characteristics of these alternative approaches are similar, they will not be discussed (for brevity).

### 3.4 CONCLUSIONS

Modeling highly dynamic flows conditions in collection systems is very challenging. The accuracy of SWMM link–node solution to represent these situations is uncertain. Therefore, a field investigation was conducted to obtain data of rapid inflows in a collection system. The traditional layout proposed in the SWMM User's Manual was not capable of properly simulating the water level variation during rapid filling. However, adding the conceptual spatial discretization proposed in this paper significantly improved the SWMM modeling of extreme inflows compared to the traditional layout.

Three alternative model layouts using spatial discretization were evaluated. First, a regular interval discretization was constructed by placing 10 dummy junctions between the risers. Second, a fixed interval discretization was constructed by limiting the discretization length to a minimum length of 1 m and maximum of 3 m. A third alternative layout, diameter based, was created using 10x the diameter of each conduit link as the discretization length.

All approaches showed different results at the inlet (PV02). The traditional layout simulation was the one that produced most disagreement between the observed and simulated data. All the alternative layouts gave satisfactory results at this node. The reason for this is that the PV02 results using a traditional SWMM link–node approach are affected by only one downstream junction. This situation causes some sort of water storage in the conduit that affects the upstream node and is reflected in the continuity error (more than  $\pm 4.5\%$ ). When using spatial discretization, as in the alternative layouts, this situation does not occur (0 % continuity error). At the other monitored riser (PV07), not all approaches predicted the correct water arrival time. However, when using artificial spatial discretization significant improvements are achieved in terms of water rise and decrease, water peak level, and continuity error, although the statistical indicators did not show good results. Thus, based on the findings of this experiment, the authors recommend the use of additional spatial discretization when modeling highly dynamic flows in SWMM, especially the alternative approach based on 10x conduit diameter, because it requires less computational effort when compared to other alternative approaches to improve the results.

It is also important to note that the physical drainage system used in this experiment is aged and poorly maintained. The system can be damaged at various

points or have detritus in its interior that can cause some unaccounted losses or storage that are not characterized in the SWMM models. Furthermore, there may be some illegal and unaccounted connections that can delay water arrival or cause significant variations in water level. The authors believe that this may be the main reason for the small values of  $r^2$  and NSE.

In conclusion, the use of artificial spatial discretization in links leads to improvements in modeling extreme inflows by SWMM. These improvements lead to a more precise unsteady flow modeling using a well-known and globally established model. However, using artificial spatial discretization in SWMM significantly increases the computational time to perform a single simulation, but this additional time is comparable to other models that are able to represent transient flows in stormwater systems. For this reason, the authors recommend setting up the model with additional spatial discretization only when highly dynamic situations are expected. Also, the selected routing time step for the performed simulations was very small and variations of the time step were not thoroughly investigated. In some situations, the number of dummy nodes and the magnitude of the inflow may require smaller or variable time steps for a precise simulation, depending on a careful analysis by the user.

Moving forward, perhaps a new system must be used for validation in new studies. Moreover, since a new SWMM release (5.1.013) which has the Preissmann Slot option is available, the impact of using the Preissmann slot along with spatial discretization should also be evaluated. Other needs to be studied are the effect of discretization in other system geometries, including conditions with multiple time-varying inflow hydrographs.

## REFERENCES

- ARDUINO. 2018. Accessed in 16 January, 2018. Available at: <<http://www.arduino.cc/en/Guide/Introduction>>.
- ASCE. Criteria for Evaluation of Watershed Models. **Journal of Irrigation and Drainage Engineering**, v. 119, n. 3, p. 429–442, 1993.
- CAMORANI, G.; CASTELLARIN, A.; BRATH, A. Effects of land-use changes on the hydrologic response of reclamation systems. **Physics and Chemistry of the Earth**, v. 30, p. 561–574, 2005. DOI: 10.1016/j.pce.2005.07.010.
- CHOW, M. F.; YUSOP, Z.; TORIMAN, M. E. Modelling runoff quantity and quality in tropical urban catchments using Storm Water Management Model. **International Journal of Environmental Science and Technology**, p. 737–748, 2012. DOI: 10.1007/s13762-012-0092-0.
- DHI. **Mouse Pipe Flow**. MIKE URBAN, 2017.

GUIZANI, M.; JOSE, G.; STEVEN, J.; KHLIFA, M. et al. Investigation of rapid filling of empty pipes. **The Journal of Water Management Modeling**, Computational Hydraulics International (CHI), v. 225, n. 20, p. 463–482, 2006.

LEGATES, D. R.; JR., G. J. M. Evaluating the use of "goodness-of-fit" measures in hydrologic and hydroclimatic model validation. **WATER RESOURCES RESEARCH, VOL.**, v. 35, n. 1, p. 233–241, 1999.

NASH, E.; SUTCLIFFE, V. River Flow Forecasting Through Conceptual Models Part I - A Discussion of Principles. **Journal of Hydrology**, v. 10, p. 282–290, 1970.

NIAZI, M.; NIETCH, C.; MAGHREBI, M.; JACKSON, N.; BENNETT, B. R.; TRYBY, M.; MASSOUDIEH, A. Storm Water Management Model: Performance Review and Gap Analysis. **Journal of Sustainable Water Built Environment**, v. 3, n. 2, 2017. DOI: 10.1061/JSWBAY.0000817..

OBROPTA, C. C.; KARDOS, J. S. Review of Urban Stormwater Quality Models: Deterministic, Stochastic, and Hybrid Approaches. **Journal of the American Water Resources Association**, v. 43, n. 6, p. 1508–1523, 2007. DOI: 10.1111/j.1752-1688.2007.00124.x.

POPESCU, I. **Computational Hydraulics**. London: IWA Publishing, 2014. ISBN 9781780400440.

QIN, H.-p.; LI, Z.-x.; FU, G. The effects of low impact development on urban flooding under different rainfall characteristics. **Journal of Environmental Management**, Elsevier Ltd, v. 129, p. 577–585, 2013. ISSN 0301-4797. DOI: 10.1016/j.jenvman.2013.08.026. Available at: <<http://dx.doi.org/10.1016/j.jenvman.2013.08.026>>.

RIDGWAY, K. E.; KUMPULA, G. Surge Modeling in Sewers using the Transient Analysis Program (TAP). **Journal of Water Management Modeling**, v. 6062, p. 155–164, 2007. DOI: 10.14796/JWMM.R228-10..

ROESNER, L. A.; ALDRICH, J. A.; DICKINSON, R. E.; BARNWELL, T. O. **Storm Water Management Model User's Manual, Version 4: EXTRAN Addendum**. Athens: Environmental Research Laboratory, Office of Research e Development, US Environmental Protection Agency, 1988.

ROSSMAN, L. A. Storm Water Management Model Quality Assurance Report: Dynamic Wave Flow Routing. **Storm Water Management Model Quality Assurance Report**, EPA/600/R-06/097, p. 1–115, 2006.

\_\_\_\_\_. Storm Water Management Model User's Manual Version 5.1. **U.S. Environmental Protection Agency**, EPA/600/R-14/413b, p. 1–353, 2015.

\_\_\_\_\_. Storm Water Management Model Reference Manual Volume II – Hydraulics. **U.S. Environmental Protection Agency**, Mayo, p. 190, 2017.



STURM, T. **Open channel hydraulics**. New York: Mc Graw Hill, 2001.

TEMPRANO, J.; ARANGO, Ó.; CAGIAO, J.; SUÁREZ, J.; TEJERO, I. Stormwater quality calibration by SWMM: A case study in Northern Spain. **Water SA**, v. 32, Jan. 21, 2002, p. 5, 2006. ISSN 0959-3330. DOI: 10.1080/09593332308618381.

TSIHRINTZIS, V. A.; HAMID, R. Runoff quality prediction from small urban catchments using SWMM. **Hydrological Processes**, v. 12, June 1996, p. 311–329, 1998.

VASCONCELOS, J. G.; ELDAYIH, Y.; JAMILY, J. A. Evaluating Storm Water Management Model accuracy in mixed flows conditions. **Journal of Water Management Modeling**, p. 1–21, 2018.

WYLIE, E. B.; STREETER, V. L.; SUO, L. **Fluid transients in systems**. Prentice Hall Englewood Cliffs, NJ, 1993. v. 1.

ZHOU, F. et al. Transient flow in a rapidly filling horizontal pipe containing trapped air. **Journal of Hydraulic Engineering**, American Society of Civil Engineers, v. 128, n. 6, p. 625–634, 2002.

## 4 ARTICLE 2 - COMPARING SWMM 5.1 CALCULATION ALTERNATIVES TO REPRESENT UNSTEADY STORMWATER SEWER FLOWS<sup>1</sup>

### Abstract

The Storm Water Management Model 5.1 (SWMM) is an open-source model widely used to simulate urban drainage systems. SWMM modeling uses a link-node discretization approach that represents well typical inflows scenarios, but may underestimate surges and other unsteady flow characteristics during extreme inflows. Adopting artificial spatial discretization (ASD) has shown to improve SWMM model accuracy in rapid inflows conditions. Additionally, an alternative pressurization algorithm based on the Preissmann slot was recently added to SWMM, but a systematic assessment of SWMM performance considering the use of ASD and the Preissmann slot algorithm is still missing. The present work provides this assessment, by comparing link-node and ASD approaches along with the original EXTRAN and Preissmann slot algorithms. Scenarios used in the comparison were selected from the SWMM QA/QC report and assessed in terms of continuity errors and numerical stability. Results indicate accuracy improvements when adequate temporal and spatial discretization are selected.

### 4.1 INTRODUCTION AND OBJECTIVE

The Environmental Protection Agency (EPA) Stormwater Management Model 5.1 (SWMM) is one of the most successful and popular hydrologic-hydraulic models currently in use worldwide (OBROPTA et al., 2007; NIAZI et al., 2017; KULLER et al., 2017). This model, which results from a multi-decade development effort (HUBER et al., 2012), is able to simulate runoff quantity and quality for single-event or continuous hydrologic modeling (GIRONÁS et al., 2010; USEPA, 2018). Operating on a collection of subcatchments areas which receives precipitation and generates runoff, SWMM transports this runoff through system of pipes, channels, and others using its unsteady flow formulation presented by Roesner et al. (1988) and Rossman (2006).

SWMM unsteady formulation solves the flow conditions in a network of conduits (also referred as links) and junctions (also referred as nodes) through the St. Venant equations (USEPA, 2018). In this work, this standard SWMM approach is referred as link-node solution. The St. Venant equations are a system of two partial differential equations based on the conservation of mass and linear momentum that represent the unsteady open-channel flows (STURM, 2001). SWMM applies these equations to solve the flow along an individual conduit and an additional continuity relationship for the junctions, such as manholes, that connect two or more conduits together

---

<sup>1</sup>Article submitted to **Journal of Hydraulic Engineering**.

(ROSSMAN, 2006). Even though SWMM is able to apply simplified versions of the St. Venant equations, such as the Zero-Inertia Wave or the Kinematic Wave, the complete St. Venant equations are frequently necessary when modeling rapid filling scenarios leading to pressurization (USEPA, 2018). However, when very long conduits are present or when highly dynamic flow conditions happen, SWMM modeling results may yield significant flow continuity errors and/or numerical instabilities (RIDGWAY, 2008; VASCONCELOS; ELDAYIH et al., 2018; HODGES et al., 2019; PACHALY; VASCONCELOS; ALLASIA; MINETTO, 2019).

In its version 5.1.013, SWMM allows the selection between two options to represent pressurized flows in conduits: EXTRAN and SLOT. EXTRAN denotes the traditional pressurization algorithm initially present in earlier SWMM versions (< 5.1.012) (ROESNER et al., 1988), which uses a variation of the surcharge algorithm to update nodal heads and link flows when the node's water level exceeds the crown of the highest conduit connected to it (ROSSMAN, 2006). When this situation occurs, an alternative nodal continuity condition expressed in the form of a perturbation equation is used to update nodal heads at the new time step. When both upstream and downstream nodes are surcharged, another set of equations is applied because the flow is considered pressurized (ROSSMAN, 2006).

The SLOT pressurization algorithm is based on the Preissmann slot concept (CUNGE et al., 1980), which adds an hypothetical vertical and narrow slot at the pipe crown. This artificial slot allows the maintenance of free surface flow conditions, but also enables the increasing of cross-sectional pressure force in the momentum equation when conduit flow is pressurized. Using this method, SWMM's normal procedure for updating nodal heads can continue to be used (USEPA, 2018). While there are significant differences in the solution procedure adopted by the EXTRAN and SLOT algorithms, to date no studies have been conducted evaluating eventual differences yielded by these algorithms when extreme flow conditions are considered.

Parallel to the comparison between pressurization algorithms, other SWMM-related studies evaluated the impact of catchment discretization (scale-effect) in hydrologic simulations and models (e.g Wood et al. (1988), Tripathi et al. (2006), Muleta et al. (2007)). In some of these studies it was analyzed the modeling improvements in terms of runoff quantity and peak levels by altering the spatial resolution in subcatchments (e.g. Zaghoul (1981), Park et al. (2008), Dongquan et al. (2009), Ghosh et al. (2012), Krebs et al. (2014), Sun et al. (2014)). By comparison, fewer studies (e.g. Ridgway (2008), Vasconcelos, Eldayih et al. (2018), Pachaly, Vasconcelos, Allasia e Minetto (2019)) evaluated the improvements in terms of numerical stability and flow continuity error in hydraulic computations by the means of adding artificial spatial discretization (ASD) between SWMM nodes. ASD implies in splitting links into smaller ones by placing dummy nodes as intermediate calculation

points, often performed with the selection of smaller routing time steps to ensure numerical stability. As pointed out by Popescu (2014), reducing the approximation error by using small temporal and spatial discretization when solving the St. Venant equations can lead to significant improvements in accuracy. On the other hand, using the traditional link-node approach in SWMM reduces computational efforts, since there is no need to calculate intermediate points.

Simultaneously to these studies, different SWMM applications have emerged. Some of them allowed SWMM to simulate situations that the model was not originally conceived to perform. In some cases it might require alterations in its source code (CHO et al., 2007; BURGER et al., 2014) or coupling it with other software (RIAÑO-BRICEÑO et al., 2016; BUAHIN et al., 2018), but sometimes only adjusting the model setup (RIDGWAY, 2008; VASCONCELOS; ELDAYIH et al., 2018; PACHALY; VASCONCELOS; ALLASIA; MINETTO, 2019) is enough. For example, some studies have shown that SWMM is able to represent intermittent water distribution systems (CAMPISANO; GULLOTTA et al., 2019), mixed flows (VASCONCELOS; ELDAYIH et al., 2018), rapid inflows (PACHALY; VASCONCELOS; ALLASIA; MINETTO, 2019), or force main transients (RIDGWAY, 2008) when coupling it with other software or setting the model properly for these specific situations.

Back in 2006, when SWMM was being upgraded from version 4.4 to version 5, a rigorous Quality Assurance (QA) report (ROSSMAN, 2006) was elaborated to assure that the numerical results obtained by the SWMM's new version were compatible with the results from the previous version, especially regarding the dynamic wave routing (i.e. solution by St. Venant equations). The examples used in this QA are available online and contain many characteristics that are useful for testing highly dynamic flows in SWMM, including the newly implemented SLOT surcharge method and the additional spatial discretization.

Therefore, the objective of this work is to present results related to a systematic analysis in terms of continuity errors and numerical stability by comparing the existing surcharge algorithms present in SWMM and the use of ASD versus the traditional link-node modeling approach. This systematic evaluation was performed using the modeling conditions presented in the SWMM QA report by Rossman (2006). Besides the comparison in terms of continuity and stability, this work includes a comparison of computational effort associated with ASD usage and different surcharge algorithms. Since adding ASD to SWMM models is a very time-demanding task, an application named ReSWMM was developed in order to automatize this task and it is available for download.

## 4.2 METHODS

### 4.2.1 SWMM formulation

The unsteady flow solver is one of the key modules presented in SWMM (USEPA, 2018). This module is based on the EXTRAN algorithm originally proposed by Roesner et al. (1988) and, due to its simplicity and versatility, SWMM 5.1 continues to use this solution technique. However, some modifications were implemented in order to bring improvements in the model stability (ROSSMAN, 2017). Using a link-node approach, SWMM solves the complete form of St. Venant equations for unsteady free surface flow through a channel or pipe (ROESNER et al., 1988; ROSSMAN, 2006, 2017). The St. Venant equations, conservation of mass (Eq. 4.1) and momentum (Eq. 4.2), can be expressed as:

$$\frac{\partial A}{\partial t} + \frac{\partial Q}{\partial x} = 0 \quad (4.1)$$

$$\frac{\partial Q}{\partial t} + \frac{\partial(Q^2/A)}{\partial x} + gA \frac{\partial H}{\partial x} + gAS_f + gAh_L = 0 \quad (4.2)$$

where  $A$  denotes cross-sectional area;  $t$  denotes time;  $Q$  denotes flow rate;  $x$  denotes distance;  $H$  denotes the hydraulic head of water in the conduit;  $g$  denotes gravity;  $h_L$  denotes the local energy loss per unit length of conduit; and  $S_f$  denotes the friction slope, which is implemented with the Manning equation (ROSSMAN, 2006).

Within SWMM, these equations are converted into an explicit set of finite difference formulas and then solved using a method of successive approximations with under relaxation (ROSSMAN, 2006). To compute the flow in each conduit and head in each node, SWMM uses, respectively, Eq. 4.3 and Eq. 4.4 for time  $t + \Delta t$  as function of known values at time  $t$  (ROSSMAN, 2006).

$$Q_{t+\Delta t} = \frac{Q_t + \Delta Q_{gravity} + \Delta Q_{inertial}}{1 + \Delta Q_{friction} + \Delta Q_{losses}} \quad (4.3)$$

$$H_{t+\Delta t} = H_t + \frac{\Delta Vol}{(A_{store} + \sum A_s)_{t+\Delta t}} \quad (4.4)$$

Where  $\Delta Q_{gravity}$ ,  $\Delta Q_{inertial}$ ,  $\Delta Q_{friction}$ , and  $\Delta Q_{losses}$  denote the type of force they represent;  $\Delta Vol$  denotes net volume flowing through the node over the time step;  $A_{store}$  denotes surface area of the node; and  $\sum A_s$  denotes surface area contributed by the conduits connected to the node. More details are provided in Rossman (2006).

When the nodal water level exceeds the crown of the highest conduit connected to it, the surcharge condition exists (ROSSMAN, 2006, 2017). In this situation, the surface area contributed by any closed conduits would be zero and, because

of that, additional formulation is needed to update nodal head at new time steps (ROESNER et al., 1988; ROSSMAN, 2006). As pointed earlier, the current SWMM version (5.1.013) allows for the selection between two surcharge methods to handle pressurized conditions: EXTRAN or SLOT (USEPA, 2018). The first uses a form of a perturbation equation (Eq. 4.5) when the flow depth is greater than 96% of link diameter (USEPA, 2018) to enforce the flow continuity condition:

$$\Delta H = \frac{-\sum Q}{\sum \partial Q / \partial H} \quad (4.5)$$

where  $\Delta H$  is the adjustment to the node's head that must be made to achieve a flow balance (ROSSMAN, 2017). Within a conduit, the combination of Eq. 4.5 and Eq. 4.3 results in:

$$\frac{\partial Q}{\partial H} = \frac{-g\bar{A}\Delta t/L}{1 + \Delta Q_{friction} + \Delta Q_{losses}} \quad (4.6)$$

where the negative sign is because the flow directed out of a node is considered negative while the flow into the node is considered positive (ROSSMAN, 2006). It can be shown that Eq. 4.6 is similar to a lumped inertia equation frequently used to represent slow transients (WYLIE et al., 1993).

The SLOT surcharge method is based on the Preissmann Slot. This technique has been extensively used since 1960 (CHAUDHRY, 2008) and eliminates the need to switch to the surcharge algorithm for surcharged nodes (USEPA, 2018). Using a vertical and narrow slot over each pipe, the free surface flow condition prevails allowing the use of St. Venant Equations (CUNGE et al., 1980). When using this method in SWMM, the Preissmann Slot is attached to closed conduits flowing more than 98.5% full (USEPA, 2018). Since surcharge conditions frequently occur during rapid fillings and/or highly dynamic situations, differences in modeling results between the EXTRAN and SLOT algorithms are expected.

Also, another change introduced by SWMM version 5.1.013 affected the calculation of the Minimum Nodal Surface Area (MNSA) during unsteady flow calculations. In previous SWMM versions, the MNSA was being used as a surface area always available at a node instead of an amount of area available only when the surface area of the node's connecting links falls below it. Therefore, the results generated by EXTRAN surcharge algorithm from SWMM version 5.1.012 were compared with the EXTRAN results yielded by SWMM 5.1.013.

#### 4.2.1.1 Routing time-step and artificial discretization

The routing time-step recommendation originally proposed by Roesner et al. (1988) to ensure SWMM numerical stability was shown to be inadequate to represent

modeling conditions involving rapid filling and ASD (VASCONCELOS; ELDAYIH et al., 2018). Vasconcelos, Eldayih et al. (2018) suggested a simple modification of the original recommendation by Roesner et al. (1988), presented in Eq. 4.7, which was shown to reduce continuity errors in extreme inflows and pressurization conditions.

$$\Delta t = 0.1 \frac{\Delta x}{\sqrt{gD}} \quad (4.7)$$

Where  $\Delta t$  denotes recommended routing time-step;  $\Delta x$  denotes size of the spatial discretization;  $g$  denotes gravity acceleration; and  $D$  denotes link diameter. Eq. 4.7 is used to set routing time-step for the discretized examples presented in this work. To ensure that this smaller time step was always adopted by SWMM simulations, the use of variable time step was disabled. The routing-time step was not modified for the original link-node examples presented in the QA, except when mentioned.

According to Ridgway (2008), Vasconcelos, Eldayih et al. (2018), and Pachaly, Vasconcelos, Allasia e Minetto (2019), adding ASD in the links could lead to significant improvements in SWMM accuracy to simulate dynamic conditions. Therefore, an alternative modelling setup was conceived for each example considered in this work placing intermediate nodes between actual nodes. For a given link with length  $L$ , the discretization length is:

$$\Delta x = \frac{L}{n+1}, \quad (4.8)$$

where  $n$  is the number of intermediate junctions being calculated based on a ratio (Eq. 4.9) between the conduit length and diameter/max depth:

$$n = \max \left[ \text{round} \left( 0.1 \frac{L}{D} \right) - 1, 0 \right]. \quad (4.9)$$

For instance, in the case of a 100-m long, 0.5-m diameter sewer, the number of intermediate junctions  $n$  would be 19, resulting in 20 links with a length of  $\Delta x = 5$  m. However, in the case of short conduits (i.e.  $L/D < 15$ ), there is no need of ASD and the results of Eq. 4.9 and Eq. 4.8 are  $n = 0$  and  $\Delta x = L$ , respectively. The advantage of this approach is that long and short conduits will have the discretization based on its own characteristics and not in a general pattern. According Pachaly, Vasconcelos, Allasia e Minetto (2019), this ASD procedure is the one that produces better results with less computational effort when compared to other discretization approaches. Furthermore, it is important to highlight that the links generated by the ASD inherit the original link roughness and the entry and exit losses will be accounted only in the first and last links connected to the original nodes.

Due to the time-consuming operation of creating manually the dummy nodes, a software/add-on called ReSWMM (PACHALY; VASCONCELOS; ALLASIA, 2018) was

used to perform this discretization automatically. Some commercial implementations of SWMM model have similar features that enable the discretization of conduits.

#### 4.2.2 Quality assurance examples

The original link-node approach in SWMM implies that stormwater structures such as manholes and storage units are represented through nodes, while sewers, channels and other conduits are represented through links. These conditions are also present in a set of examples provided by the SWMM QA report (ROSSMAN, 2006). Using several examples, this report compares the dynamic wave flow routing procedures of SWMM 4.4 against SWMM 5 in order to assure that the numerical results obtained by SWMM 5 were compatible with the results from the previous version (ROSSMAN, 2006). Three types of cases were present in the QA report:

1. Models that were presented in SWMM-EXTRAN 4.4 User's Manual (ROESNER et al., 1988). These examples include conditions that are representative of stormwater systems, such as side orifices, weirs, storage units, pumps, surcharged flows, etc. The great majority of these examples modifies hydraulic elements present in 2 branches of circular conduits that converge into a pair of trapezoidal channels (Fig. 4.1 (A)).
2. Challenge Test Cases, which are a set of conditions compiled by Robert E. Dickson for the QA report. These cases consist of circular pipes arranged in way that challenges the dynamic flow modeling including flat and adverse slopes, steep drops, etc. A total of five models are present: (1) 10 pipes with 100-foot lengths of 4-foot diameter on a flat slope; (2) 5 pipes with 1000-foot lengths alternating sections of 12-foot diameter into a 3-foot diameter with a slope of 0.05%; (3) 12 pipes with 500-foot lengths with the first 6 having 6-foot diameter and the last 6 having 3-foot diameter with a 40 feet drop between them and a slope of 0.10%; (4) inverted siphon with 10 pipes with 100-foot lengths of 4-foot diameter; and (5) 10 conduits with 100-foot lengths of 4-foot diameter with adverse slopes of 3% (Fig. 4.1 (B)).
3. Real-world models representing storm sewer systems, combined sewer systems, and natural channel systems, corresponding to the User-Submitted Test Cases in the SWMM QA report. Valuable results are accounted when analyzing the modeling performance in real-world cases due to the variety of situations and the large number of nodes and links occurring in these datasets (Fig. 4.1 (C)).

Because of very irregular geometries or due to the absence of links, four of the twenty QA examples were not used in this work. Table 4.1 summarizes the elements



present in each example for both traditional and discretized layouts. Fig. 4.1 shows samples of one layout for each set of cases. More information about these examples are presented in Rossman (2006). For each of the 16 examples studied here, three surcharge algorithms were used (EXTRAN 5.1.012 / EXTRAN 5.1.013 / SLOT), along with traditional (i.e. link-node) and discretized approaches. A total of 96 simulations were thus performed in this investigation.

Table 4.1 – QA report test cases summary.

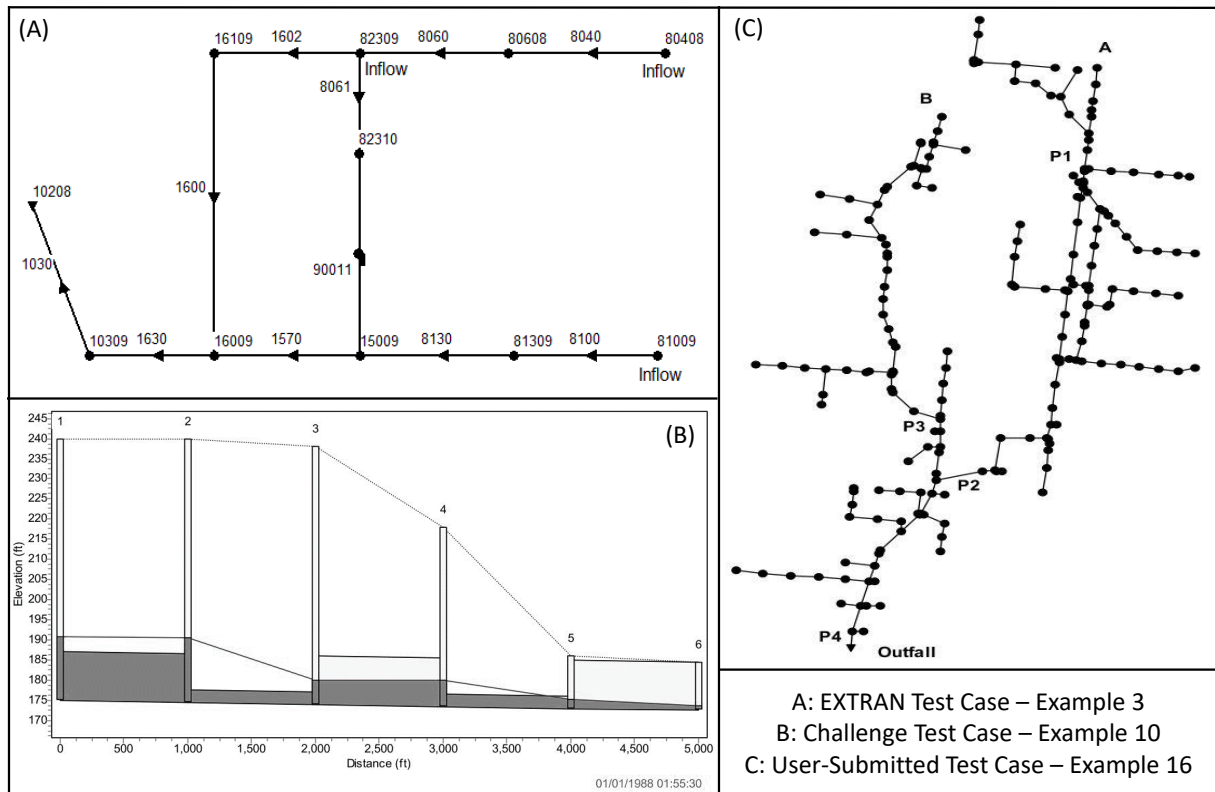
(continues)

Ex.	Layout	Junctions	Stor. Unit	Outfalls	Conduits	$\Delta t$	Sim. Time
1	Trad.	9	-	1	9	20 s	8:00:00
	Disc.	540	-	1	540	0.64 s	8:00:00
2	Trad.	9	-	1	9	20 s	8:00:00
	Disc.	540	-	1	540	0.64 s	8:00:00
3	Trad.	9	-	1	9	20 s	8:00:00
	Disc.	540	-	1	540	0.53 s	8:00:00
4	Trad.	9	-	1	9	20 s	8:00:00
	Disc.	540	-	1	540	0.53 s	8:00:00
5	Trad.	9	1	1	9	20 s	8:00:00
	Disc.	540	1	1	540	0.53 s	8:00:00
6	Trad.	10	-	1	10	20 s	8:00:00
	Disc.	548	-	1	548	0.60 s	8:00:00
7	Trad.	9	-	1	9	20 s	8:00:00
	Disc.	540	-	1	540	0.64 s	8:00:00
8	Trad.	-	2	1	1	60 s	5:00:00
	Disc.	24	2	1	25	0.64 s	5:00:00
9	Trad.	10	-	1	10	5 s	5:00:00
	Disc.	20	-	1	20	0.80 s	5:00:00
10	Trad.	5	-	1	5	5 s	6:00:00
	Disc.	90	-	1	90	0.56 s	6:00:00
11	Trad.	12	-	1	12	5 s	6:00:00
	Disc.	150	-	1	150	0.54 s	6:00:00
12	Trad.	10	-	1	10	5 s	5:00:00
	Disc.	20	-	1	20	0.80 s	5:00:00
13	Trad.	10	-	1	10	5 s	12:00:00
	Disc.	20	-	1	20	0.80 s	12:00:00
14	Trad.	59	-	1	59	5 s	7:00:00
	Disc.	1116	-	1	1116	0.15 s	7:00:00

Ex.	Layout	Junctions	Stor. Unit	Outfalls	Conduits	$\Delta t$	Sim. Time
15	Trad.	5	130	6	134	0.5 s	6:00:00
	Disc.	2094	130	6	2223	0.25 s	6:00:00
16	Trad.	208	-	1	209	5 s	24:00:00
	Disc.	1520	-	1	1521	0.02 s	24:00:00

Source: The Author.

Figure 4.1 – Test cases samples.



Source: Adapted from Rossman (2006).

### 4.2.3 Criteria for evaluation of numerical solutions

In the present study, three different criteria were used to evaluate numerical solutions yielded by the modeling performed with SWMM 5.1: Flow continuity errors, numerical stability and computational effort analyses. According to the SWMM User’s Manual Version 5.1 (ROSSMAN, 2015), the flow continuity error represents the sum of the all outflow from the network divided by the sum of all inflow to the network. Likewise, the manual states that continuity errors greater than  $\pm 10\%$  must be examined to guarantee the validity of the simulation. Too short conduits or too long time-steps are likely to be a reason for larger flow continuity errors. In order to

evaluate eventual improvements achieved by using ASD, a comparison between flow continuity errors from the traditional approach and those from discretized approach was realized. Differences in flow continuity errors were grouped according to the surcharging algorithm used in the simulation.

Rossmann (2015) states that, due to the explicit nature of the numerical methods used in its solution, the flow in some links or water depth may fluctuate or oscillate as a result of numerical instabilities. SWMM is fitted with the ability to adjust and reduce the routing time step as a means to reduce instability in the simulation. Often times, reducing routing time or increasing short length links tend to help mitigate stability issues. Also, a more severe action of dampening or ignoring the inertial terms of the St. Venant equation can be implemented but this action can affect the modeling accuracy. Since SWMM 5, a criterion for determining if a nodal head has converged is used. This criterion is called Head Convergence Tolerance and reducing this value can lead to improvements in terms of numerical stability. Therefore, this work compares differences in numerical stability between the surcharge algorithms for selected cases.

Moreover, the size, complexity, and dynamic situations occurring in a system may require small time steps (VASCONCELOS; ELDAYIH et al., 2018), and the combination of small time steps along with the presence of many nodes must demand higher computational time to perform a single simulation when compared to the traditional link-node approach. In order to analyze this additional computational effort, a comparison between the computational time spent to execute the traditional and discretized simulations with different surcharge methods was performed using the QA examples.

## 4.3 RESULTS AND DISCUSSION

Results presented in this section are grouped by discretization approach (traditional link-node vs discretized) and by surcharge algorithm used in calculations (EXTRAN 5.1.012, EXTRAN 5.1.013 and SLOT). Initially a comparison of continuity errors is presented, followed by a discussion on numerical stability of the solutions yielded by the different modeling strategies in SWMM, and concluding with a comparison of the computational effort associated with the modeling of each approach.

### 4.3.1 Evaluation of flow continuity errors

After running the SWMM QA report examples present in Table 4.1, results for continuity errors were extracted and summarized on Table 4.2. As it is noticed, most continuity errors are small, only Example 12 using the traditional link-node approach with the SLOT pressurization algorithm exceeded more than 68% of continuity error.

The reason for this high value of continuity error was the routing time-step, reducing it from 5 s to 1 s decreased the continuity error to almost 0%. However, it is important to highlight that for 12 out of 16 examples the continuity errors were equal or smaller when spatial discretization was used.

For practical purposes, most of these continuity error values are not larger than other error sources in a modeling effort, and thus possibly acceptable in actual modeling applications. Yet, these comparisons with the SWMM QA cases indicate that both SLOT and the latest EXTRAN algorithms have a tendency of presenting smaller continuity errors. Adding ASD, which was shown to improve modeling results of flows involving surges, appears to also reduce continuity errors when routing time step was selected according to Eq. 4.7. In these cases, the routing time-steps selected were always smaller than those values reported in the original QA report, which should help in increasing the stability of the solutions.

Table 4.2 – Flow continuity error summary.

Ex.	Traditional Layout			Spatial Discretized Layout		
	EXTRAN (5.1.012)	EXTRAN (5.1.013)	SLOT (5.1.013)	EXTRAN (5.1.012)	EXTRAN (5.1.013)	SLOT (5.1.013)
1	-0.03%	0.01%	0.01%	-0.13%	-0.04%	-0.01%
2	-4.08%	-4.05%	-4.23%	-0.10%	-0.06%	-0.05%
3	0.09%	0.09%	0.10%	-0.01%	-0.04%	-0.01%
4	0.02%	0.02%	-0.10%	-0.01%	0.00%	0.00%
5	-0.22%	-0.20%	-0.41%	-0.12%	-0.06%	-0.01%
6	-0.05%	-0.05%	-0.16%	-0.01%	-0.13%	-0.00%
7	0.10%	0.05%	-0.11%	0.12%	0.10%	-0.01%
8	0.13%	0.13%	-0.18%	0.09%	0.03%	0.04%
9	-0.01%	-0.01%	-2.20%	-0.02%	-0.02%	-0.03%
10	-0.06%	-0.05%	-0.29%	-0.12%	-0.05%	-0.09%
11	-0.17%	-0.20%	-0.12%	-0.01%	-0.21%	0.03%
12	0.36%	0.34%	-68.16%	0.07%	0.03%	0.38%
13	-0.02%	-0.01%	-0.01%	-0.06%	-0.05%	-0.02%
14	-0.08%	0.13%	0.10%	-0.12%	0.78%	0.81%
15	-0.03%	-0.02%	-0.13%	-0.16%	-0.15%	-0.36%
16	0.05%	0.05%	0.05%	-0.02%	0.01%	0.04%

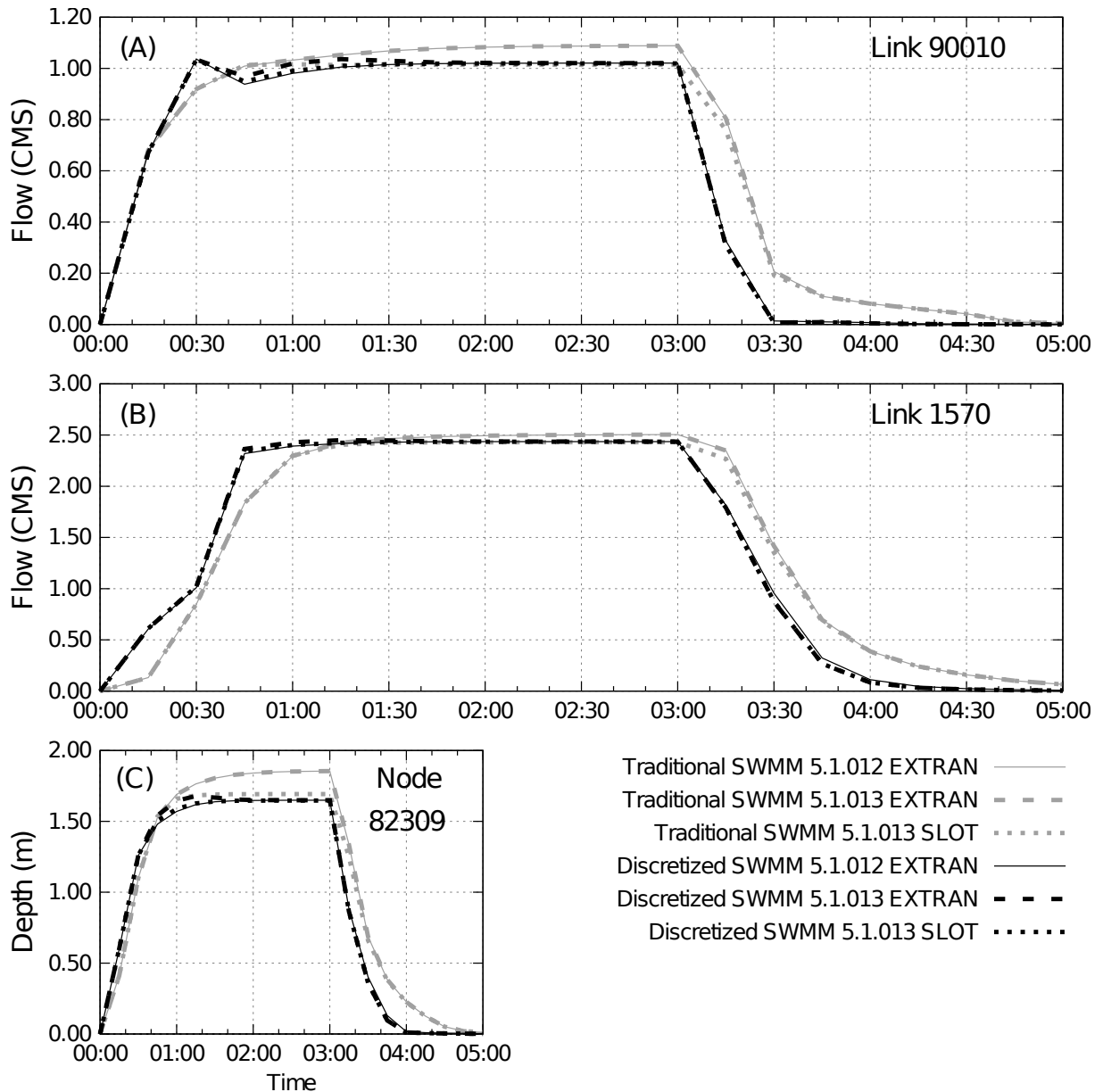
Source: The Author.

### 4.3.2 Evaluation of numerical stability

Numerical stability, in the context of the present work, is reflected in a numerical solution that yields predictions that would be theoretically anticipated, without presenting spurious spikes and/or oscillations. Results in this way were observed for simulation conditions performed for Examples 1, 2, 4, 5, 7, 8, 9 and 16. In this light, following results presented are focused on QA report examples in which differences between the modeling approaches were noticed, and when numerical stability issues were detected.

For instance, different simulation results obtained for Example 3 are presented in Fig. 4.2 (A, B, C), showing that there are no apparent spikes in the solution although it is noticed differences between solutions obtained with discretized and non-discretized modeling. The latter approach tends to show a delayed arrival of inflow fronts, as well a delayed recession curve during the dewatering of the system. This result, which was also noticed in Example 7, is consistent with Vasconcelos, Eldayih et al. (2018), who pointed out that the use of ASD in SWMM helped to create a sharp description of inflow fronts. It can also be noticed that peak depths yielded by discretized approaches are smaller. However, without field data it is hard to estimate which scenario is more accurate, although Pachaly, Vasconcelos, Allasia e Minetto (2019) showed that discretized models represented more accurately the flow in terms of water peak level and arrival of inflow fronts in a monitored rapid filling case.

Figure 4.2 – Example 3 SWMM results showing delayed flow arrivals and recession of traditional (i.e. link-node) approaches, compared to discretized modeling

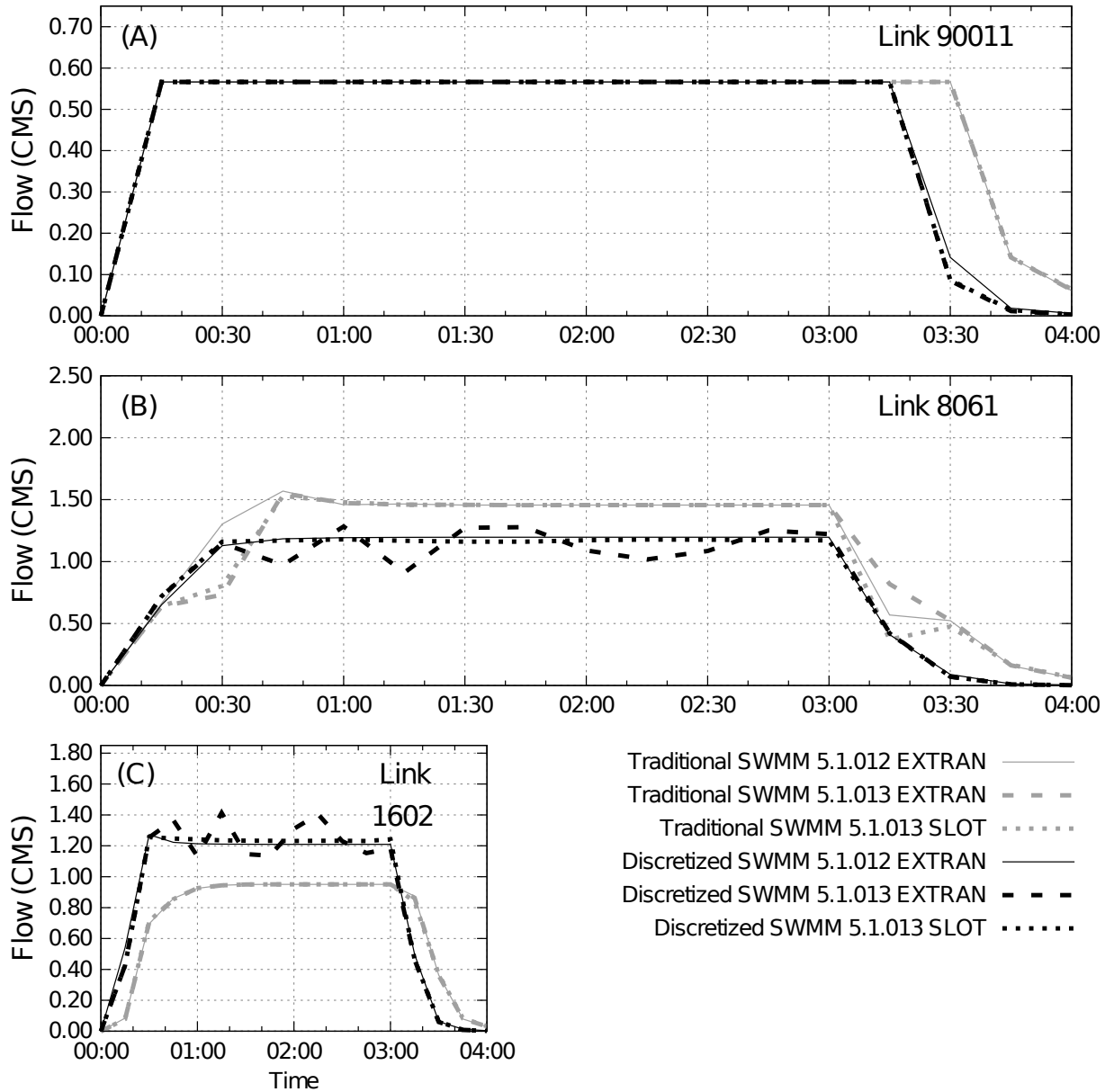


Source: The Author.

Example 6 in the SWMM QA report changes conditions in Example 3 by placing an off-line pump station (SWMM Type 1 pump) where formerly an orifice connected two junctions. In Fig.4.3, it is possible to observe the same delayed recession curve during the dewatering of the system at the link 90011 for all non-discretized models. Some signs of numerical spikes are noticed in the solution at link 8061 and 1602 using ASD along with the EXTRAN 5.0.13 pressurization algorithm. Additionally, flow results for some links are significantly different between traditional and discretized solutions. Interestingly, when Eq.4.7 is used to estimate the routing time-step ( $\Delta t = 3.19$  s) for the non-discretized models instead of the original routing time step presented in the

QA, the solution produces many numerical spikes as can be seen in Fig.4.4.

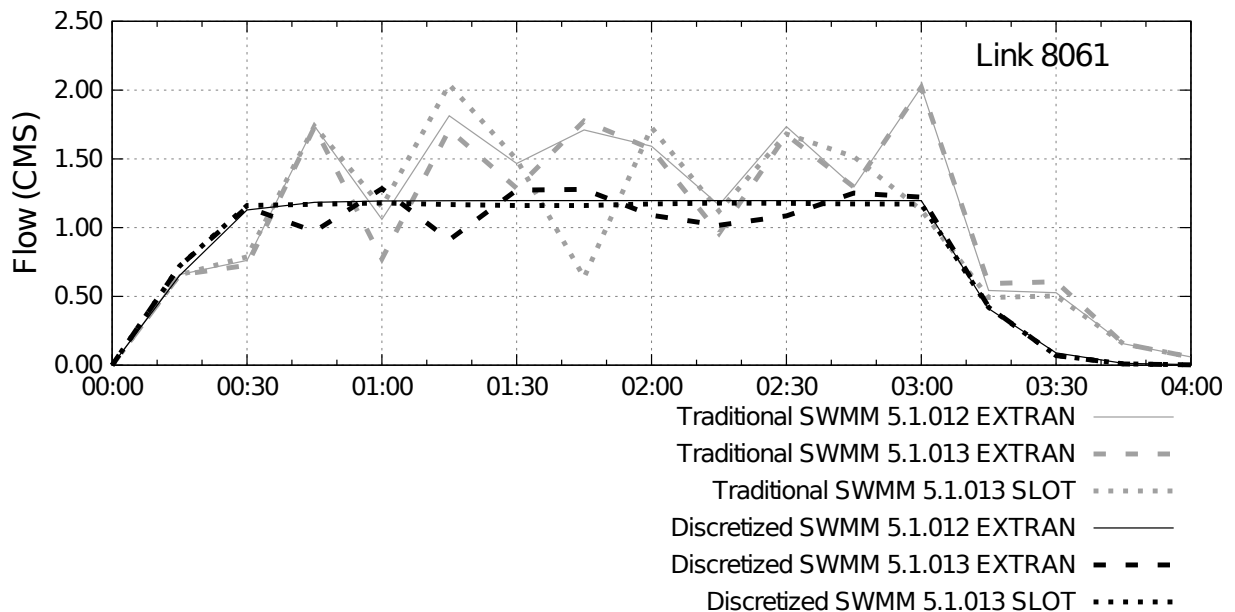
Figure 4.3 – Selected SWMM results for Example 6 for all modeling conditions tested.



Source: The Author.



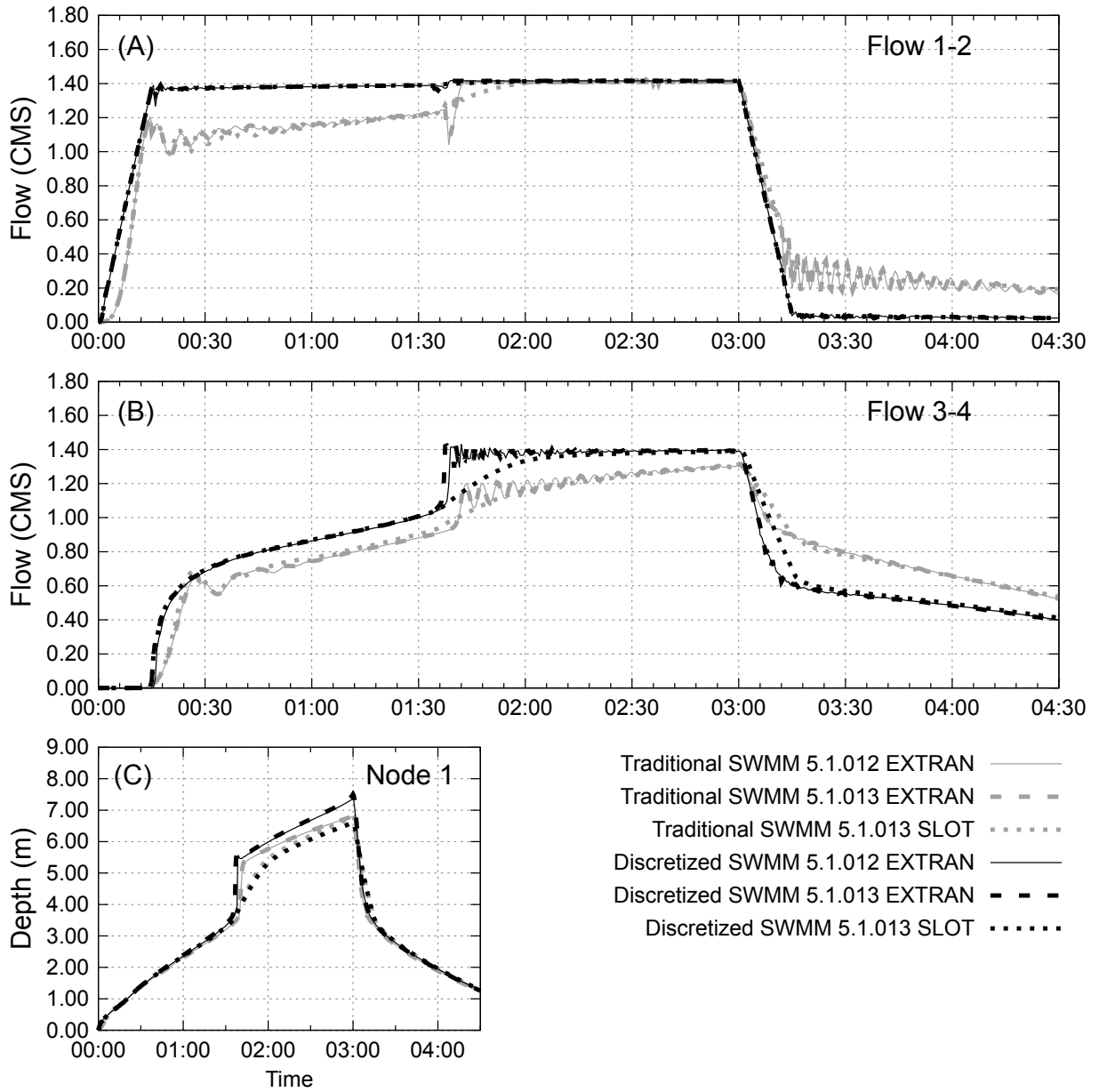
Figure 4.4 – Example 6 link 8061 results showing numerical instabilities when Eq.4.7 is used to estimate the routing time-step for both traditional and discretized approaches.



Source: The Author.

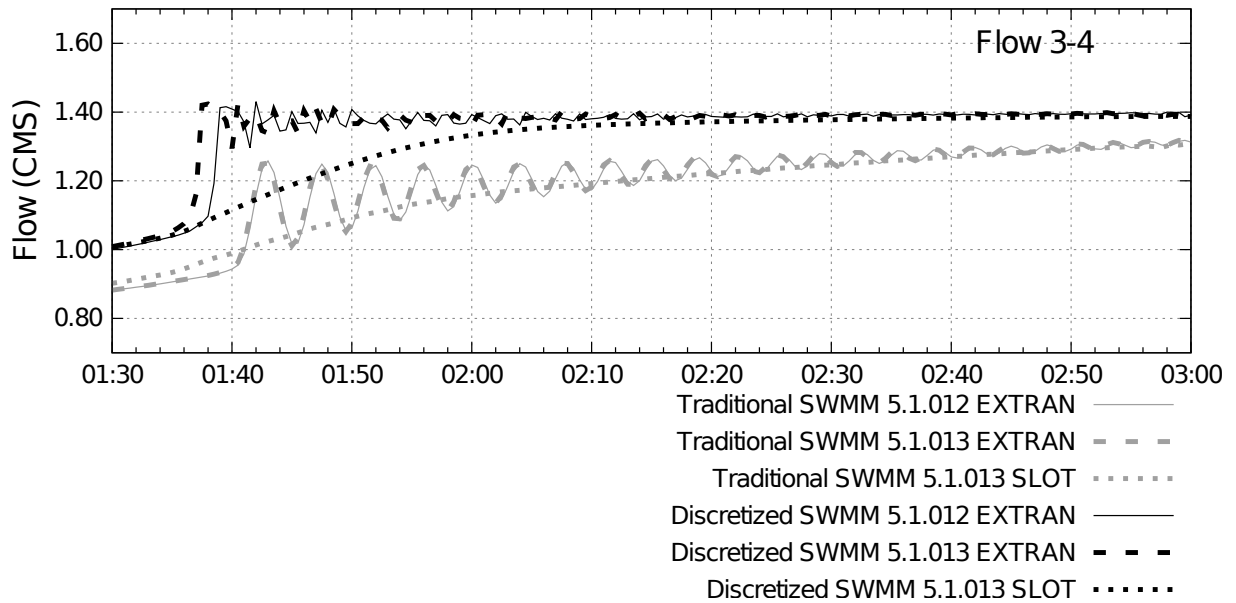
Fig. 4.5 shows the most relevant results generated by Example 10. In Fig. 4.5 (A), all discretized models diminished the oscillations presented in the traditional layouts. Yet in Fig. 4.5 (B), the SLOT algorithm produced results without apparent numerical instability for both traditional and discretized models, with the first showing smaller flow values than the latter. This situation is easier to visualize in Fig. 4.6, which shows Fig. 4.5 (B) in detail during the simulation period of 01:30-03:00. Still, some minor instabilities are found in the discretized models using EXTRAN pressurization algorithm but less than the oscillations found in the non-discretized models using EXTRAN pressurization algorithm. However, the nature of the instability seems to be different between them. In the non-discretized models it is periodic when in the discretized layouts it is more like a “noise”. Reducing the head convergence tolerance may reduce this noise in the discretized models. Furthermore, it is important to highlight that the discretized results have, in general, higher values of flow and water depth than the traditional ones. Lastly, Fig. 4.5 (C) shows that the selection of the surcharge method impairs directly in the water level in this example.

Figure 4.5 – Selected SWMM results for Example 10 indicating numerical oscillations in traditional modeling approaches.



Source: The Author.

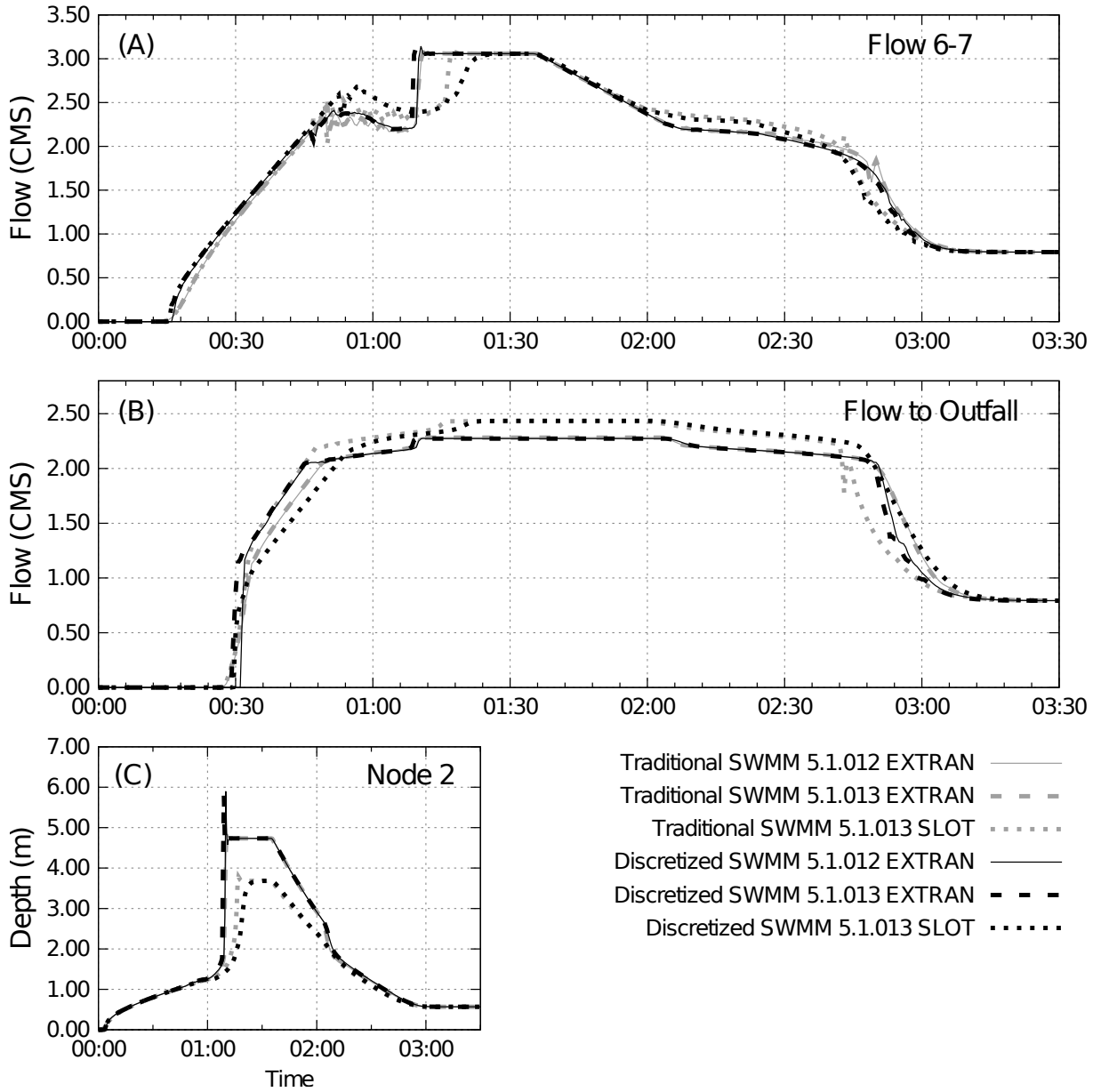
Figure 4.6 – Detail of the predicted flows between nodes 3 and 4 in Example 10.



Source: The Author.

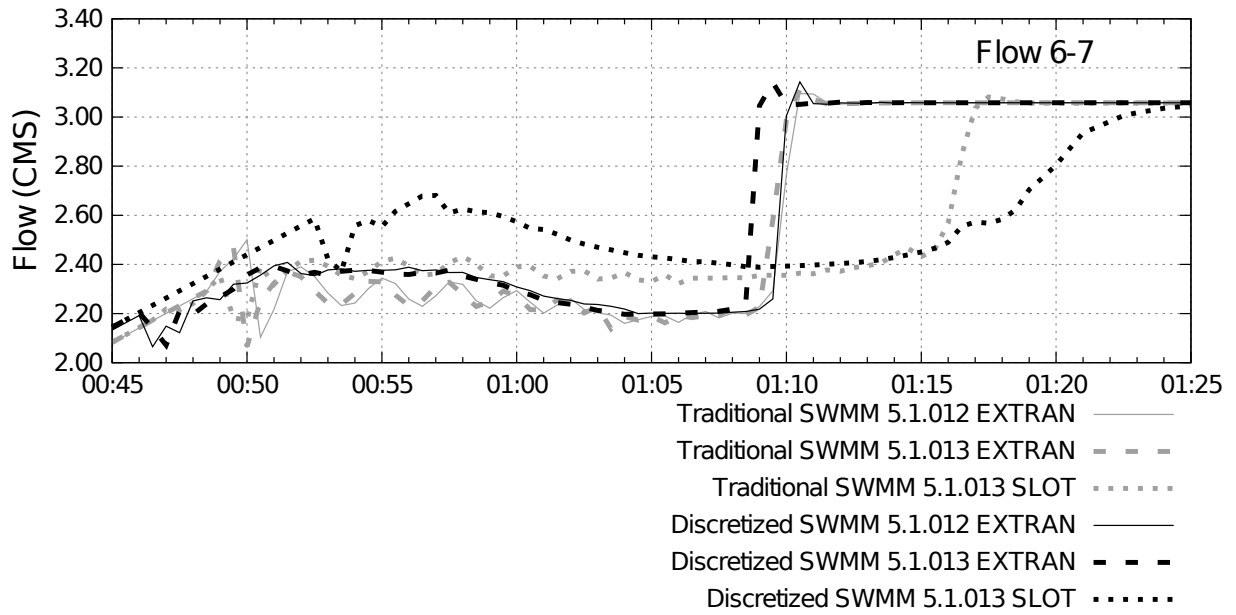
Fig. 4.7 shows the most pertinent results of Example 11. In Fig. 4.7 (A), it is possible to identify that all the non-discretized models results showed significant oscillations not observed on discretized layouts. Fig. 4.8 magnifies Fig. 4.7 (A) during the simulation period of 00:45-1:25 in order to elucidate this statement. Moreover, there are relevant differences between the EXTRAN and SLOT pressurization algorithm, mainly in the timing where the peak occurs. Fig. 4.7 (B) and (C) confirm that there are significant differences in the results obtained from these surcharge algorithms. The SLOT algorithm overestimates the flow (Fig. 4.7 (B)) and underestimates the water depth (Fig. 4.7 (C)) for both traditional and discretized layouts.

Figure 4.7 – Example 11 results.



Source: The Author.

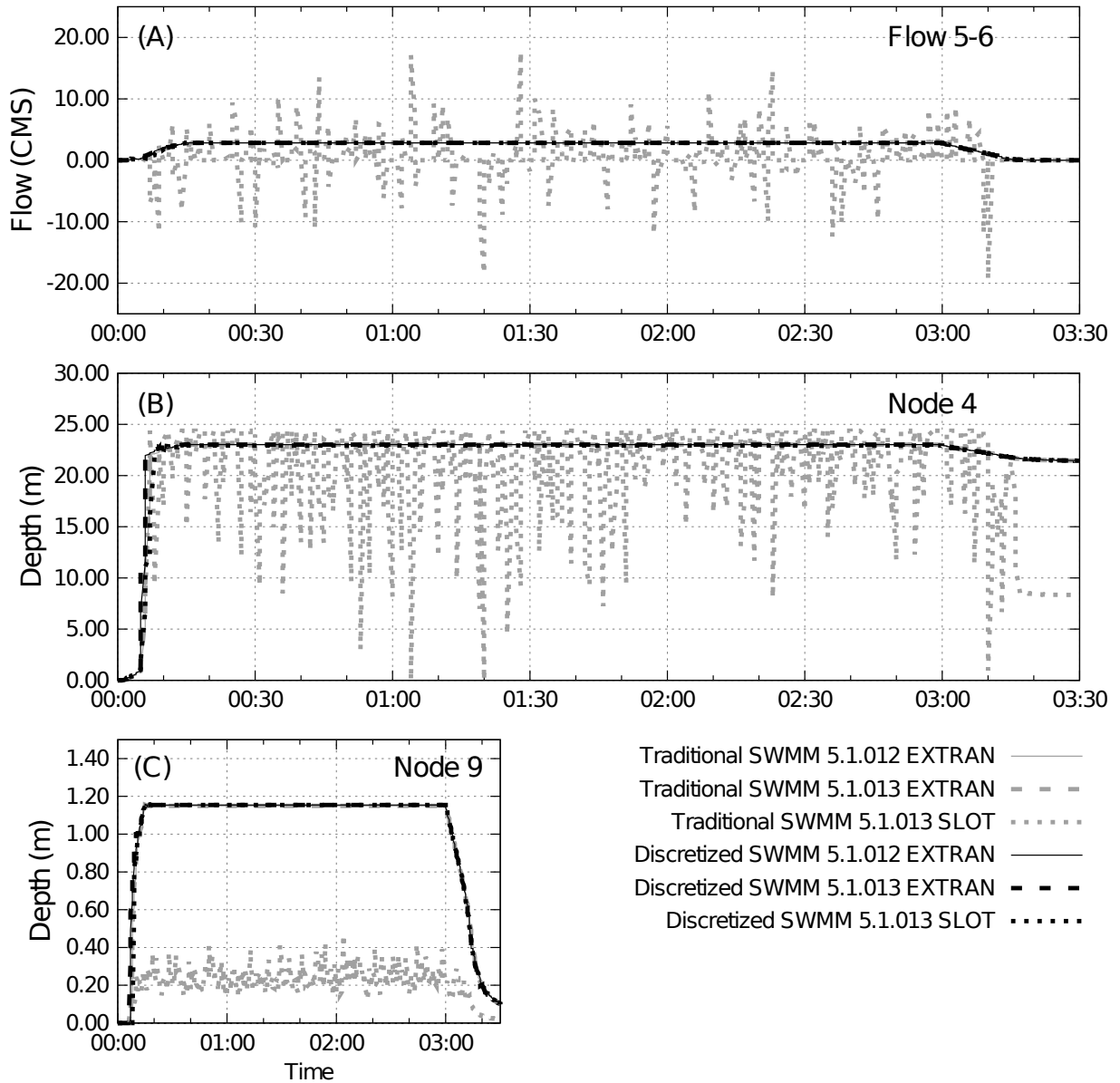
Figure 4.8 – Example 11 - Fig. 4.7 (A) in detail.



Source: The Author.

Example 12 simulates an inverted siphon and its results are presented in Fig. 4.9. In general, the results from both discretized and non-discretized models are alike, excepting the non-discretized model using the SLOT pressurization algorithm. When the system starts to receive inflow, all models have similar behavior, however, the non-discretized model with the SLOT pressurization algorithm becomes highly unstable in the moment that the water touches the siphon crown. Using Eq.4.7 to estimate routing time-step ( $\Delta t = 1.60$  s) for the link-node approach, the instability produced by SLOT pressurization algorithm was removed and the flow continuity error was reduced to 0.21%.

Figure 4.9 – Example 12 results showing instabilities using the non-discretized model with the SLOT pressurization algorithm.

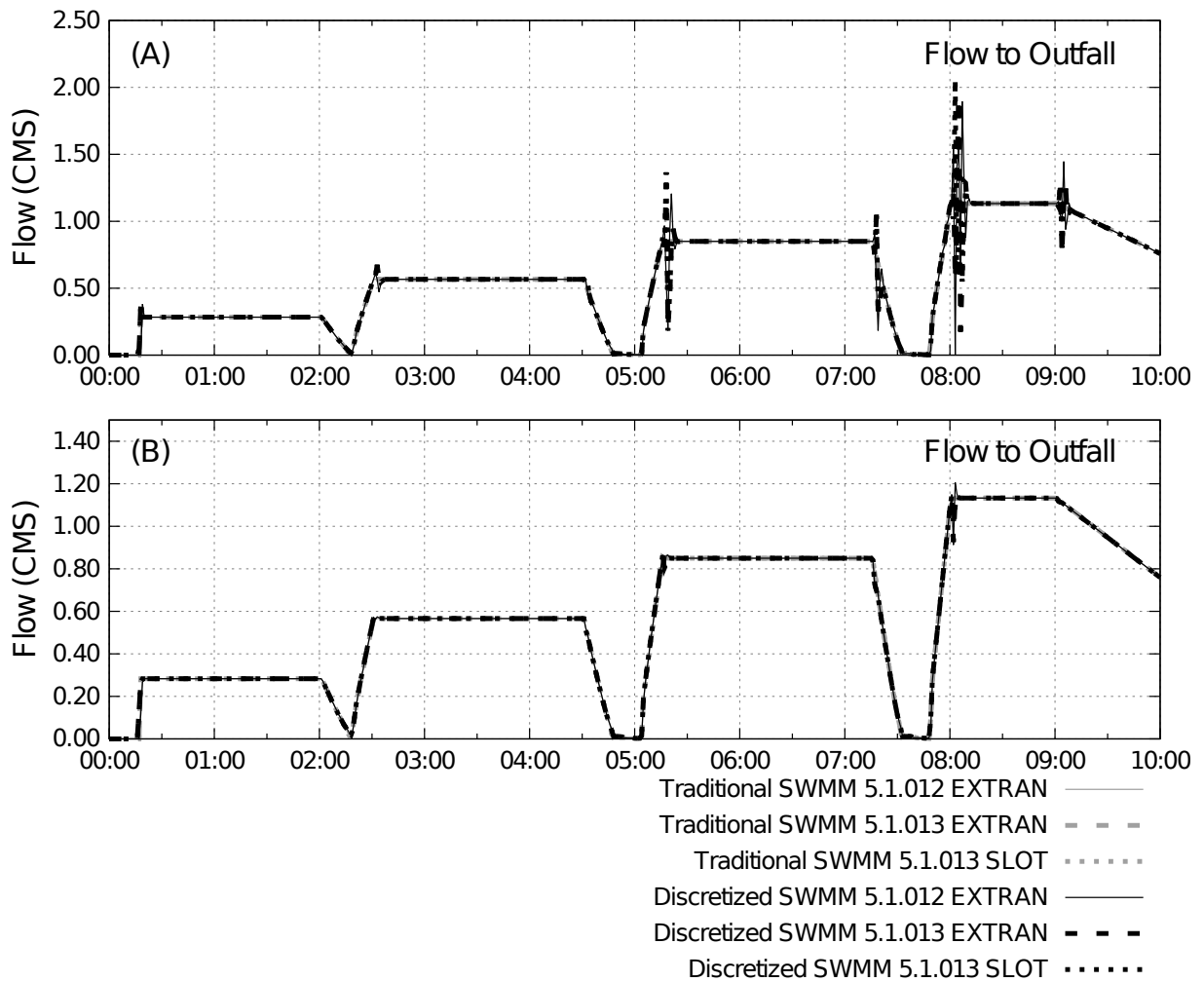


Source: The Author.

The results obtained in Example 13 were unsatisfactory for the discretized layouts (Fig. 4.10). Fig. 4.10 (A) shows that discretized models have numerical spikes in the solution that are not present in the non-discretized layouts. This example is very challenging to dynamic flow modeling since there are adverse slopes in the order of 3%, a situation hardly present in real-world cases. Dampening or ignoring the inertial terms of the St. Venant equations could be a good procedure to try to avoid these numerical spikes (USEPA, 2018). However, instead of dropping the inertial terms and, consequently, losing some accuracy, the strategy used was to reduce the head convergence tolerance. First, the head convergence tolerance was divided by 100 and

improved results were found but still insufficient. Then, the original head convergence tolerance was divided by  $10^6$  and the results had significant improvements, as can be seen in Fig. 4.10 (B). There are some numerical spikes around 08:00 but nothing compared to the ones presented using the original head convergence tolerance. Hence, the head convergence tolerance needs to be more stringent when ASD is added to the model since smaller  $\Delta t$  or  $\Delta x$  could led to truncation and rounding error.

Figure 4.10 – Example 13 results using the original head convergence tolerance (A) and the improvements achieved in terms of numerical stability when reducing the head convergence tolerance (B).



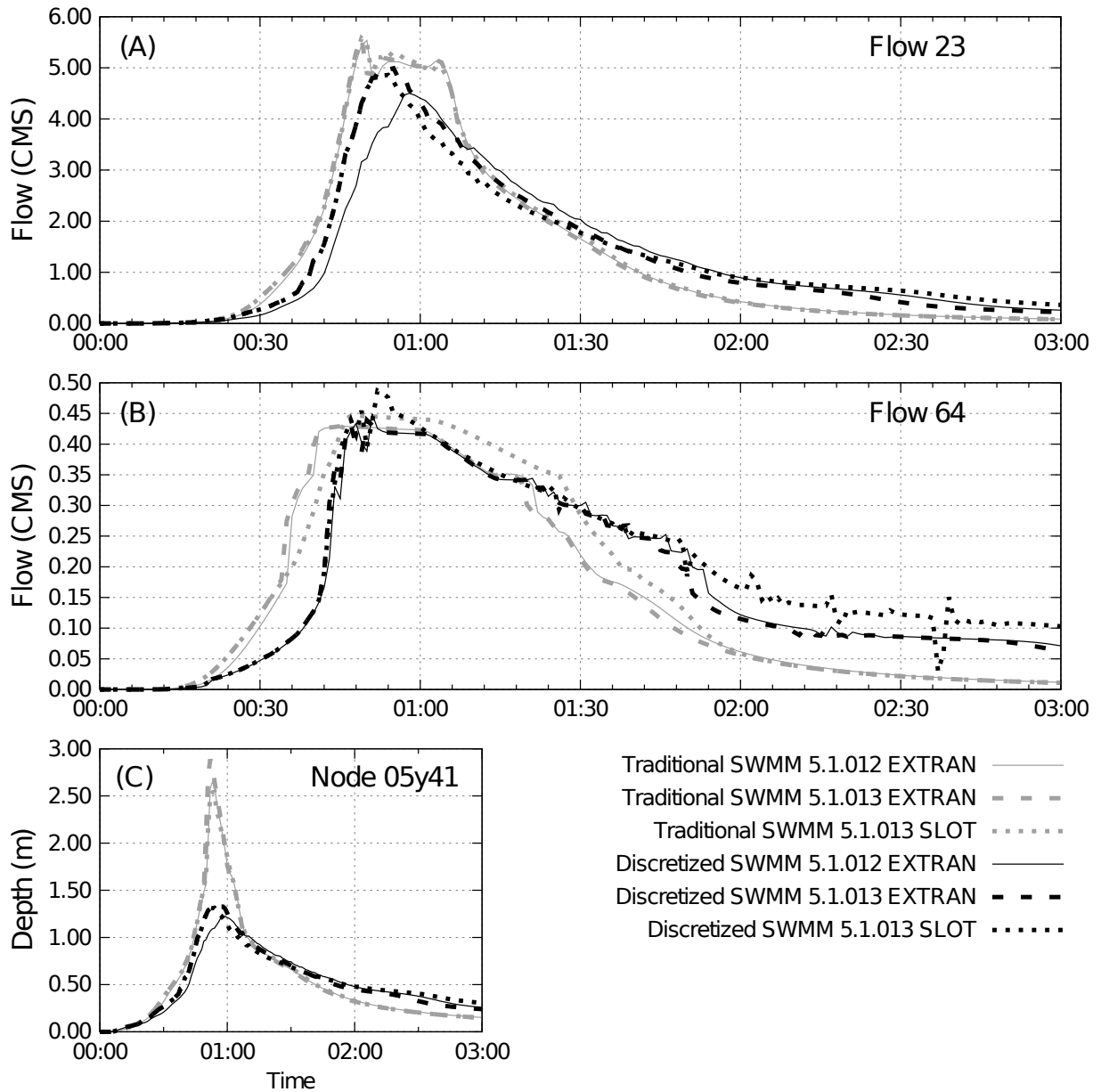
Source: The Author.

Example 14 results are demonstrated in Fig. 4.11. Fig. 4.11 (A) and (B) show that, in general, the water rise and decline are different between the discretized and non-discretized models. The first show a delay of water rise during the system watering and a longer recession curve during the system dewatering. The latter show the opposite, an advanced water rise during the system watering and a shorter recession curve during the system dewatering. Fig. 4.11 (C) shows water depth results allowing

to identify accentuated difference between discretized and non-discretized models. The discretized models show small water depth values while non-discretized show high ones. Probably these results are related to the wave produced when discretization is added to the model that is not captured by the SWMM traditional link-node approach (PACHALY; VASCONCELOS; ALLASIA; MINETTO, 2019). In the discretized models, the wave passes through several dummy nodes until it arrives at the downstream node, representing more accurately the wave. In non-discretized models, the water depth starts to rise at the next node when the link connecting two nodes starts to fill. This can speed up the system filling and, at the same time, it promotes more water storage specially within the nodes, increasing water depth values. The system used in this case has many nodes (>1000), amplifying this situation not so evident in the previous examples. However, due to the lack of field data it is not possible to guarantee which discretization best represented the real flow propagation. Moreover, in this example, EXTRAN 5.1.012 surcharged method results are different from those obtained by EXTRAN 5.1.013 and SLOT pressurization algorithm generated peaks that were not produced by EXTRAN surcharge methods.



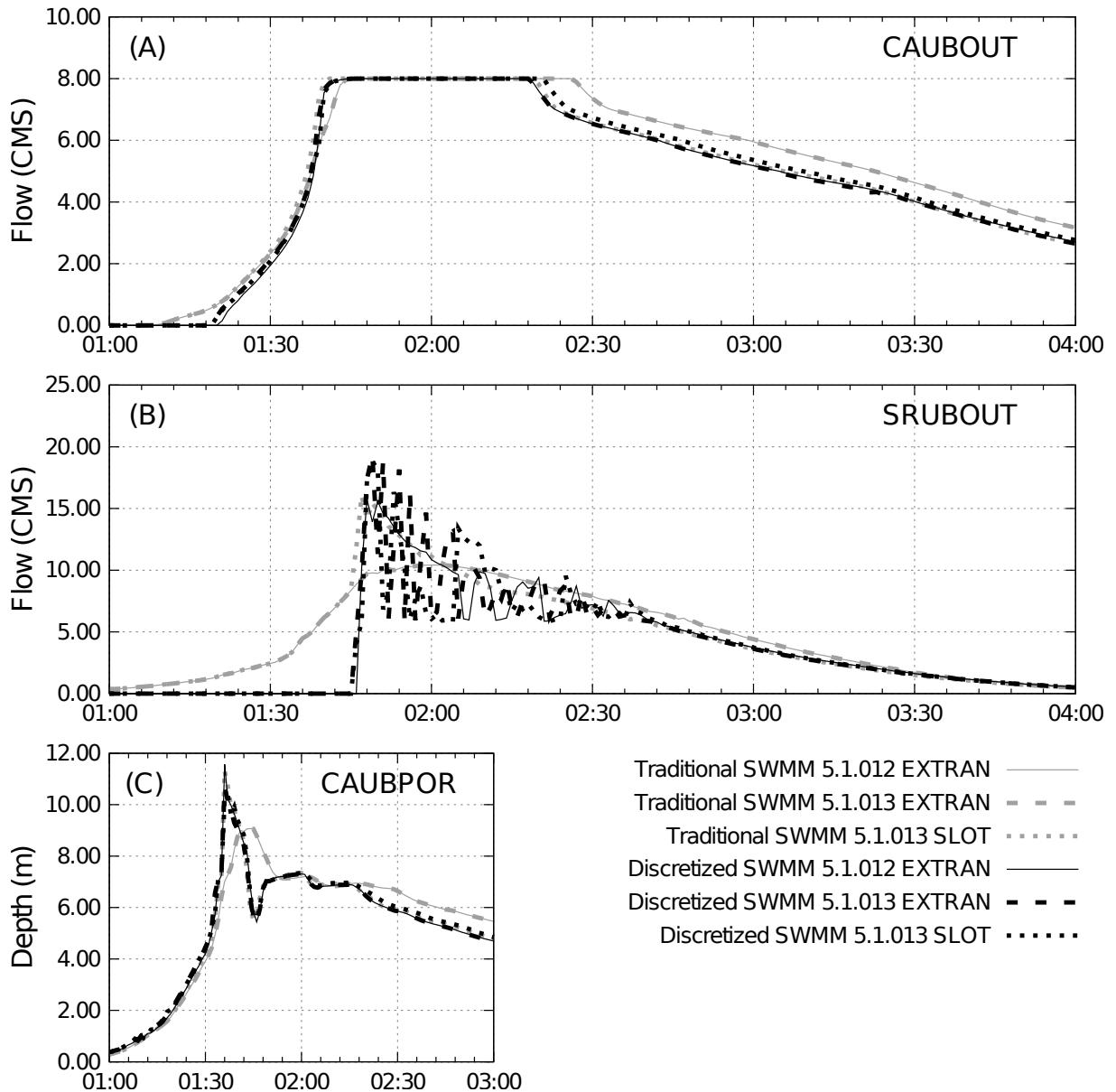
Figure 4.11 – Example 14 results.



Source: The Author.

Finally, in Example 15 the discretized models produced many numerical spikes. So, a reduction of two decimal places of the head convergence tolerance was performed and these spikes were, in general, diminished as can be seen in Fig. 4.12 (A) and (C). However, at links near outfalls (SRUBOUT), numerical spikes were still present. Ignoring the inertial terms of the St. Venant equations also did not bring improvements in this case. Considering the current results, there are differences in the system dewatering (Fig. 4.12 (A) and (C)) and there is a noteworthy difference in the timing of water arrival (Fig. 4.12 (B)). As this system also has many nodes, the reason for these differences can be the same explained at Example 14.

Figure 4.12 – Example 15 adjusting the head convergence tolerance.



Source: The Author.

### 4.3.3 Computational time

The computational time spent for each simulation was analyzed and Table 4.3 shows the results. As expected, the computational time spent to perform the simulations using discretized layouts is higher when compared to traditional layouts. When analyzing the discretized layouts, it is possible to assert that EXTRAN 5.1.0.12 surcharge method requires more time to perform a simulation than the others. Also, the SLOT surcharge method has a slight reduction of the computation time spent when compared to the EXTRAN 5.1.013 pressurization algorithm.

The computational time spent to perform a single simulation was more relevant in the cases that have higher number of elements (Example 14, 15, and 16). Examples 14 and 15, using the ASD, required a computational time in the order of minutes while the traditional layout required only 1 to 2 seconds to perform the simulation. In the Example 16 it was more remarkable, moving from a computational time in the order of minutes to hours. However, in this set of cases the SLOT surcharge method does not seem to reduce the computational time when compared to the EXTRAN surcharge method.

Table 4.3 – Computational time spent summary.

Ex.	Traditional Layout			Spatial Discretized Layout		
	EXTRAN (5.1.012)	EXTRAN (5.1.013)	SLOT (5.1.013)	EXTRAN (5.1.012)	EXTRAN (5.1.013)	SLOT (5.1.013)
1	<1	<1	<1	0:00:33	0:00:22	0:00:22
2	<1	<1	<1	0:00:30	0:00:23	0:00:22
3	0:00:01	<1	<1	0:00:35	0:00:28	0:00:28
4	<1	<1	<1	0:00:33	0:00:29	0:00:28
5	<1	<1	<1	0:00:38	0:00:27	0:00:26
6	0:00:01	<1	<1	0:00:31	0:00:27	0:00:25
7	<1	<1	<1	0:00:29	0:00:24	0:00:26
8	<1	<1	<1	0:00:01	0:00:01	0:00:01
9	<1	<1	<1	<1	<1	0:00:01
10	<1	<1	<1	0:00:04	0:00:02	0:00:03
11	<1	<1	<1	0:00:07	0:00:04	0:00:05
12	<1	<1	<1	0:00:01	<1	0:00:01
13	<1	0:00:01	<1	0:00:01	0:00:01	0:00:01
14	0:00:02	0:00:01	0:00:01	0:04:40	0:03:33	0:03:45
15	0:00:11	0:00:08	0:00:08	0:05:18	0:03:45	0:03:11
16	00:00:07	0:00:07	0:00:06	2:29:56	1:37:57	1:38:04

Source: The Author.

#### 4.4 CONCLUSIONS

This work presented simulation results of using ASD in SWMM links instead of the traditional link-node approach. Examples presented in Rossman (2006) were used with the purpose of analyzing the improvements achieved in terms of flow continuity error and numerical stability. A total of 96 simulations were performed, including the old surcharged method presented in SWMM version 5.1.012 and the new ones (EXTRAN and SLOT) presented in SWMM version 5.1.013.

The results demonstrated that the Vasconcelos, Eldayih et al. (2018) recommended routing time-step generates small flow continuity error for discretized models, showing less than  $\pm 1\%$  in all simulations. However, even though it improves significantly the SWMM modeling, when many intermediate nodes are added or when there are many source terms such as steep slopes, this recommendation may not be enough to maintain stability. The head convergence tolerance reduction appeared to be a solution for diminishing numerical spikes without altering the inertial terms of the St. Venant equations. However, in this work this criteria was not systematically studied and a deeper analysis ought to be performed in order to estimate a more precise value.

There were considerable differences when using ASD in SWMM. Some oscillations or fluctuations that may be due to numerical instabilities were reduced when using the ASD. In some simulations, significant results differences were present between the surcharge method presented in SWMM versions (5.1.012 & 5.1.013) and the SLOT method. The latter reduced significantly the oscillations when compared to the EXTRAN surcharged method. Moreover, significant computational time differences occurred when analyzing both traditional and discretized layouts. As expected, the discretized layouts required more computational time to perform a simulation due to additional nodes. Also, in some cases the SLOT surcharge method reduced the computational time when compared to the others surcharged methods.

Finally, based on the results presented in this work and in earlier contributions on unsteady flow SWMM modeling using artificial discretization, an appropriate selection of routing time step and ASD will result in significant improvements in hydraulic modeling. It is believed that the additional computational effort associated with ASD can be justified with the gain in terms of the model accuracy, particularly in highly dynamic conditions. In such cases, much care is needed in modeling setup, with the modeler encouraged to evaluate the effect of parameters such as head convergence tolerance and how inertial terms are accounted for in SWMM. Future research is also being developed to understand the ability of SWMM to represent other types of transient flows, and how to setup models to represent closed conduit as well fast transients.

## REFERENCES

- BUAHIN, C. A.; HORSBURGH, J. S. Advancing the Open Modeling Interface (OpenMI) for integrated water resources modeling. **Environmental Modelling and Software**, v. 108, April, p. 133–153, 2018. ISSN 13648152. DOI: 10.1016/j.envsoft.2018.07.015.
- BURGER, G.; SITZENFREI, R.; KLEIDORFER, M.; RAUCH, W. Parallel flow routing in SWMM 5. **Environmental Modelling and Software**, v. 53, p. 27–34, 2014. ISSN 13648152. DOI: 10.1016/j.envsoft.2013.11.002.
- CHAUDHRY, M. H. **Open Channel Flow**. Springer Science & Business Media, 2008. P. 523. ISBN 9780387301747. DOI: 10.1007/978-0-387-68648-6.
- CUNGE, J. A.; HOLLY, F. M.; VERWEY, A. **Practical aspects of computational river hydraulics**. London: Pitman publishing, 1980.
- DONGQUAN, Z.; JINING, C.; HAOZHENG, W.; QINGYUAN, T.; SHANGBING, C.; ZHENG, S. GIS-based urban rainfall-runoff modeling using an automatic catchment-discretization approach: A case study in Macau. **Environmental Earth Sciences**, v. 59, n. 2, p. 465–472, 2009. ISSN 18666280. DOI: 10.1007/s12665-009-0045-1.
- GHOSH, I.; HELLWEGER, F. L. Effects of Spatial Resolution in Urban Hydrologic Simulations. **Journal of Hydrologic Engineering**, v. 17, January, p. 129–137, 2012. ISSN 1084-0699. DOI: 10.1061/(ASCE)HE.1943-5584.0000405.
- GIRONÁS, J.; ROESNER, L. A.; ROSSMAN, L. A.; DAVIS, J. A new applications manual for the Storm Water Management Model (SWMM). **Environmental Modelling & Software**, v. 25, n. 6, p. 813–814, 2010. ISSN 13648152. DOI: 10.1016/j.envsoft.2009.11.009. Available at: <<http://linkinghub.elsevier.com/retrieve/pii/S1364815209002989>>.
- HODGES, B. R.; LIU, F.; ROWNEY, A. C. **A New Saint-Venant Solver for SWMM**. Springer International Publishing, 2019. v. 1, p. 582–586. ISBN 9783319998671. DOI: 10.1007/978-3-319-99867-1. Available at: <[http://dx.doi.org/10.1007/978-3-319-99867-1%7B%5C\\_%7D100](http://dx.doi.org/10.1007/978-3-319-99867-1%7B%5C_%7D100)>.
- HUBER, W.; ROESNER, L. The History and Evolution of the EPA SWMM" in "Fifty Years Of Watershed Modeling - Past, Present And Futur. **Engineering Conferences International Symposium Series**. <http://dc.engconfintl.org/watershed/29>, 2012. Available at: <<http://dc.engconfintl.org/cgi/viewcontent.cgi?article=1001&context=watershed>>.

KREBS, G.; KOKKONEN, T.; VALTANEN, M.; SETÄLÄ, H.; KOIVUSALO, H. Spatial resolution considerations for urban hydrological modelling. **Journal of Hydrology**, Elsevier B.V., v. 512, p. 482–497, 2014. ISSN 00221694. DOI: 10.1016/j.jhydrol.2014.03.013. Available at: <<http://dx.doi.org/10.1016/j.jhydrol.2014.03.013>>.

KULLER, M.; BACH, P. M.; RAMIREZ-LOVERING, D.; DELETIC, A. Framing water sensitive urban design as part of the urban form: A critical review of tools for best planning practice. **Environmental Modelling and Software**, Elsevier Ltd, v. 96, p. 265–282, 2017. ISSN 13648152. DOI: 10.1016/j.envsoft.2017.07.003. Available at: <<http://dx.doi.org/10.1016/j.envsoft.2017.07.003>>.

MULETA, M. K.; PH, D.; NICKLOW, J. W.; PH, D.; BEKELE, E. G.; PH, D. Sensitivity of a Distributed Watershed Simulation Model. **Journal of Hydrologic Engineering**, v. 0699, March, 2007. DOI: 10.1061/(ASCE)1084-0699(2007)12.

NIAZI, M.; NIETCH, C.; MAGHREBI, M.; JACKSON, N.; BENNETT, B. R.; TRYBY, M.; MASSOUDIEH, A. Storm Water Management Model: Performance Review and Gap Analysis. **Journal of Sustainable Water Built Environment**, v. 3, n. 2, 2017. DOI: 10.1061/JSWBAY.0000817..

OBROPTA, C. C.; KARDOS, J. S. Review of Urban Stormwater Quality Models: Deterministic, Stochastic, and Hybrid Approaches. **Journal of the American Water Resources Association**, v. 43, n. 6, p. 1508–1523, 2007. DOI: 10.1111/j.1752-1688.2007.00124.x.

PACHALY, R. L.; VASCONCELOS, J. G.; ALLASIA, D. G. P. **ReSWMM v0.1**. GitHub, 2018. Available at: <<https://github.com/ecotecnologias/ReSWMM>>.

PACHALY, R. L.; VASCONCELOS, J. G.; ALLASIA, D. G. P.; MINETTO, B. Field evaluation of discretized model setups for the Storm Water Management Model. **Journal of Water Management Modeling**, p. 1–16, 2019. ISSN 2292-6062. DOI: 10.14796/JWMM.C465.

PARK, S.; LEE, K.; PARK, I.; HA, S. Effect of the aggregation level of surface runoff fields and sewer network for a SWMM simulation. **Desalination**, v. 226, n. 1, p. 328–337, 2008. 10th IWA International Specialized Conference on Diffuse Pollution and Sustainable Basin Management. ISSN 0011-9164. DOI: <https://doi.org/10.1016/j.desal.2007.02.115>. Available at: <<http://www.sciencedirect.com/science/article/pii/S0011916408001653>>.

POPESCU, I. **Computational Hydraulics**. London: IWA Publishing, 2014. ISBN 9781780400440.

RIAÑO-BRICEÑO, G.; BARREIRO-GOMEZ, J.; RAMIREZ-JAIME, A.; QUIJANO, N.; OCAMPO-MARTINEZ, C. MatSWMM - An open-source toolbox for designing real-time control of urban drainage systems. **Environmental Modelling and Software**, v. 83, p. 143–154, 2016. ISSN 13648152. DOI: 10.1016/j.envsoft.2016.05.009.

RIDGWAY, K. E. Evaluating Force Main Transients with SWMM5 and Other Programs. v. 6062, p. 43–54, 2008. DOI: 10.14796/JWMM.R236-04..

ROESNER, L. A.; ALDRICH, J. A.; DICKINSON, R. E.; BARNWELL, T. O. **Storm Water Management Model User's Manual, Version 4: EXTRAN Addendum**. Athens: Environmental Research Laboratory, Office of Research e Development, US Environmental Protection Agency, 1988.

ROSSMAN, L. A. Storm Water Management Model Quality Assurance Report: Dynamic Wave Flow Routing. **Storm Water Management Model Quality Assurance Report**, EPA/600/R-06/097, p. 1–115, 2006.

\_\_\_\_\_. Storm Water Management Model User's Manual Version 5.1. **U.S. Environmental Protection Agency**, EPA/600/R-14/413b, p. 1–353, 2015.

\_\_\_\_\_. Storm Water Management Model Reference Manual Volume II – Hydraulics. **U.S. Environmental Protection Agency**, Mayo, p. 190, 2017.

STURM, T. **Open channel hydraulics**. New York: Mc Graw Hill, 2001.

SUN, N.; HALL, M.; HONG, B.; ZHANG, L. Impact of SWMM Catchment Discretization: Case Study in Syracuse, New York. **Journal of Hydrologic Engineering**, v. 19, n. 1, p. 223–234, 2014. ISSN 1084-0699. DOI: 10.1061/(ASCE)HE.1943-5584.0000777. Available at: <<http://ascelibrary.org/doi/10.1061/%7B%5C%7D28ASCE%7B%5C%7D29HE.1943-5584.0000777>>.

TRIPATHI, M. P.; RAGHUWANSHI, N. S.; RAO, G. P. Effect of watershed subdivision on simulation of water. **Hydrological Processes**, v. 1156, December 2005, p. 1137–1156, 2006. DOI: 10.1002/hyp.5927.

USEPA. **Storm Water Management Model (SWMM) ver. 5.0.13**. 2018. Available at: <<https://www.epa.gov/water-research/storm-water-management-model-swmm>>.

VASCONCELOS, J. G.; ELDAYIH, Y.; JAMILY, J. A. Evaluating Storm Water Management Model accuracy in mixed flows conditions. **Journal of Water Management Modeling**, p. 1–21, 2018.

WOOD, E. F.; SIVAPALAN, M.; BEVEN, K.; BAND, L. Effects of spatial variability and scale with implications to hydrologic modeling. **Journal of Hydrology**, v. 102, n. 1-4, p. 29–47, 1988. ISSN 00221694. DOI: 10.1016/0022-1694(88)90090-X.

WYLIE, E. B.; STREETER, V. L.; SUO, L. **Fluid transients in systems**. Prentice Hall Englewood Cliffs, NJ, 1993. v. 1.

ZAGHLOUL, N. A. SWMM model and level of discretization. **Journal of the Hydraulics Division**, ASCE, v. 107, n. 11, p. 1535–1545, 1981.



## 5 ARTICLE 3 - EVALUATING SWMM CAPABILITIES TO SIMULATE SLOW AND FAST TRANSIENTS OF STORMWATER SYSTEMS<sup>1</sup>

### Abstract

One of the most used 1D approaches to model drainage systems is the link-node technique employed by the Storm Water Management Model 5.1 (SWMM). This model is widely used in many hydrological and hydraulic applications, especially in urban drainage systems. Solving the full form of the St. Venant equations, this model represents well the unsteady flows usually present in stormwater systems. However, the representation of more dynamic flows, such as transient flows in sewers systems operating in pressurized flow conditions, this solution technique may be insufficient to properly represent these hydraulic phenomena. Adopting spatial discretization (i.g. more intermediate calculation points in-between nodes) is a solution often used by more contemporary transient solvers. The last SWMM version released (5.1.013) implemented the Preissmann Slot (SLOT) as surcharge method apart from the traditional EXTRAN solution. Although this pressurization algorithm has been extensively used since 1960, to date, no studies were found analyzing the applicability of SWMM to represent closed-pipe transient flows applying the Preissmann slot algorithm. Therefore, the present work investigates different simulation conditions to represent transients in SWMM, comparing it to analytical solutions of well-known cases of slow and fast transients. Various spatial and temporal discretizations along different pressurization algorithms were tested to verify the SWMM capacity of modeling these phenomena. Using an alternative implementation of the SLOT pressurization algorithm along with routing time-steps estimated by the Courant equation and artificial spatial discretization indicate that SWMM is capable to perform satisfactory transient simulations.

### 5.1 INTRODUCTION

The Stormwater Management Model (SWMM) is a dynamic hydrologic-hydraulic model (USEPA, 2018), result of a multi-decade development among many researchers, users, and collaborators (HUBER et al., 2012). The model is often used for planning, analysis, and design related to drainage systems, mainly in urban areas (ROSSMAN, 2015). Many studies have been performed using SWMM, such as runoff quality (TSIHRINTZIS et al., 1998; DI MODUGNO et al., 2015), quantity (DENAULT et al., 2006; MEIERDIERCKS et al., 2010; ABDUL-AZIZ et al., 2016), and, more recently, analysis of low impact development structures (QIN et al., 2013; ZAHMATKESH et al., 2015; CAMPISANO; CATANIA et al., 2017). Due to these variety of applications,

---

<sup>1</sup>Article submitted to **Urban Water Journal**.

SWMM is considered by researchers one of the most popular and successful models worldwide (OBROPTA et al., 2007; NIAZI et al., 2017; VASCONCELOS; ELDAYIH et al., 2018).

The SWMM formulation solves the complete form of the St. Venant equations (ROESNER et al., 1988; ROSSMAN, 2006, 2017), which are a set of two differential equations based on the conservation of mass and linear momentum (STURM, 2001). This formulation allows the representation of unsteady free surface flow in channels and pipes (STURM, 2001). Since these equations cannot be solved analytically, SWMM uses a link-node approach based on finite differences in order to compute head in each node or junction and the flow in each link or conduit (ROESNER et al., 1988; ROSSMAN, 2006, 2017). This solution technique is suitable for the great majority of SWMM applications because it can properly simulate the filling process of drainage systems.

Over the last years, many researchers have attempted to expand the uses of SWMM for more diverse situations, adapting and verifying the applicability for cases where SWMM was not originally conceived. For instance, representation of intermittent water distribution systems (CAMPISANO; GULLOTTA et al., 2019), mixed flows (VASCONCELOS; ELDAYIH et al., 2018), rapid inflows (PACHALY; VASCONCELOS; ALLASIA; MINETTO, 2019), or force main transients (RIDGWAY, 2008) are some of these recent new SWMM applications. In some cases, changing the source code is required in order to add or modify features (CHO et al., 2007) but in others, as shown by Pachaly, Vasconcelos, Allasia e Minetto (2019), just altering the conventional SWMM setup could lead to improvements in SWMM modeling.

All hydraulic systems are likely to experience operational issues such as equipment breakdowns, starting and shutting down operations, human errors, and others (THORLEY, 1991; WOOD, 2014). Transient flows, which are the intermediate-state flow between one steady-state and another steady-state (CHAUDHRY, 2013), occur and, as a consequence, significant changes in pressure and velocity, vibrations, reverse flows, and other situations are expected to arise (THORLEY, 1991). In some cases, such as a pump startup or a pipeline filling, these situations are expected and the hydraulic system is designed to withstand such transient flow conditions. However, in other cases, where this situation is not expected or planned, such as a pump failure, these situations may lead to unacceptable operational conditions, and even significant damage to systems. Some computer models attempt to represent such cases and assess the variations in pressure and flow rates. However, it is unknown if a model such as SWMM can be used to represent key closed-pipe transient flow conditions that may occur in storm and sewer systems.

In this context, the present work aims to evaluate the accuracy and potential limitations of the current version of SWMM to represent three well-known cases of

transient flows through a comparison with available analytical solutions. The first case analyzed is a type of the slow transient characterized by inertial oscillations in a surge tank, resulting from a sudden valve maneuver presented in Parmakian (1963). The second case is also a slow transient corresponding to a pipeline flow startup presented in Wylie et al. (1993). And the last one is a type of fast transient, resulting from an instantaneous valve closure at the end of a pipeline, as presented in Wylie et al. (1993). These flow conditions are tested with the original EXTRAN pressurization algorithm in SWMM, and with the newly implemented surcharge algorithm based on the Preissmann Slot (PREISSMANN, 1961; USEPA, 2018). These three transient flows were also modeled applying varying spatial and temporal discretizations to determine the most appropriate modeling approach for these types of transient flows.

## 5.2 METHODS

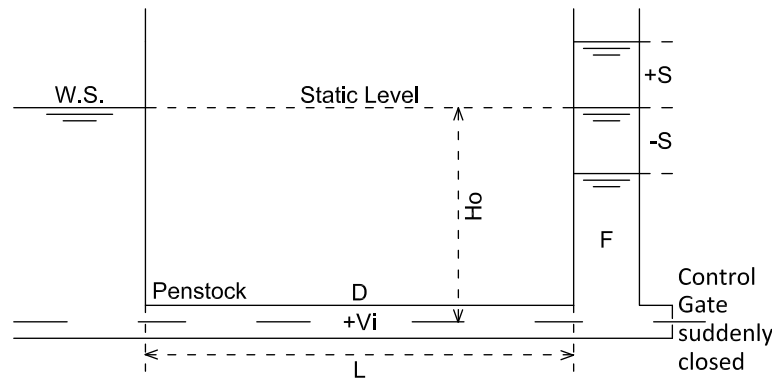
### 5.2.1 Analytical solutions

The St. Venant equations are too complex to be solved by an analytical closed-form solution, requiring approximate solutions using numerical techniques (STURM, 2001; CHAUDHRY, 2013). In specific situations and considering some simplifications such as neglecting or linearizing the nonlinear terms, analytical solutions are available but cannot be used to analyze large systems or systems with complex boundary conditions (CHAUDHRY, 2013). Even though analytical solutions may have considerable simplifications, they may be a useful tool to assess model accuracy. In the context of this work, three cases of typical slow and fast transients were selected to evaluate the SWMM capacity to represent these phenomena.

#### 5.2.1.1 Case 1: Surge tank

Surge tanks are devices often used at power or pumping plants to control pressure changes resulting from rapid changes in the flow such as gate openings or closures (PARMAKIAN, 1963; NOVAK et al., 2010). The device, represented by Figure 5.1, corresponds to a vertical reservoir, usually open to the atmosphere, attached by its base to a pipe (ZÁRUBA, 1993; CHAUDHRY, 2013). The surge tank purpose is to reduce the amplitude of pressure fluctuations by reflecting the incoming pressure waves or by storing or providing water (CHAUDHRY, 2013). In other words, it converts the kinetic energy generated by operations into potential energy, reducing the rate of change of flow and the waterhammer effect in the pipe (PARMAKIAN, 1963; ZÁRUBA, 1993).

Figure 5.1 – Surge tank.



Source: Adapted from Parmakian (1963).

Even though there are recent studies (e.g. Kim (2010), Zhang et al. (2012), Kendir et al. (2013), Lan Lan Guo et al. (2013) e Mohamed. Yossef (2015), and other) showing different approaches to numerically solve the water level variations in a surge tank due to a rapid gate closure, a classical analytical solution is available (PARMAKIAN, 1963; CHAUDHRY, 2013). Considering the system presented in Figure 5.1 and the following assumptions:

1. The tunnel walls are rigid.
2. The water is incompressible.
3. The inertia of the water in the surge tank is negligible compared to that of the water in the tunnel.
4. The head losses in the system during the transient state may be computed by using the steady-state equations for the corresponding flow velocities.

There are no spatial derivatives and the resulting equations are ordinary differential equations instead of partial differential equations. Thus, the flow variables are only functions of time (CHAUDHRY, 2013).

According to Parmakian (1963), the mass of water which is moving in the penstock is  $LAw/g$  prior to the gate closure and  $wAS$  after the gate closure. Where  $L$  denotes conduit length;  $A$  denotes conduit area;  $w$  denotes specific weight of water;  $g$  denotes gravity; and  $S$  denotes the water level in surge tank. Therefore, the deceleration of the water column (Eq. 5.1) in the penstock can be expressed as:

$$-\frac{dVi}{dt} = \frac{gS}{L}, \quad (5.1)$$

where  $V_i$  denotes the velocity in the penstock. The continuity condition states that the flow of water into the surge tank right after the gate closure is the same leaving the penstock, which is:

$$\frac{dS}{dt} = \frac{AV_i}{F}, \quad (5.2)$$

where  $F$  denotes the cross-section area of surge tank. Considering the boundary conditions as  $t = 0$ ,  $S = 0$ , and  $dS/dt = Q_o/F$ , it is possible to solve Eq. 5.1 and 5.2 simultaneously for  $S$ :

$$S(t) = \frac{Q_o}{F} \sqrt{\frac{FL}{Ag}} \sin \left( \sqrt{\frac{Ag}{FL}} t \right), \quad (5.3)$$

where  $Q_o$  denotes the initial flow in the penstock. From Eq. 5.3, it is possible to obtain the maximum upsurge (Eq. 5.4) and the time required to reach the maximum upsurge (Eq. 5.5):

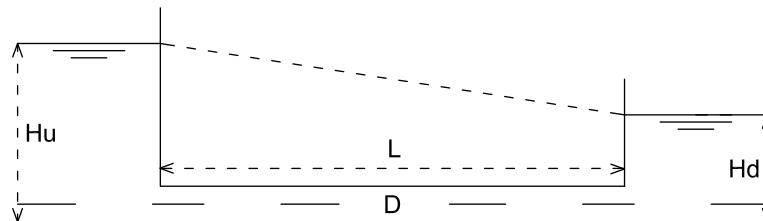
$$S_{max} = \frac{Q_o}{F} \sqrt{\frac{FL}{Ag}}, \quad (5.4)$$

$$T = \frac{\pi}{2} \sqrt{\frac{FL}{Ag}}. \quad (5.5)$$

### 5.2.1.2 Case 2: Pipeline flow startup

The flow startup in a transmission main is a typical slow transient flow condition that occurs when pumps are initiated or when a pressure gradient is created by the opening of a valve. Considering the system shown in Figure 5.2, it is possible to find an analytical solution when solving the pipe flow startup using the rigid water column theory (WATTERS, 1979).

Figure 5.2 – Pipeline flow startup.



Source: The Author.

This theory can be considered as an intermediate approach between the quasi-

steady and the waterhammer approaches (JUNG et al., 2017). The flow is updated at each time step using an ordinary differential equation (ODE) based on a momentum balance in a rigid column represented by the pressurized portion of the flow (WYLIE et al., 1993). In the case of Figure 5.2, for a horizontal constant-diameter pipe and the  $f$ -value in unsteady flow considered the same as for a steady at a velocity equal to the instantaneous value and neglecting the local head losses (WATTERS, 1979), Eq. 5.6 is used to update the flow at each time step:

$$\frac{dQ}{dt} = \frac{gA}{L} \left( \Delta H - \left( f \frac{L}{D} \frac{1}{2gA^2} \right) Q^2 \right), \quad (5.6)$$

where  $Q$  denotes flow;  $V$  denotes velocity;  $g$  denotes gravity;  $A$  denotes cross-sectional area;  $L$  denotes pipe length;  $D$  denotes pipe diameter;  $\Delta H$  denotes the difference between upstream and downstream reservoir; and  $f$  denotes the friction factor.

$$Q(t) = \frac{\sqrt{2}A\sqrt{D}\sqrt{g}\sqrt{H}\tanh\left(\frac{\sqrt{f}\sqrt{g}\sqrt{H}t}{\sqrt{2}\sqrt{D}\sqrt{L}}\right)}{\sqrt{f}\sqrt{L}} \quad (5.7)$$

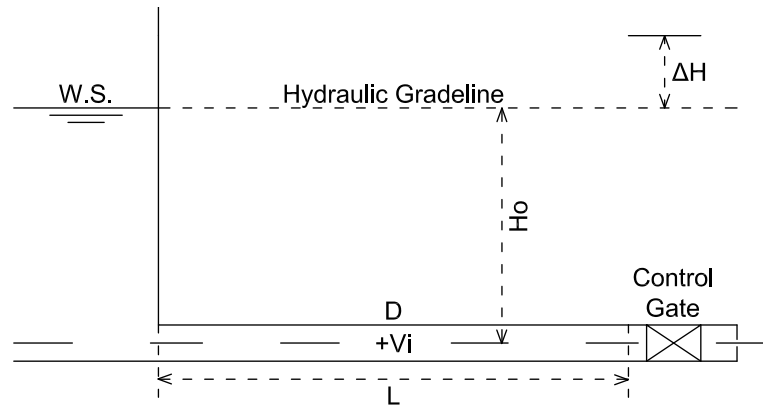
With Eq. 5.7, it is possible to solve the transient occurring in this system analytically. The flow in the steady-state occurring after the filling process can be determined using the Darcy-Weisbach formula (Eq. 5.8):

$$\Delta H = f \frac{L}{D} \frac{Q^2}{2gA^2}. \quad (5.8)$$

### 5.2.1.3 Case 3: Instantaneous valve closure transient

Figure 5.3 shows a typical case of a transient caused by an instantaneous valve closure at a downstream control gate. Neglecting friction, minor losses and considering an instantaneous closing movement, when the valve is closed ( $V_i = 0$ ), a pressure wave of magnitude  $\Delta H$  will be produced at the lower end of the pipe and it will travel upstream at some sonic wavespeed (PARMAKIAN, 1963; WYLIE et al., 1993; CHAUDHRY, 2013).

Figure 5.3 – Instantaneous valve closure.



Source: Adapted from Wylie et al. (1993).

The Joukowski Equation (JOUKOWSKI, 1904) (Eq. 5.9), also known as the fundamental equation of waterhammer, describes the change in flow related to a change in head due to an instantaneous valve closure (WYLIE et al., 1993; GHIDAOUI et al., 2005):

$$\Delta H = \pm \frac{a}{g} \Delta V, \quad (5.9)$$

where  $\Delta H$  denotes increment of head change;  $a$  denotes wave celerity;  $g$  denotes gravity; and  $\Delta V$  denotes the increment of flow velocity. The plus sign is used for waves traveling downstream and the minus sign for wave traveling upstream (WYLIE et al., 1993). This equation states that the magnitude of the pressure wave is proportional to the change in the water velocity and to the speed of propagation of the pressure wave (PARMAKIAN, 1963).

However, the wavespeed has not been determined. Considering a pressurized flow in a very thick-walled pipe, the wavespeed can be determined by:

$$a = \sqrt{\frac{K}{\rho}} \quad (5.10)$$

where  $K$  denotes the bulk modulus of elasticity of the fluid and  $\rho$  denotes the mass density of the fluid. For open-channel flows, the celerity can be estimated using Eq. 5.11:

$$a = \sqrt{g \frac{A}{B}} \quad (5.11)$$

where  $A$  denotes area; and  $B$  denotes free surface width.

It is important to point out that the pressure wave caused by the valve closure can have its period determined based on pipe length and celerity using Eq. 5.12:

$$T = \frac{4L}{a} \quad (5.12)$$

where  $T$  denotes the wave period and  $L$  the pipe length.

### 5.2.2 SWMM formulation

SWMM uses the St. Venant equations to solve the unsteady free surface flow through a network of links and nodes (USEPA, 2018). These equations form a system of partial differential equations which represent the unsteady open-channel flows (STURM, 2001) based on the conservation of mass (Eq. 5.13) and linear momentum (Eq. 5.14):

$$\frac{\partial A}{\partial t} + \frac{\partial Q}{\partial x} = 0 \quad (5.13)$$

$$\frac{\partial Q}{\partial t} + \frac{\partial(Q^2/A)}{\partial x} + gA \frac{\partial H}{\partial x} + gAS_f + gAh_L = 0 \quad (5.14)$$

where  $A$  denotes cross-sectional area;  $t$  denotes time;  $Q$  denotes flow rate;  $x$  denotes distance;  $H$  denotes the hydraulic head of water in the conduit;  $g$  denotes gravity;  $h_L$  denotes the local energy loss per unit length of conduit; and  $S_f$  denotes the friction slope, which is implemented with the Manning equation (ROSSMAN, 2006).

SWMM solves these equations using a link-node approach, computing the flow at each link and the head in each node (ROSSMAN, 2006; ROESNER et al., 1988). In order to perform this, SWMM 5.1 converts Eq. 5.13 and Eq. 5.14 into an explicit set of finite difference formulas and then solve it using a method of successive approximations with under relaxation (ROSSMAN, 2006).

In situations where the water level at a node exceeds the crown of the highest conduit connected to it, the surcharge condition occurs (ROSSMAN, 2006, 2017). SWMM 5.1.013 can handle the surcharge condition using two methods: EXTRAN or SLOT (USEPA, 2018). The EXTRAN pressurization algorithm uses an additional formulation when the flow depth is greater than 96% of link diameter (USEPA, 2018). This formulation is required to update heads since the surface contributed by any closed conduits is zero when surcharge condition occurs (ROESNER et al., 1988; ROSSMAN, 2006). So, Eq. 5.15 is used to enforce the flow continuity condition:

$$\Delta H = \frac{-\sum Q}{\sum \partial Q / \partial H} \quad (5.15)$$

where  $\Delta H$  is the adjustment to the node's head that must be made to achieve a flow balance (ROSSMAN, 2017). Therefore, EXTRAN applies another set of equations (Eq. 5.16 and Eq. 5.17) when a conduit flow is pressurized:



$$Q = A_f V \quad (5.16)$$

$$\frac{dQ}{dt} = \left( \frac{gA}{L} \right) \left( \frac{\Delta H}{1 + \Delta Q_{friction} + \Delta Q_{losses}} \right) \quad (5.17)$$

The SLOT pressurization algorithm is based on the Preissmann Slot (USEPA, 2018). This technique uses a narrow and vertical slot over each pipe, eliminating the need to switch equations and allowing the use of the St. Venant equations (CUNGE et al., 1980) throughout the entire simulation. SWMM uses a formula (Eq. 5.18) based on the Sjöberg equation (YEN, 1986; USEPA, 2018) to set the slot width when the flow depth is greater than 98.5% of link diameter (USEPA, 2018):

$$B = D * 0.5423 * \exp(-(y/D)^{2.4}) \quad (5.18)$$

where  $B$  denotes the slot width;  $D$  denotes the link diameter; and  $y$  the flow depth. For ratio of  $y/D$  greater than 1.78, the slot width is equal to 1% of conduit diameter.

The Preissmann Slot method has two deficiencies: it cannot sustain negative pressures and spurious numerical oscillations are present when the flow switches to pressurized flow (MALEKPOUR et al., 2015). Even though there are some works that remedied the negative pressure issues (VASCONCELOS; WRIGHT; ROE, 2006a; KERGER et al., 2011), the spurious numerical oscillations are still a current concern. Some studies (TRAJKOVIC et al., 1999; CAPART et al., 1997) showed that reducing the acoustic wave speed by increasing the slot width is a good approach to control the numerical oscillations but, on the other hand, wider slots can create unrealistic storage that can have considerable consequences in the simulation (MALEKPOUR et al., 2015).

The SWMM source code was altered in order to verify potential improvements of removing the Sjöberg equation and decreasing the slot width with a method based on celerity. Since within the SLOT method is valid the open-channel flow assumption, the celerity can be estimated using Eq. 5.11. Re-arranging this equation for  $B$  (Eq. 5.19) gives the free surface or slot width based on a specific celerity for a known link diameter.

$$B = g \frac{A}{a^2}. \quad (5.19)$$

In this work, three values of celerity were used to set the slot width: 250 m/s, 500 m/s and 1000 m/s. These celerity values represent the range of wavespeeds usually present in stormwater systems. If there is no gas inside a pipe (air, methane), the celerity may be close to 1000 m/s. However, usually there is gas in stormwater pipes, therefore, celerity values of 250 m/s or 500 m/s come as alternatives to simulate flow conditions in such scenarios (WYLIE et al., 1993). In the case of a 1-m diameter

link, the SWMM SLOT implementation has a celerity of of 27.75 m/s for the 0.01 m slot width. The proposed SLOT implementation based on a celerity value of 250 m/s resulted in  $1.23 \times 10^{-4}$  m slot width or 1.23% of the original implementation. The 500 m/s SLOT implementation resulted in  $3.08 \times 10^{-5}$  m slot width or 0.31% of the original implementation. The last SLOT implementation (1000 m/s) resulted in  $7.70 \times 10^{-6}$  m slot width or 0.08% of the original implementation.

In order to produce the most theoretically accurate results, the dynamic wave was selected as routing model keeping all inertial terms under all conditions. The normal flow criteria chosen was the slope and Froude number, and the main equation selected to compute friction losses during pressurized flow was Hazen-Williams. Also, since the SWMM solution method uses a convergence tolerance and a maximum number of trials to verify if the solution converged, these values were changed, respectively, from  $5 \times 10^{-3}$  to  $5 \times 10^{-6}$  and from 8 to 20 in order to improve the simulations.

#### 5.2.2.1 Spatial discretization

The routing algorithm used by SWMM does not employ discretization in-between two adjacent nodes. In some highly dynamic situations, such as pressurization of conduits, entrapment of air pockets within the pipes, pressure surges, pipe-filling bores and even waterhammers (ZHOU et al., 2002; GUIZANI et al., 2006), artificial spatial discretization along with the full form of the St. Venant equations brings significant improvements in SWMM results (RIDGWAY; KUMPULA, 2007; VASCONCELOS; ELDAYIH et al., 2018; PACHALY; VASCONCELOS; ALLASIA; MINETTO, 2019).

Artificial spatial discretization is conceived by placing dummy nodes between actual nodes, forcing SWMM to solve the St. Venant equations in the same way that more contemporary unsteady flow solvers solve. However, adding more nodes may have a significant impact in the computational time to perform a single simulation since there are more nodes and links to be solved at each time-step (PACHALY; VASCONCELOS; ALLASIA; MINETTO, 2019) and a smaller routing time-step may be required to maintain the stability and flow continuity (VASCONCELOS; ELDAYIH et al., 2018).

In this work, the arrangement of the dummy nodes used a ratio between the link length ( $L$ ) and spatial discretization ( $\Delta x$ ). Thus, besides the SWMM traditional link-node approach ( $L/\Delta x = 1$ ), two ratios were used:  $L/\Delta x = 30$  and  $L/\Delta x = 120$ . In order to reduce the storage effects caused by the artificial spatial discretization, the minimum nodal surface area (MNSA), which is the surface area available when the surface area of the node's connecting links fell below it, was changed from

the default value of 1.167 m<sup>2</sup> (US standard manhole area) to a smaller value of 1 × 10<sup>-6</sup> m<sup>2</sup>. Moreover, since the disposal of dummy nodes is a time-demanding task, the application/add-on called ReSWMM (PACHALY; VASCONCELOS; ALLASIA, 2018) was used.

### 5.2.2.2 Temporal discretization

In this study, two formulas were used to estimate the routing-time step. The first one is the EXTRAN routing-time step recommendation proposed by Roesner et al. (1988). The original equation is referred as Eq. 5.20a. Also, an improvement of this formula was proposed by Vasconcelos, Eldayih et al. (2018) when mixed flows are expected, considering only 10% of Eq. 5.20a, referred as Eq. 5.20b.

$$\Delta t = \frac{\Delta x}{\sqrt{gD}}, \quad (5.20a)$$

$$\Delta t = 0.1 \frac{\Delta x}{\sqrt{gD}}, \quad (5.20b)$$

where  $\Delta t$  denotes recommended routing time-step;  $\Delta x$  denotes size of the spatial discretization (or link length); and  $D$  denotes link diameter.

The other formula used was the Courant-Friedrich-Lewy (CFL) stability condition. This condition states that the routing time-step depends upon the spatial discretization  $\Delta x$  and celerity ( $a$ ) to maintain the stability in a finite-difference scheme (CHAUDHRY, 2008):

$$\Delta t = Cr \frac{\Delta x}{a}. \quad (5.21)$$

The  $Cr$  term in Eq. 5.21 is called the Courant number and has its maximum where  $a$  is maximum. All the calculation should have a local Courant number lesser than the maximum to avoid numerical instabilities. Therefore, the  $Cr$  term should be less than 1 throughout the simulation (CHAUDHRY, 2008).

This formula has an advantage when compared to Eq. 5.20 because it uses the flow characteristics to estimate the routing time-step instead of the system geometry. In this work, three variations of this formula were tested:

$$\Delta t = 0.1 \frac{\Delta x}{a}, \quad (5.22a)$$

$$\Delta t = 0.9 \frac{\Delta x}{a}, \quad (5.22b)$$

$$\Delta t = 3 \frac{\Delta x}{a}. \quad (5.22c)$$

These values were selected in order to provide a deeper analysis of the SWMM

behavior considering routing time-steps close to the Courant number and far from it. Furthermore, the option of variable time-steps was disabled in order to keep the routing time-step value fixed throughout the entire simulation.

### 5.2.3 Model performance evaluation

The metric selected to evaluate the simulations performance is the  $L^2$  norm, also known as Euclidean norm. This metric measures the distance between two points or vectors. In this work, it evaluates the distance between the simulated and analytical values. Many studies in computational fluid dynamics (CFD) (FALCÃO DE CAMPOS et al., 2006; MEYERS et al., 2007; MATHEOU et al., 2008; MARCHI, 2010) employ this metric.

Equation 5.23 describes the  $L^2$  norm:

$$L^2 = \frac{1}{N} \sqrt{\sum (x^{sim} - x^{anl})^2} \quad (5.23)$$

where  $N$  denotes the number of data points;  $x^{sim}$  denotes the simulated data series and  $x^{anl}$  denotes the analytical solution data series. Values closer to 0 indicate better agreement between the data analyzed.

It is important to highlight that the data series may have different sizes because some SWMM simulations have a report time of 5 s and others of 1 s. Therefore, the  $1/N$  is used in order to normalize the  $L^2$  norm results.

## 5.3 RESULTS AND DISCUSSION

### 5.3.1 Simulations Summary

In this work, several spatial and temporal discretizations were used along with different pressurization algorithms for the analytical solutions selected. For each of the three closed-pipe transient flow problems, a total of 75 modeling conditions were considered, according to the Table 5.1:

Table 5.1 – Simulations summary

<b>Simulation variables</b>	<b>Range of variation</b>
Pressurization algorithms	EXTRAN, SLOT, SLOT 250 m/s, SLOT 500 m/s, SLOT 1000 m/s
Spatial discretization	$L/\Delta x = 1$ , $L/\Delta x = 30$ , $L/\Delta x = 120$
Temporal discretization	Eq. 5.20a, Eq. 5.20b, Eq. 5.22a, Eq. 5.22b, Eq. 5.22c

Source: The Author.

The routing time-steps estimated based on Eq. 5.20a resulted in time-steps greater than 5 s. This routing time-step is too large to represent the transient dynamics. Therefore, simulations that the estimated routing time-step were greater than 5 s were discarded. Also, simulation conditions that did not yield the expected behavior or oscillations were omitted from this discussion.

### 5.3.2 Case 1: Surge tank

Parmakian (1963) solved the system shown in Figure 5.1 for a 914.4 m long, 3.05-m diameter penstock. The author considered a reservoir having a static water level height ( $H_o$ ) of 152.4 m and a surge tank area ( $A$ ) of 29.17m<sup>2</sup>. Also, a flow rate ( $Q_o$ ) of 23.87 m<sup>3</sup>/s was defined as initial condition. Solving Eq. 5.4 and Eq. 5.5 resulted in a maximum upsurge ( $S_{max}$ ) of 168.19 m at 30.3 s after the gate closure.

In order to represent this solution in SWMM, an outfall node with a fixed stage of 153.92 m ( $H_o + D/2$ ) was selected to represent the water level at the upstream reservoir. Then, a circular conduit having the same characteristics of the Parmakian (1963) solution was used as penstock. However, since SWMM requires a value of roughness in links, a small value of  $10^{-6}$  was selected in an attempt to minimize the friction accounted by SWMM. The surge tank was represented by a storage unit with a max. depth of 237.7 m, initial depth of 152.4 m and a constant area of 29.2 m<sup>2</sup>. Prior to the gate closure, a small conduit having the same characteristics of the penstock followed by a huge storage unit were used as system outlet. A control rule closing the conduit after the surge tank was created to simulate the rapid gate closure.

Table 5.2 summarizes the selected routing-time steps for all the simulation conditions used in the Surge Tank analysis.

Table 5.2 – Surge tank routing time-steps (s) summary.

Press. Algor.	Spatial Disc.	Temporal Discretization			
		Eq. 5.22a	Eq. 5.22b	Eq. 5.22c	Eq. 5.20b
EXTRAN	$L/\Delta x = 1$	0.062	0.560	1.867	1.01
	$L/\Delta x = 30$	0.002	0.019	0.062	1.01
	$L/\Delta x = 120$	0.001	0.005	0.016	0.25
SLOT Original	$L/\Delta x = 1$	1.767	>5	>5	1.01
	$L/\Delta x = 30$	0.059	0.530	1.767*	1.01
	$L/\Delta x = 120$	0.015	0.133	0.442*	0.25
SLOT 250m/s	$L/\Delta x = 1$	1.151	>5	>5	1.01
	$L/\Delta x = 30$	0.038	0.345*	1.151*	1.01*
	$L/\Delta x = 120$	0.010	0.086*	0.288*	0.25*
SLOT 500m/s	$L/\Delta x = 1$	0.587	>5	>5	1.01
	$L/\Delta x = 30$	0.020	0.176*	0.587*	1.01*
	$L/\Delta x = 120$	0.005	0.044*	0.147*	0.25*
SLOT 1000m/s	$L/\Delta x = 1$	0.297	2.671	>5	1.01
	$L/\Delta x = 30$	0.010	0.089*	0.297*	1.01*
	$L/\Delta x = 120$	0.003	0.022*	0.074*	0.25*

Source: The Author.

\* Results did not represent the expected behavior.

The first results analyzed represent the surge tank maximum upsurge occurring right after the control gate closure. The surge tank analytical results and the SWMM simulation results for all modeling conditions evaluated are shown in Table 5.3.

Table 5.3 – Surge tank maximum upsurge results (m).

Press. Algor.	Spatial Disc.	Temporal Discretization				Analytical Solution
		Eq. 5.22a	Eq. 5.22b	Eq. 5.22c	Eq. 5.20b	
EXTRAN	$L/\Delta x = 1$	157.43	157.43	157.40	157.41	169.72
	$L/\Delta x = 30$	164.46	164.45	164.45	164.14	169.72
	$L/\Delta x = 120$	167.71	167.71	167.71	167.23	169.72
SLOT Original	$L/\Delta x = 1$	163.62	-	-	163.78	169.72
	$L/\Delta x = 30$	164.61	164.38	*	164.21	169.72
	$L/\Delta x = 120$	164.90	164.61	*	164.55	169.72
SLOT 250m/s	$L/\Delta x = 1$	169.18	-	-	169.26	169.72
	$L/\Delta x = 30$	169.61	*	*	*	169.72
	$L/\Delta x = 120$	169.62	*	*	*	169.72
SLOT 500m/s	$L/\Delta x = 1$	169.50	-	-	169.34	169.72
	$L/\Delta x = 30$	169.68	*	*	*	169.72
	$L/\Delta x = 120$	169.69	*	*	*	169.72
SLOT 1000m/s	$L/\Delta x = 1$	169.61	168.70	-	169.36	169.72
	$L/\Delta x = 30$	169.71	*	*	*	169.72
	$L/\Delta x = 120$	169.71	*	*	*	169.72

Source: The Author.

- Routing time-steps greater than 5s.

\* Results did not represent the expected behavior.

The results showed that the EXTRAN pressurization algorithm was able to generate results for all time-steps and spatial discretizations used. However, it is important to highlight that there were significant differences using the artificial spatial discretization. Finer  $\Delta x$  produced results closer to the analytical solution, underestimating it by 2 m, when large  $\Delta x$  tended to show distant results to the analytical solution, underestimating it by 12 m.

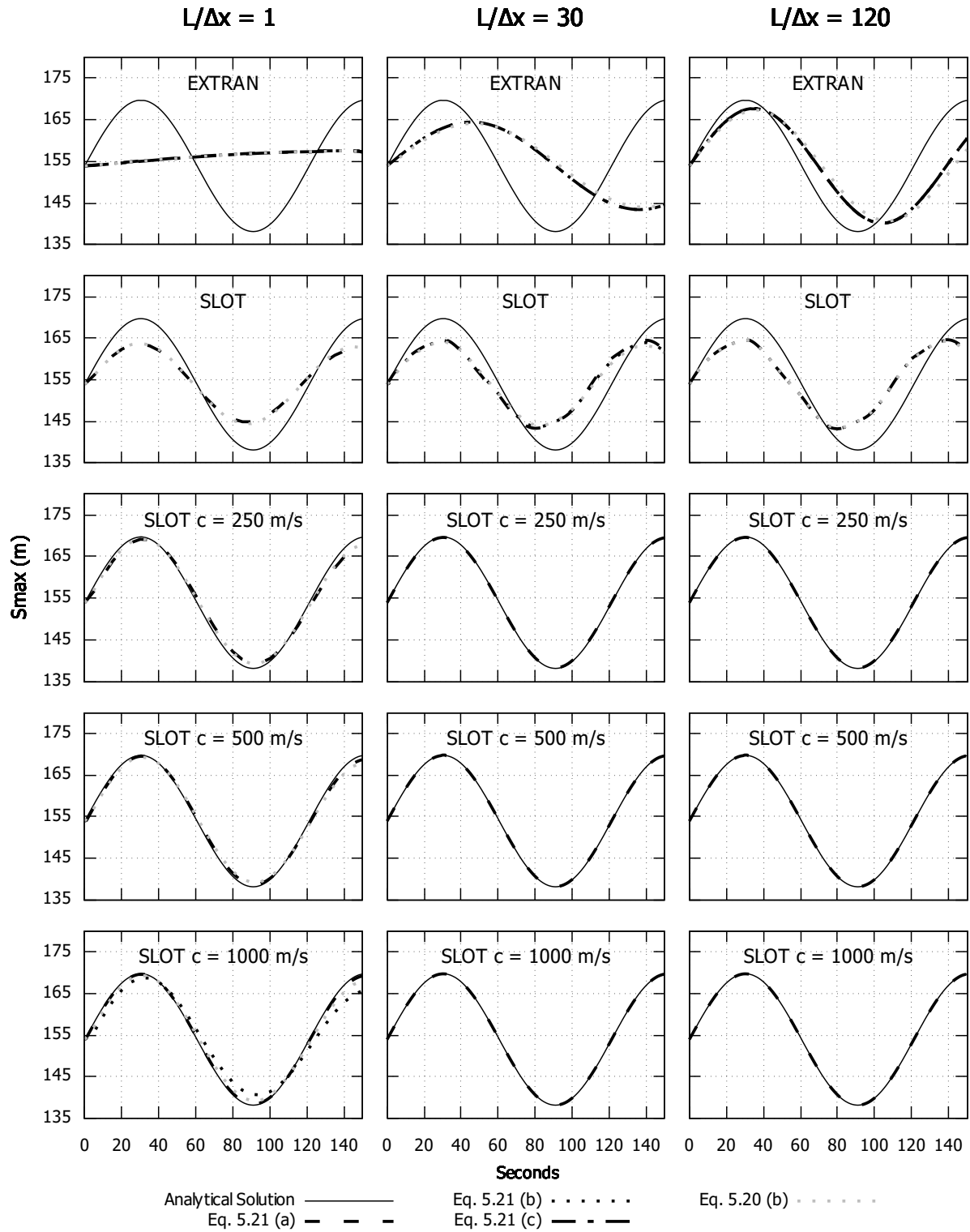
In turn, the original implementation of SLOT was not able to simulate all spatial discretizations when the time-step was selected based on Eq. 5.22c. Also, the traditional link-node approach simulation using Eq. 5.22b was discarded because the routing time-step estimated was greater than 5 s. The remaining results were consistent, underestimating the analytical solution by 4.5 m.

The other SLOT implementations (250 m/s, 500 m/s, 1000 m/s) simulations produced results closer to the analytical solution. The results were consistent when the time-step was based on Eq. 5.22a, underestimating the analytical solution by less than 0.3 m when spatial discretization is used. However, using the Eq. 5.20b to estimate routing time-steps produced accurate results when the traditional link-node approach was used. It is noticeable that when the slot size is estimated based on  $c = 1000$  m/s, the traditional link-node approach using routing time-steps based Eq. 5.22b was able to generate results close to the analytical solution. As the original implementation of

SLOT, using the time-step estimated by Eq. 5.22c crashed the simulations.

Figure 5.4 shows the graphical results for all simulation conditions used in this work.

Figure 5.4 – Surge tank graphical results.



Source: The Author.

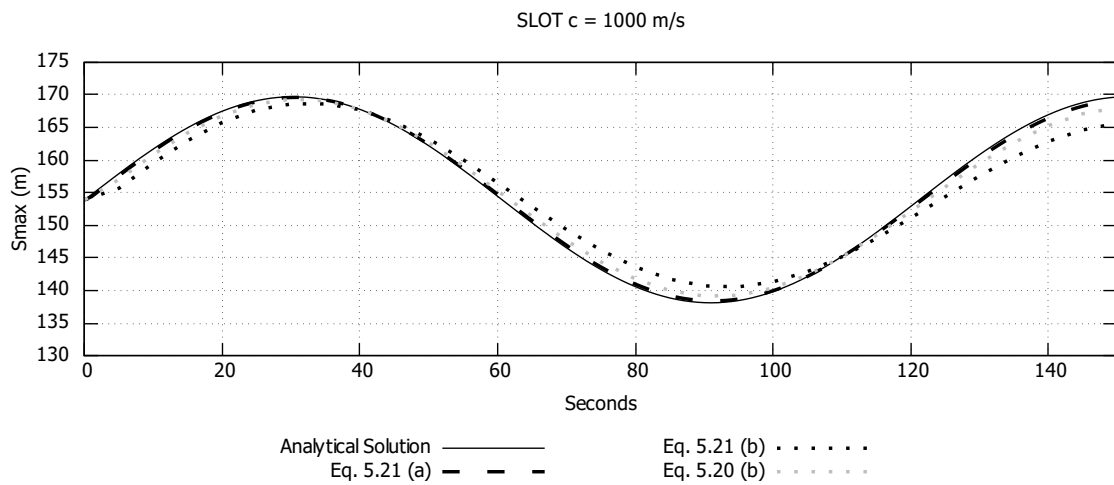


The EXTRAN pressurization algorithm using the traditional link-node approach did not represent either the wavelength or amplitude of the oscillatory behavior presented in the analytical solution. When adopting artificial spatial discretization, the representation of the oscillatory behavior was improved. This is possible to visualize in the first row of Figure 5.4. Finer  $\Delta x$  seemed to improve the results because the maximum upsurge and wavelength estimated by  $L/\Delta x = 120$  was closer to the analytical solution when compared to  $L/\Delta x = 1$  or  $L/\Delta x = 30$ . However, the results should not be altered by additional spatial discretization since it is just more computational cells to be computed.

The original SLOT pressurization algorithm had a closer wavelength and amplitude when compared to the analytical solution but the results still have a significant discrepancy (Figure 5.4 second row). The reason for this discrepancy can be the extra storage caused by the slot width, affecting the wave front (VASCONCELOS; WRIGHT; ROE, 2006a) and reducing the water level (MALEKPOUR et al., 2015). It is important to highlight that, differently from the EXTRAN pressurization algorithm, results from the original SLOT method were not influenced by the varying discretization in the simulation.

The use of narrower SLOT values has clearly improved the solution, with near perfect results in terms of peak level, timing of peak level, and oscillatory behavior. Similarly to the original SLOT, there were slightly improvements when using spatial discretization. Figure 5.5 presents details of simulation results for the narrowest SLOT ( $c = 1000$  m/s). The time step associated with Eq. 5.22b presented greater damping of surge oscillation amplitude, whereas the results using routing time-steps based Eq. 5.22a and Eq. 5.20b showed lesser damping. These results may be seen with all time steps using the non-discretized simulation conditions.

Figure 5.5 – Surge tank simulation using the non-discretized model and setting the slot width based on  $c = 1000$  m/s.



Source: The Author.

Table 5.4 shows the  $L^2$  norm results obtained for each simulation condition. In order to perform this analysis, the data of two entire oscillations were used, 244 s for report time of 1 s and 250 s for report time of 5 s.

Table 5.4 –  $L^2$  norm results for surge tank analysis.

Press. Algor.	Spatial Disc.	Temporal Discretization			
		Eq. 5.22a	Eq. 5.22b	Eq. 5.22c	Eq. 5.20b
EXTRAN	$L/\Delta x = 1$	0.738	0.738	1.590	1.589
	$L/\Delta x = 30$	0.953	0.953	0.952	2.018
	$L/\Delta x = 120$	0.557	0.553	0.553	0.632
SLOT Original	$L/\Delta x = 1$	0.772	-	-	0.728
	$L/\Delta x = 30$	0.488	0.473	*	1.005
	$L/\Delta x = 120$	0.506	0.503	*	0.501
SLOT 250m/s	$L/\Delta x = 1$	0.197	-	-	0.164
	$L/\Delta x = 30$	0.011	*	*	*
	$L/\Delta x = 120$	0.011	*	*	*
SLOT 500m/s	$L/\Delta x = 1$	0.046	-	-	0.161
	$L/\Delta x = 30$	0.003	*	*	*
	$L/\Delta x = 120$	0.003	*	*	*
SLOT 1000m/s	$L/\Delta x = 1$	0.024	0.388	-	0.161
	$L/\Delta x = 30$	0.001	*	*	*
	$L/\Delta x = 120$	0.001	*	*	*

Source: The Author.

- Routing time-steps greater than 5s.

\* Results did not represent the expected behavior.

The EXTRAN pressurization algorithm showed smaller values of  $L^2$  when the

$L/\Delta x = 120$  discretization is used, independently of the selected routing time-step. When  $L/\Delta x = 30$  discretization is adopted, the  $L^2$  results were higher than those for the  $L/\Delta x = 1$  discretization. Based on this and on the previous analysis, it is possible to infer that the EXTRAN pressurization algorithm simulates results closer to the analytical solution when a finer spatial discretization is adopted. Furthermore, higher routing time-steps (Eq. 5.22c or Eq. 5.20b) produced higher values of  $L^2$ . The SLOT original implementation also had some improvements when artificial spatial discretization is adopted. The best simulation was when the routing time-step was estimated using Eq. 5.22b along with  $L/\Delta x = 30$  discretization. In this case, finer discretization ( $L/\Delta x = 120$ ) increased the  $L^2$  values. In general, excepting the  $L/\Delta x = 30$  discretization along Eq. 5.20b routing time-step and the  $L/\Delta x = 1$  discretizations, the results were comparable. The proposed SLOT implementations based on celerity were also consistent in its  $L^2$  results. In these cases, the impact of adopting artificial spatial discretization is more relevant. The discretization improved results accuracy but some minor variation was noticed among discretized solutions. It is also noticeable that the discretized models were only successful using the small routing time-step estimated by Eq. 5.22a. Another point to mention is that smaller slot width - higher celerity values - decreased unquestionably the  $L^2$  values.

In general, the best routing time-step estimation for the Surge Tank case is based on Eq. 5.22a. Also, it is important to highlight that none of the simulation conditions analyzed generated any kind of numerical instabilities and showed small continuity errors.

### 5.3.3 Case 2: Pipeline flow startup

Considering the system shown in Figure 5.2, a 3000-m long, 1-m diameter pipe with a Darcy-Weisbach  $f$  friction of 0.012 connects the two reservoirs. The upstream reservoir has a static water level ( $H_u$ ) of 200 m and the downstream reservoir is empty ( $H_d = 0$  m). Solving Eq. 5.8 for  $Q$  results in a flow value of 8.1998 m<sup>3</sup>/s.

To represent this situation in SWMM, two storage units with large area of 10<sup>6</sup> m<sup>2</sup> were used to maintain the water level static in the upstream and downstream reservoirs. The reservoirs have the same water level of the analytical solution. As the links in SWMM require the Manning Roughness Coefficient as input, the following relationship (BRATER et al., 1996) was used to relate the Darcy-Weisbach  $f$  friction coefficient and the Manning Roughness  $n$  friction factor:

$$\frac{Rh^{1/6}}{n} = \sqrt{\frac{8g}{f}}. \quad (5.24)$$

Thus, the conduit has the same characteristics of the analytical solution but a

Roughness of 0.0098.

Since the link-node approach creates a piezometric line between the upstream and downstream reservoirs, the nodes' water level in the discretized layouts were set to match this piezometric line. The flow results for the discretized layouts were retrieved on the link closest to the downstream reservoir.

Table 5.5 shows the routing time-steps estimated for this analysis.

Table 5.5 – Pipeline flow startup routing time-steps (s) summary.

Press. Algor.	Spatial Disc.	Temporal Discretization			
		Eq. 5.22a	Eq. 5.22b	Eq. 5.22c	Eq. 5.20b
EXTRAN	$L/\Delta x = 1$	0.203	1.828	>5	>5
	$L/\Delta x = 30$	0.007	0.061	0.203	3.19
	$L/\Delta x = 120$	0.002	0.015	0.051	0.80
SLOT Original	$L/\Delta x = 1$	>5	>5	>5	>5
	$L/\Delta x = 30$	0.262	2.356	>5	3.19
	$L/\Delta x = 120$	0.065	0.589	1.964	0.80
SLOT 250m/s	$L/\Delta x = 1$	1.152	>5	>5	>5
	$L/\Delta x = 30$	0.038	0.346	1.152	3.19
	$L/\Delta x = 120$	0.010	0.086	0.288	0.80
SLOT 500m/s	$L/\Delta x = 1$	0.588	>5	>5	>5
	$L/\Delta x = 30$	0.020	0.176	0.588	3.19
	$L/\Delta x = 120$	0.005	0.044	0.147	0.80
SLOT 1000m/s	$L/\Delta x = 1$	0.297	2.672	>5	>5
	$L/\Delta x = 30$	0.010	0.090	0.297	3.19
	$L/\Delta x = 120$	0.003	0.022	0.074	0.80

Source: The Author.

The analytical solution and SWMM results obtained for the case of a pipeline flow startup are shown in Table 5.6. These results represent the steady state flow after the transient.

Table 5.6 – Pipeline startup flow (m<sup>3</sup>/s) results.

Press. Algor.	Spatial Disc.	Temporal Discretization				Analytical Solution
		Eq. 5.22a	Eq. 5.22b	Eq. 5.22c	Eq. 5.20b	
EXTRAN	$L/\Delta x = 1$	5.505	5.504	-	-	8.199
	$L/\Delta x = 30$	7.628	7.628	7.628	7.628	8.199
	$L/\Delta x = 120$	7.682	7.682	7.682	7.682	8.199
SLOT Original	$L/\Delta x = 1$	-	-	-	-	8.199
	$L/\Delta x = 30$	18.845	18.809	-	18.806	8.199
	$L/\Delta x = 120$	18.927	18.926	*	18.925	8.199
SLOT 250m/s	$L/\Delta x = 1$	8.102	-	-	-	8.199
	$L/\Delta x = 30$	8.105	8.105	*	*	8.199
	$L/\Delta x = 120$	8.105	8.105	*	*	8.199
SLOT 500m/s	$L/\Delta x = 1$	8.012	-	-	-	8.199
	$L/\Delta x = 30$	8.012	8.012	*	*	8.199
	$L/\Delta x = 120$	8.012	8.012	*	*	8.199
SLOT 1000m/s	$L/\Delta x = 1$	7.989	7.989	-	-	8.199
	$L/\Delta x = 30$	7.989	7.989	*	*	8.199
	$L/\Delta x = 120$	*	7.989	*	*	8.199

Source: The Author.

- Routing time-steps greater than 5s.

\* Results did not represent the expected behavior.

Source: The Author.

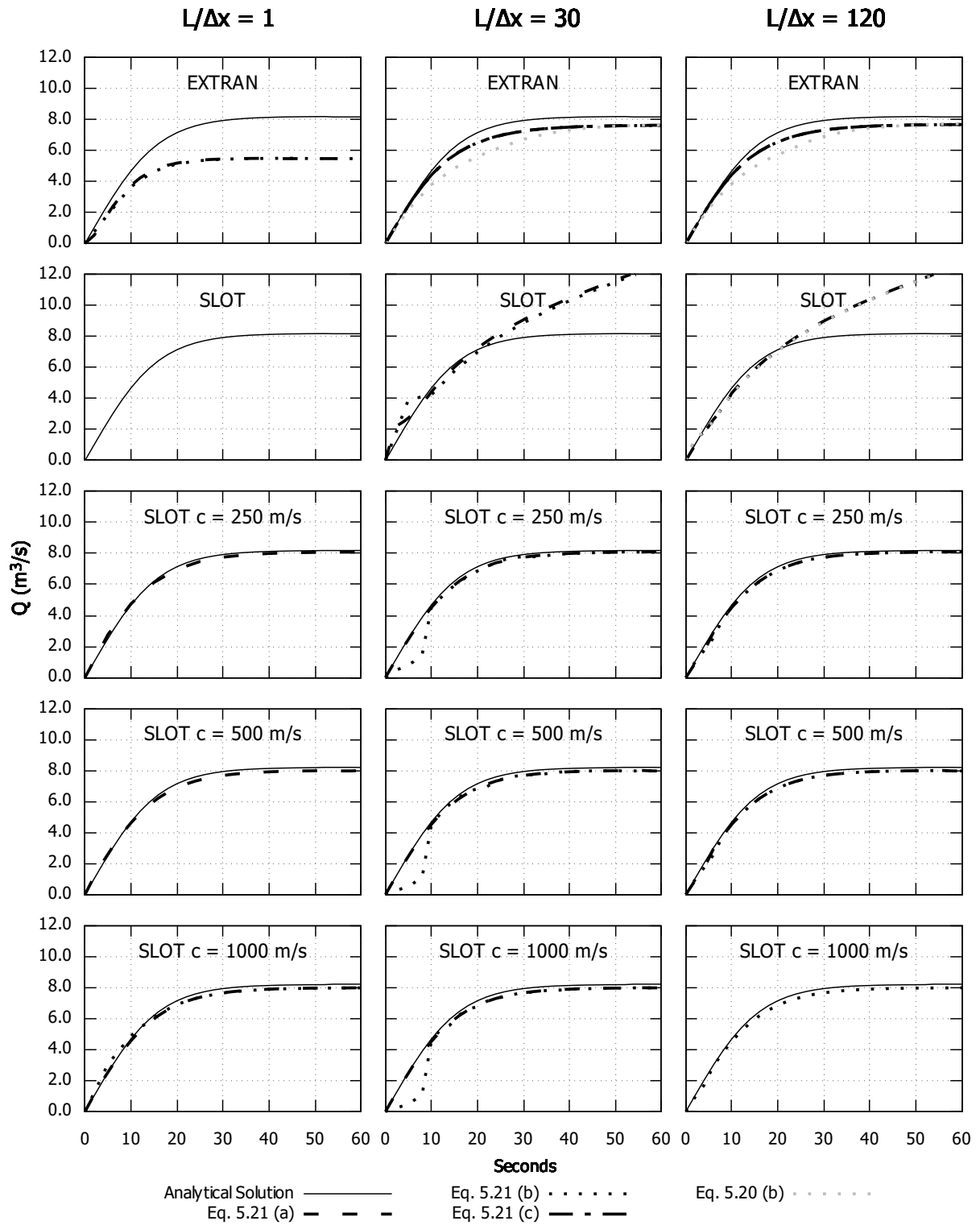
The EXTRAN pressurization algorithm results were similar to the previous case. It was able to simulate the pipeline flow startup using all proposed time-steps, excepting the routing time-steps based on Eq. 5.20a. Also, there were significant differences when the spatial discretization is adopted. When it is used, the simulations produced results closer to the analytical solution, underestimating the results by 0.5 m<sup>3</sup>/s. Using the non-discretized models, it underestimated the analytical solution by 2.7 m<sup>3</sup>/s.

The results using the SLOT original implementation produced the worst results. It was only capable to simulate when artificial discretization is used. Even though the results were consistent, estimating the same value of flow for the artificial spatial discretizations adopted and for the time-steps that were able to simulate, this pressurization algorithm overestimated the flow values by more than 10 m<sup>3</sup>/s.

The proposed SLOT implementations produced consistent results close to the analytical solution. These simulations underestimated the analytical solution by 0.1 m<sup>3</sup>/s. However, they were not capable to simulate using higher values of time-step based on Eq. 5.22c and Eq. 5.20b. In these proposed implementations, using the Courant condition to estimate the routing time-step was better than the EXTRAN based recommendations.

Figure 5.6 shows the graphical results for the transient happening in a pipeline startup for all simulation conditions analyzed.

Figure 5.6 – Pipeline flow startup graphical results.



Source: The Author.

These results are consistent with the ones presented in the surge tank

simulations. Results indicate that the traditional link-node approach with EXTRAN pressurization algorithm produces significant under-prediction of flow rates. This under-prediction was reduced when discretization was adopted, though it was still noticeable.

The original SLOT implementation yielded a poor representation of the pipeline flow startup for cases using the traditional link-node approach. The results were not representative of expected flows. Even when additional spatial discretization was adopted, the simulation results highly overestimated flow rates.

The proposed SLOT implementations represented more accurately the analytical solution. The flow startup until the steady state was well represented by the slot width adjusted based on celerity, even when the traditional link-node approach was used. A little discrepancy was found in the beginning of the pipeline filling when the discretization  $L/\Delta x = 30$  along routing time-step based on Eq. 5.22b is adopted for all modifications in the slot. This problem is solved adopting a finer discretization.

Table 5.7 shows the  $L^2$  results obtained for the Pipeline Flow Startup. In this case, the data used to perform this analysis was the first 82 s of simulation when the report time is 1 s and the first 85 s of simulation when the report time is 5 s.

Table 5.7 –  $L^2$  norm results for pipeline flow startup analysis.

Press. Algor.	Spatial Disc.	Temporal Discretization			
		Eq. 5.22a	Eq. 5.22b	Eq. 5.22c	Eq. 5.20b
EXTRAN	$L/\Delta x = 1$	0.351	0.568	-	-
	$L/\Delta x = 30$	0.083	0.084	0.084	0.232
	$L/\Delta x = 120$	0.076	0.076	0.076	0.115
SLOT Original	$L/\Delta x = 1$	-	-	-	-
	$L/\Delta x = 30$	0.567	0.851	-	0.844
	$L/\Delta x = 120$	0.576	0.572	*	0.571
SLOT 250m/s	$L/\Delta x = 1$	0.054	-	-	-
	$L/\Delta x = 30$	0.021	0.080	*	*
	$L/\Delta x = 120$	0.022	0.024	*	*
SLOT 500m/s	$L/\Delta x = 1$	0.030	-	-	-
	$L/\Delta x = 30$	0.030	0.094	*	*
	$L/\Delta x = 120$	0.031	0.033	*	*
SLOT 1000m/s	$L/\Delta x = 1$	0.033	0.075	-	-
	$L/\Delta x = 30$	0.033	0.096	*	*
	$L/\Delta x = 120$	*	0.034	*	*

Source: The Author.

- Routing time-steps greater than 5s.

\* Results did not represent the expected behavior.

As the Surge Tank analysis, the EXTRAN pressurization algorithm maintains the same behavior of small  $L^2$  values when artificial spatial discretization is adopted.

Also, higher routing time-steps (Eq. 5.20b) produced higher values of  $L^2$ . For this pressurization algorithm, the best results were associated with  $L/\Delta x = 120$  discretization. The  $L^2$  results for the original SLOT implementation are alike, excepting the routing time-steps based on Eq. 5.22b and Eq. 5.20b for the  $L/\Delta x = 30$  discretization. The proposed SLOT implementations showed agreement between the values obtained by the simulation and the analytical solution.

### 5.3.4 Case 3: Instantaneous valve closure transient

The instantaneous valve closure transient presented in this work is analytically solved by the Joukowski Equation (JOUKOWSKI, 1904). It is important to highlight that in this case the analytical solution yields the maximum upsurge and this value is directly related to celerity, as can be seen in Eq. 5.9. Therefore, all pressurization algorithms have different maximum upsurges estimated by the analytical solution because the celerity changes for each one. However, the velocity ( $V_i$ ) does not vary and it is defined as 0.1 m/s. Also, a 3000-m long pipe is used to estimate the wave period (Eq. 5.12).

In order to represent this situation in SWMM, two storage units with large area were used. The first has a static water level ( $H_o$ ) of 20 m and the second is empty. Between them, a 3000-m long, 1-m diameter pipe followed by a side circular orifice of 0.1-m height and discharge coefficient of 0.505 was set. This orifice was used to limit the flow velocity to 0.1 m/s. After the simulation enters in steady state, a control rule was used to close the orifice, creating an instantaneous valve closure. The head results obtained at the downstream junction were used to compare with the analytical solution.

Table 5.8 summarizes the selected routing time-steps for the instantaneous valve closure transient.



Table 5.8 – Instantaneous valve closure transient routing time-steps (s) summary.

Press. Algor.	Spatial Disc.	Temporal Discretization			
		Eq. 5.22a	Eq. 5.22b	Eq. 5.22c	Eq. 5.20b
EXTRAN	$L/\Delta x = 1$	0.205*	1.841*	>5	>5
	$L/\Delta x = 30$	0.007*	0.061*	0.205	3.19
	$L/\Delta x = 120$	0.002*	0.015*	0.051	0.80
SLOT Original	$L/\Delta x = 1$	>5	>5	>5	>5
	$L/\Delta x = 30$	0.359**	3.231	>5	3.19
	$L/\Delta x = 120$	0.090**	0.808	2.692*	0.80
SLOT 250m/s	$L/\Delta x = 1$	1.200	>5	>5	>5
	$L/\Delta x = 30$	0.040**	0.360	0.800	3.19*
	$L/\Delta x = 120$	0.010**	0.090	0.200	0.80*
SLOT 500m/s	$L/\Delta x = 1$	0.600	>5	>5	>5
	$L/\Delta x = 30$	0.020**	0.180	0.600*	3.19*
	$L/\Delta x = 120$	0.005**	0.045	0.150*	0.80*
SLOT 1000m/s	$L/\Delta x = 1$	0.300	2.700	>5	>5
	$L/\Delta x = 30$	0.001**	0.090	0.300*	3.19*
	$L/\Delta x = 120$	0.003**	0.023	0.075*	0.8*

Source: The Author.

\* Results did not represent the expected behavior.

\*\* Minor instabilities present in the simulations.

Differently from the previous cases, the analytical solution changes for each pressurization algorithm. The results are shown in Table 5.9.

Table 5.9 – Instantaneous valve closure transient maximum upsurge results (m).

Press. Algor.	Spatial Disc.	Temporal Discretization				Analytical Solution
		Eq. 5.22a	Eq. 5.22b	Eq. 5.22c	Eq. 5.20b	
EXTRAN	$L/\Delta x = 1$	*	*	-	-	14.95
	$L/\Delta x = 30$	*	*	17.96	1.14	14.95
	$L/\Delta x = 120$	*	*	17.98	1.13	14.95
SLOT Original	$L/\Delta x = 1$	-	-	-	-	0.28
	$L/\Delta x = 30$	0.32**	0.27	-	0.27	0.28
	$L/\Delta x = 120$	0.31**	0.28	*	0.28	0.28
SLOT 250m/s	$L/\Delta x = 1$	3.38	-	-	-	2.55
	$L/\Delta x = 30$	3.56**	2.91	2.81	*	2.55
	$L/\Delta x = 120$	3.56**	2.91	2.80	*	2.55
SLOT 500m/s	$L/\Delta x = 1$	6.78	-	-	-	5.10
	$L/\Delta x = 30$	7.15**	5.84	*	*	5.10
	$L/\Delta x = 120$	7.15**	5.84	*	*	5.10
SLOT 1000m/s	$L/\Delta x = 1$	13.57	8.39	-	-	10.19
	$L/\Delta x = 30$	14.33**	11.71	*	*	10.19
	$L/\Delta x = 120$	14.33**	11.71	*	*	10.19

Source: The Author.

- Routing time-steps greater than 5s.

\* Results did not represent the expected behavior.

\*\* Minor instabilities present in the simulations.

For the EXTRAN pressurization algorithm, it was assumed that celerity was equal to the wavespeed in a very thick-walled pipe (Eq. 5.10), resulting in 1466.29 m/s and, consequently, a maximum upsurge of 14.95 m. This pressurization algorithm was only capable to simulate using artificial spatial discretization along routing time-steps estimated based on Eq. 5.22c and Eq. 5.20b. When the routing time-step was selected based on Eq. 5.22c, it overestimated the maximum upsurge by 3 m. These results would be corresponding to a celerity of 1760 m/s. When the time-step was selected based on Eq. 5.20b, the maximum upsurge was underestimated by almost 14 m, a result that would be corresponding to a celerity of 111 m/s. These results are interesting because changing the temporal discretization should not alter the results.

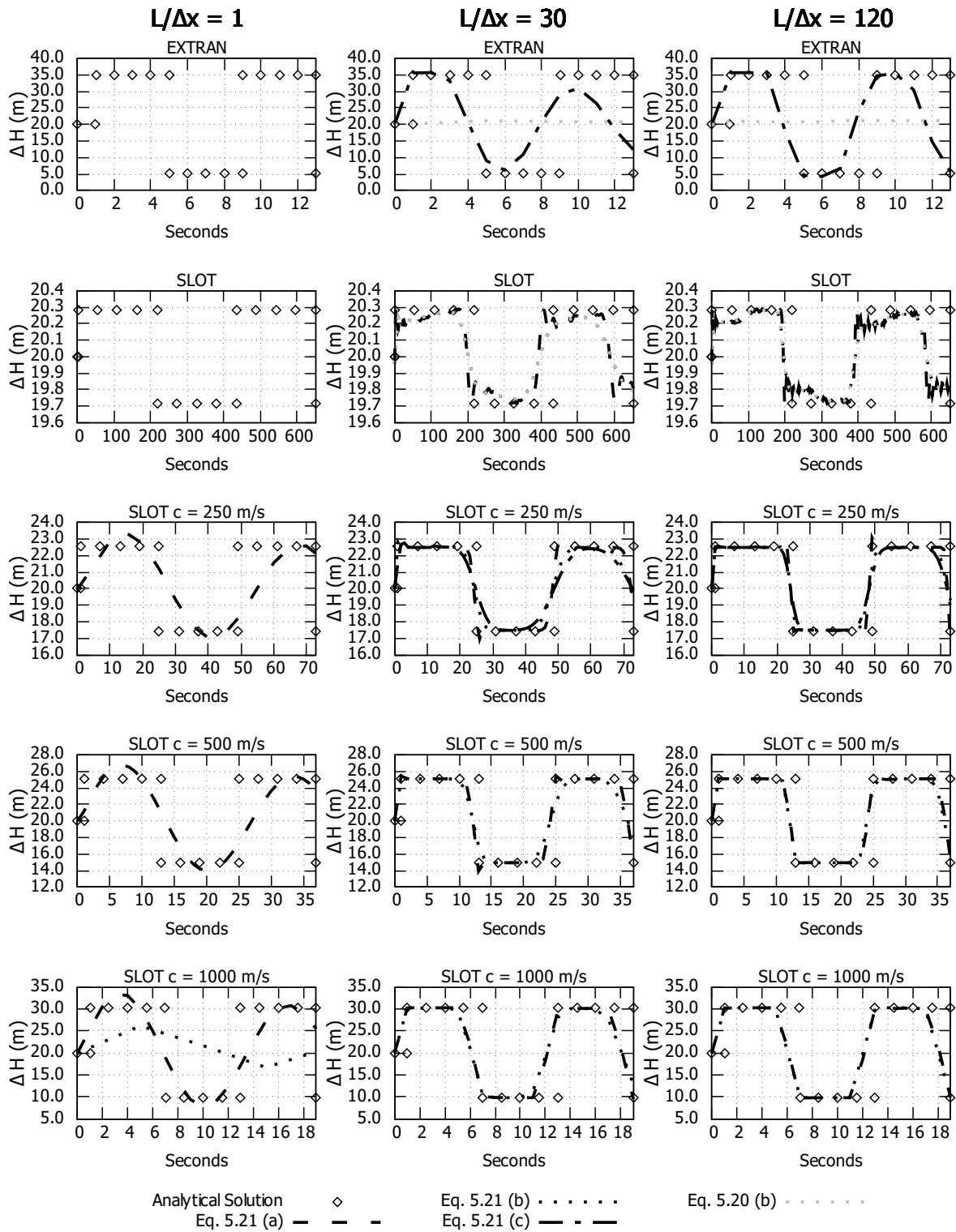
As the EXTRAN pressurization algorithm, the SLOT original implementation was not capable to simulate using the traditional link-node approach. When discretization is adopted, this implementation yielded results that represented the expected maximum upsurge and it was capable to run the simulations for almost every time-step selected, except based on Eq. 5.22c. However, it is important to highlight that the celerity was estimated based on Eq. 5.11, producing a small, and unrealistic, value of 27.76 m/s. According to Ghidaoui et al. (2005), waterhammer wave speeds ranges from 100 to 1400 m/s and, therefore, the maximum upsurge found (0.28 m) should not represent an

actual waterhammer. Despite this, the theoretical maximum upsurge from Joukowsky equation of 0.28 m was near the result obtained with this pressurization algorithm. In this case, finer discretization generated results closer to the analytical solution.

As the previous cases, the proposed SLOT implementations were consistent in its results. Minor differences were found between the traditional link-node approach and the discretized models and between the routing time-steps. When using Eq. 5.20b for estimating the routing time-step the simulations crashed. Also, some minor instabilities were found when coupling spatial discretization with a routing time-step based on Eq. 5.22a. The slot width based on a celerity value of 250 m/s was the only implementation capable to simulate using Eq. 5.22c and, in this simulation condition, its results were closer to the analytical solution. The other proposed implementations (500 m/s and 1000 m/s) were consistent: adopting artificial spatial discretization along Eq. 5.22b routing time-step generated maximum upsurges values closer to the analytical solution.

Figure 5.7 shows the graphical results for all the simulation conditions analyzed and Table 5.10 shows the simulated wave periods compared to the ones obtained by Eq. 5.12.

Figure 5.7 – Instantaneous valve closure transient graphical results.



Source: The Author.

Table 5.10 – Instantaneous valve closure transient wave period results (s).

Press. Algor.	Spatial Disc.	Temporal Discretization				Analytical Solution
		Eq. 5.22a	Eq. 5.22b	Eq. 5.22c	Eq. 5.20b	
EXTRAN	$L/\Delta x = 1$	*	*	-	-	8
	$L/\Delta x = 30$	*	*	9	145	8
	$L/\Delta x = 120$	*	*	8	148	8
SLOT Original	$L/\Delta x = 1$	-	-	-	-	432
	$L/\Delta x = 30$	406**	435	-	440	432
	$L/\Delta x = 120$	398**	435	*	430	432
SLOT 250m/s	$L/\Delta x = 1$	54	-	-	-	48
	$L/\Delta x = 30$	48**	53	55	*	48
	$L/\Delta x = 120$	48**	53	52	*	48
SLOT 500m/s	$L/\Delta x = 1$	26	-	-	-	24
	$L/\Delta x = 30$	24**	26	*	*	24
	$L/\Delta x = 120$	24**	25	*	*	24
SLOT 1000m/s	$L/\Delta x = 1$	13	16	-	-	12
	$L/\Delta x = 30$	12**	13	*	*	12
	$L/\Delta x = 120$	12**	12	*	*	12

Source: The Author.

- Routing time-steps greater than 5s.

\* Results did not represent the expected behavior.

\*\* Minor instabilities present in the simulations.

The EXTRAN pressurization algorithm continues to show the same behavior: dependent of spatial and temporal discretization. In the discretized models, decreasing the time-step seemed to increase the oscillations and peak level. Considering Eq. 5.22c, the oscillations diminished faster for  $L/\Delta x = 30$  than  $L/\Delta x = 120$  but the wave periods were alike. Yet for Eq. 5.20b, the results were different than the expected ones.

The waves generated by the SLOT original implementation adopting  $L/\Delta x = 30$  and  $L/\Delta x = 120$  were alike but when the time-step was estimated based on Eq. 5.22a some instabilities were found, specially in  $L/\Delta x = 120$  discretization. Yet the proposed SLOT implementations based on celerity represented the wave expected to occur due to a waterhammer in a frictionless pipe (CHAUDHRY, 2013), excepting the traditional link-node approach. The simulations using Eq. 5.22a as routing time-step showed instabilities that lead to a higher value of maximum upsurge and a shorter wavelength when compared to the Eq. 5.22b routing time-step. As the previous cases, the discretized layouts showed consistent results independently of the discretization.

Table 5.11 shows the  $L^2$  results for the instantaneous valve closure transient case. In this analysis, two complete oscillations were used to calculate the  $L^2$  norm.

Table 5.11 –  $L^2$  norm results for instantaneous valve closure transient analysis.

Press. Algor.	Spatial Disc.	Temporal Discretization			
		Eq. 5.22a	Eq. 5.22b	Eq. 5.22c	Eq. 5.20b
EXTRAN	$L/\Delta x = 1$	*	*	-	-
	$L/\Delta x = 30$	*	*	2.201	6.009
	$L/\Delta x = 120$	*	*	2.334	3.748
SLOT Original	$L/\Delta x = 1$	-	-	-	-
	$L/\Delta x = 30$	0.008**	0.016	-	0.016
	$L/\Delta x = 120$	0.008**	0.008	*	0.008
SLOT 250m/s	$L/\Delta x = 1$	0.677	-	-	-
	$L/\Delta x = 30$	0.052**	0.085	0.103	*
	$L/\Delta x = 120$	0.047**	0.066	0.076	*
SLOT 500m/s	$L/\Delta x = 1$	0.466	-	-	-
	$L/\Delta x = 30$	0.175**	0.247	*	*
	$L/\Delta x = 120$	0.167**	0.212	*	*
SLOT 1000m/s	$L/\Delta x = 1$	1.153	3.960	-	-
	$L/\Delta x = 30$	0.678**	0.789	*	*
	$L/\Delta x = 120$	0.679**	0.790	*	*

Source: The Author.

- Routing time-steps greater than 5s.

\* Results did not represent the expected behavior.

\*\* Minor instabilities present in the simulations.

The  $L^2$  results for the EXTRAN pressurization algorithm showed that this surcharge method was the one that resulted in higher values of  $L^2$ . Smaller routing time-steps (Eq. 5.22c) reduced the  $L^2$  values when compared to higher routing time-steps (Eq. 5.20b). The original SLOT implementation showed small  $L^2$  values for all routing time-steps and discretizations. The best simulation was achieved estimating the routing time-step based on Eq. 5.22b along the finer discretization of  $L/\Delta x = 120$ . The  $L^2$  results for the proposed SLOT implementations showed that smaller routing time-steps along finer discretizations tend to improve the simulations. In some cases, a slight increment in the  $L^2$  results were found for the  $L/\Delta x = 120$  discretization. On the one hand, finer spatial discretization along the routing time-step based on Eq. 5.22a shows smaller values of  $L^2$  but, on the other hand, some instabilities were found in these simulation conditions.

In a summary, the Eq. 5.22b based routing time-step coupled with artificial spatial discretization produced, in general, results closer to the expected ones. Even though routing time-steps based on Eq. 5.22a coupled with artificial spatial discretization also produced results closer to the analytical solution, some instabilities were found in the simulations. It is important to highlight that the celerity of these proposed SLOT implementations are inside the range stated by Ghidaoui et al. (2005),

being, therefore, more representative of waterhammer flow conditions.

#### 5.4 CONCLUSIONS AND RECOMMENDATIONS

This work evaluated the SWMM modeling capacity to simulate slow and fast transients that could be present in stormwater systems. Since the amount of field data related to transients occurring in collection systems is limited, SWMM models were set up in order to represent classic cases of transients which analytical solutions are available. Different simulation conditions were tested, such as varying pressurization algorithms, routing time-steps and spatial discretization.

The findings show that the EXTRAN pressurization algorithm is directly affected by the spatial and temporal discretization used in the simulation. Since discretizing the model only add more intermediate calculation points, this situation should not play a major role in the simulations. Therefore, this pressurization algorithm is not recommended for transient simulations in SWMM since unrealistic results, often underestimating the surges, may occur. Comparatively, adopting spatial discretization along the SLOT pressurization algorithm implemented in SWMM 5.1.013 improves the SWMM capacity to perform more dynamic simulations. However, the original SLOT algorithm has a large slot width that results in a small celerity value of 27.76 m/s. This value is not representative of transients and simulating it with a large slot width may cause a delayed wave front (VASCONCELOS; WRIGHT; ROE, 2006a) and a smaller upsurge amplitude (MALEKPOUR et al., 2015), which was confirmed in this work.

The proposed SLOT implementations, narrowing the slot width based on predefined values of celerity (250 m/s, 500 m/s, 1000 m/s), consistently produced results closer to the analytical solutions. Only small differences were found when the traditional link-node is used or when the routing time-step is not correctly estimated. In general, setting the SWMM slot width based on celerity improved the SWMM capacity to simulate slow and fast transients. Moreover, it is important to highlight that these wave celerity are more representative of hydraulic transients. Thus, it is recommended to select the proposed SLOT implementations based on the expected celerity range of the transient in analysis.

The Courant equation estimated more reliable routing time-steps for pressurized conduits and transient analysis than those obtained by EXTRAN based equations. In general, the transients seemed to be better simulated when the Eq. 5.22b is used to set the routing time-step along spatial discretization. Smaller routing time-step (Eq. 5.22a) also produced accurate simulations but it showed signals of instability in some cases. Furthermore, spatial discretization is required for a proper simulation, especially  $L/\Delta x = 120$  discretization that yielded, in general, results closer to the analytical solutions. Based on this, reducing the slot width along a proper selection

of spatial and temporal discretization can make SWMM a valuable tool to analyze transients in collection systems.

Finally, it is important to emphasize that the modeler should use the proposed implementations carefully because different results may occur depending on the transient in analysis. Careful judgment is always needed when transient models are applied, but these results are an initial indication that SWMM with narrow slots, spatial discretization and small routing time-steps can be used to simulate closed-pipe transient flows in sewer systems operating in pressurized flow conditions.

## REFERENCES

ABDUL-AZIZ, O. I.; AL-AMIN, S. Climate, land use and hydrologic sensitivities of stormwater quantity and quality in a complex coastal-urban watershed. **Urban Water Journal**, v. 13, n. 3, p. 302–320, 2016. ISSN 17449006. DOI: 10.1080/1573062X.2014.991328.

BRATER, E. F.; KING, H. W.; LINDELL, J. E.; WEI, C. Y. **Handbook of Hydraulics**. 7. ed. New York: McGraw-Hill, 1996.

CAMPISANO, A.; CATANIA, F. V.; MODICA, C. Evaluating the SWMM LID Editor rain barrel option for the estimation of retention potential of rainwater harvesting systems. **Urban Water Journal**, Taylor & Francis, v. 14, n. 8, p. 876–881, 2017. ISSN 17449006. DOI: 10.1080/1573062X.2016.1254259. Available at: <<http://dx.doi.org/10.1080/1573062X.2016.1254259>>.

CAMPISANO, A.; GULLOTTA, A.; MODICA, C. Using EPA-SWMM to simulate intermittent water distribution systems. **Urban Water Journal**, Taylor & Francis, v. 00, n. 00, p. 1–9, 2019. DOI: 10.1080/1573062X.2019.1597379. Available at: <<https://www.tandfonline.com/doi/full/10.1080/1573062X.2019.1597379>>.

CAPART, H.; SILLEN, X.; ZECH, Y. Numerical and experimental water transients in sewer pipes. **Journal of Hydraulic Research**, v. 1686, 1997. DOI: 10.1080/00221689709498400.

CHAUDHRY, M. H. **Applied hydraulic transients**. Third Edit. New York: Springer, 2013. v. 9781461485, p. 1–583. ISBN 9781461485384. DOI: 10.1007/978-1-4614-8538-4.

CHO, J. H.; SEO, H. J. Parameter optimization of SWMM for runoff quantity and quality calculation in a eutrophic lake watershed using a genetic algorithm. **Water Science and Technology: Water Supply**, v. 7, n. 5-6, p. 35–41, 2007. ISSN 16069749. DOI: 10.2166/ws.2007.114.



CUNGE, J. A.; HOLLY, F. M.; VERWEY, A. **Practical aspects of computational river hydraulics**. London: Pitman publishing, 1980.

DENAULT, C.; MILLAR, R. G.; LENCE, B. J. Assessment of possible impacts of climate change in an urban catchment. **Journal of the American Water Resources Association**, v. 42, n. 3, p. 685–697, 2006. ISSN 1093474X. DOI: 10.1111/j.1752-1688.2006.tb04485.x.

DI MODUGNO, M.; GIOIA, A.; GORGOGNONE, A.; IACOBELLIS, V.; FORGIA, G. la; PICCINNI, A. F.; RANIERI, E. Build-up/wash-off monitoring and assessment for sustainable management of first flush in an urban area. **Sustainability (Switzerland)**, v. 7, n. 5, p. 5050–5070, 2015. ISSN 20711050. DOI: 10.3390/su7055050.

FALCÃO DE CAMPOS, J. A.; FERREIRA DE SOUSA, P. J.; BOSSCHERS, J. A verification study on low-order three-dimensional potential-based panel codes. **Computers and Fluids**, v. 35, n. 1, p. 61–73, 2006. ISSN 00457930. DOI: 10.1016/j.compfluid.2004.08.002.

GHIDAOU, M. S.; ZHAO, M.; MCINNIS, D. A.; AXWORTHY, D. H. A Review of Water Hammer Theory and Practice. **Applied Mechanics Reviews**, v. 58, n. 1, p. 49, 2005. ISSN 00036900. DOI: 10.1115/1.1828050.

GUIZANI, M.; JOSE, G.; STEVEN, J.; KHLIFA, M. et al. Investigation of rapid filling of empty pipes. **The Journal of Water Management Modeling**, Computational Hydraulics International (CHI), v. 225, n. 20, p. 463–482, 2006.

GUO, L. L.; LIU, Z. G.; GENG, J.; LI, D.; DU, G. S. Numerical study of flow fluctuation attenuation performance of a surge tank. **Journal of Hydrodynamics**, Publishing House for Journal of Hydrodynamics, v. 25, n. 6, p. 938–943, 2013. ISSN 10016058. DOI: 10.1016/S1001-6058(13)60443-6. Available at: <[http://dx.doi.org/10.1016/S1001-6058\(13\)60443-6](http://dx.doi.org/10.1016/S1001-6058(13)60443-6)>.

HUBER, W.; ROESNER, L. The History and Evolution of the EPA SWMM" in "Fifty Years Of Watershed Modeling - Past, Present And Future. **Engineering Conferences International Symposium Series**. <http://dc.engconfintl.org/watershed/29>, 2012. Available at: <<http://dc.engconfintl.org/cgi/viewcontent.cgi?article=1001&context=watershed>>.

JOUKOWSKI, N. Water hammer. **Proceedings of American Water Works Association**, v. 24, p. 341–424, 1904.

JUNG, B. S.; KARNEY, B. A practical overview of unsteady pipe flow modeling: from physics to numerical solutions. **Urban Water Journal**, v. 14, n. 5, p. 502–508, 2017. ISSN 17449006. DOI: 10.1080/1573062X.2016.1223323.

KENDIR, T. E.; OZDAMAR, A. Numerical and experimental investigation of optimum surge tank forms in hydroelectric power plants. **Renewable Energy**, Elsevier Ltd, v. 60, p. 323–331, 2013. ISSN 09601481. DOI: 10.1016/j.renene.2013.05.016. Available at: <<http://dx.doi.org/10.1016/j.renene.2013.05.016>>.

KERGER, F.; ARCHAMBEAU, P.; ERPICUM, S.; DEWALS, B. J.; PIROTON, M. Journal of Computational and Applied An exact Riemann solver and a Godunov scheme for simulating highly transient mixed flows. **Journal of Computational and Applied Mathematics**, Elsevier B.V., v. 235, n. 8, p. 2030–2040, 2011. ISSN 0377-0427. DOI: 10.1016/j.cam.2010.09.026. Available at: <<http://dx.doi.org/10.1016/j.cam.2010.09.026>>.

KIM, S. H. Design of surge tank for water supply systems using the impulse response method with the GA algorithm. **Journal of Mechanical Science and Technology**, v. 24, n. 2, p. 629–636, 2010. ISSN 1738494X. DOI: 10.1007/s12206-010-0108-y.

MALEKPOUR, A.; KARNEY, B. W. Spurious Numerical Oscillations in the Preissmann Slot Method: Origin and Suppression. **Journal of Hydraulic Engineering**, v. 142, n. 3, p. 04015060, 2015. ISSN 0733-9429. DOI: 10.1061/(asce)hy.1943-7900.0001106.

MARCHI, C. H. Effect of P-Norms on the Accuracy Order of Numerical Solution Errors in Cfd. **Fluid Dynamics**, 2010.

MATHEOU, G.; PANTANO, C.; DIMOTAKIS, P. E. Verification of a fluid-dynamics solver using correlations with linear stability results. **Journal of Computational Physics**, v. 227, n. 11, p. 5385–5396, 2008. ISSN 00219991. DOI: 10.1016/j.jcp.2008.01.055.

MEIERDIERCKS, K. L.; SMITH, J. A.; BAECK, M. L.; MILLER, A. J. Analyses of Urban Drainage Network Structure and Its Impact on Hydrologic Response. **Journal of the American Water Resources Association**, v. 46, n. 5, 2010.

MEYERS, J.; GEURTS, B. J.; SAGAUT, P. A computational error-assessment of central finite-volume discretizations in large-eddy simulation using a Smagorinsky model. **Journal of Computational Physics**, v. 227, n. 1, p. 156–173, 2007. ISSN 00219991. DOI: 10.1016/j.jcp.2007.07.012.

MOHAMED. YOSSEF. Flow Details near River Groynes: Experimental Investigation. **ASCE Journal of Hydraulic Engineering**, v. 138, July, p. 642–652, 2015. DOI: 10.1061/(ASCE)HY.1943-7900.

NIAZI, M.; NIETCH, C.; MAGHREBI, M.; JACKSON, N.; BENNETT, B. R.; TRYBY, M.; MASSOUDIEH, A. Storm Water Management Model: Performance Review and Gap Analysis. **Journal of Sustainable Water Built Environment**, v. 3, n. 2, 2017. DOI: 10.1061/JSWBAY.0000817..

- OBROPTA, C. C.; KARDOS, J. S. Review of Urban Stormwater Quality Models: Deterministic, Stochastic, and Hybrid Approaches. **Journal of the American Water Resources Association**, v. 43, n. 6, p. 1508–1523, 2007. DOI: 10.1111/j.1752-1688.2007.00124.x.
- PACHALY, R. L.; VASCONCELOS, J. G.; ALLASIA, D. G. P. **ReSWMM v0.1**. GitHub, 2018. Available at: <<https://github.com/ecotecnologias/ReSWMM>>.
- PACHALY, R. L.; VASCONCELOS, J. G.; ALLASIA, D. G. P.; MINETTO, B. Field evaluation of discretized model setups for the Storm Water Management Model. **Journal of Water Management Modeling**, p. 1–16, 2019. ISSN 2292-6062. DOI: 10.14796/JWMM.C465.
- PARMAKIAN, J. **Waterhammer analysis**. New York: Prentice-Hall, 1963. v. 9.
- POPESCU, I. **Computational Hydraulics**. London: IWA Publishing, 2014. ISBN 9781780400440.
- PREISSMANN, A. Propagation of translatory waves in channels and rivers. In: PROCEEDINGS of the 1st Congress of French Association for Computation, Grenoble, France. 1961. P. 432–443.
- QIN, H.-p.; LI, Z.-x.; FU, G. The effects of low impact development on urban flooding under different rainfall characteristics. **Journal of Environmental Management**, Elsevier Ltd, v. 129, p. 577–585, 2013. ISSN 0301-4797. DOI: 10.1016/j.jenvman.2013.08.026. Available at: <<http://dx.doi.org/10.1016/j.jenvman.2013.08.026>>.
- RIDGWAY, K. E. Evaluating Force Main Transients with SWMM5 and Other Programs. v. 6062, p. 43–54, 2008. DOI: 10.14796/JWMM.R236-04..
- RIDGWAY, K. E.; KUMPULA, G. Surge Modeling in Sewers using the Transient Analysis Program (TAP). **Journal of Water Management Modeling**, v. 6062, p. 155–164, 2007. DOI: 10.14796/JWMM.R228-10..
- ROESNER, L. A.; ALDRICH, J. A.; DICKINSON, R. E.; BARNWELL, T. O. **Storm Water Management Model User's Manual, Version 4: EXTRAN Addendum**. Athens: Environmental Research Laboratory, Office of Research e Development, US Environmental Protection Agency, 1988.
- ROSSMAN, L. A. Storm Water Management Model Quality Assurance Report: Dynamic Wave Flow Routing. **Storm Water Management Model Quality Assurance Report**, EPA/600/R-06/097, p. 1–115, 2006.
- \_\_\_\_\_. Storm Water Management Model User's Manual Version 5.1. **U.S. Environmental Protection Agency**, EPA/600/R-14/413b, p. 1–353, 2015.
- \_\_\_\_\_. Storm Water Management Model Reference Manual Volume II – Hydraulics. **U.S. Environmental Protection Agency**, Mayo, p. 190, 2017.

- STURM, T. **Open channel hydraulics**. New York: Mc Graw Hill, 2001.
- THORLEY, A. R. D. **Fluid transients in pipeline systems**. Herts: D. e L. George Ltd, 1991.
- TRAJKOVIC, B.; IVETIC, M.; CALOMINO, F.; D'IPPOLITO, A. Investigation of transition from free surface to pressurized flow in a circular pipe. In: 9. WATER Science and Technology. Great Britain: Elsevier Science, 1999. v. 39, p. 105–112.
- TSIHRINTZIS, V. A.; HAMID, R. Runoff quality prediction from small urban catchments using SWMM. **Hydrological Processes**, v. 12, June 1996, p. 311–329, 1998.
- USEPA. **Storm Water Management Model (SWMM) ver. 5.0.13**. 2018. Available at: <<https://www.epa.gov/water-research/storm-water-management-model-swmm>>.
- VASCONCELOS, J. G.; WRIGHT, S. J.; ROE, P. L. Improved Simulation of Flow Regime Transition in Sewers: Two-Component Pressure Approach. **Journal of Hydraulic Engineering**, v. 9429, JUNE 2006, p. 553–562, 2006.
- VASCONCELOS, J. G.; ELDAYIH, Y.; JAMILY, J. A. Evaluating Storm Water Management Model accuracy in mixed flows conditions. **Journal of Water Management Modeling**, p. 1–21, 2018.
- WATTERS, G. Z. **Modern Analysis and Control of Unsteady Flow in Pipelines**. US: Ann Arbor Science Publishers, 1979. P. 92–97. ISBN 0-250-40492-3.
- WOOD, D. J. Waterhammer Analysis — Essential and Easy (and Efficient). **Journal of Environmental Engineering**, v. 9372, August, p. 1123–1131, 2014. ISSN 07339372. DOI: 10.1061/(ASCE)0733-9372(2005)131.
- WYLIE, E. B.; STREETER, V. L.; SUO, L. **Fluid transients in systems**. Prentice Hall Englewood Cliffs, NJ, 1993. v. 1.
- ZAHMATKESH, Z.; BURIAN, S. J.; KARAMOUZ, M.; TAVAKOL-DAVANI, H.; GOHARIAN, E. Low-Impact Development Practices to Mitigate Climate Change Effects on Urban Stormwater Runoff : Case Study of New York City. **Journal of Irrigation and Drainage Engineering**, v. 141, n. 1, p. 1–13, 2015. DOI: 10.1061/(ASCE)IR.1943-4774.0000770..
- ZÁRUBA, J. **Water hammer in pipe-line systems**. Elsevier, 1993. ISBN 0444987223.
- ZHANG, X. X.; CHENG, Y. G. Simulation of hydraulic transients in hydropower systems using the 1-D-3-D coupling approach. **Journal of Hydrodynamics**, Publishing House for Journal of Hydrodynamics, v. 24, n. 4, p. 595–604, 2012. ISSN 10016058. DOI: 10.1016/S1001-6058(11)60282-5. Available at: <[http://dx.doi.org/10.1016/S1001-6058\(11\)60282-5](http://dx.doi.org/10.1016/S1001-6058(11)60282-5)>.

ZHOU, F. et al. Transient flow in a rapidly filling horizontal pipe containing trapped air. **Journal of Hydraulic Engineering**, American Society of Civil Engineers, v. 128, n. 6, p. 625–634, 2002.

## 6 DISCUSSION

The results produced in this Master's Thesis showed that adding artificial spatial discretization and selecting the correct routing time-step and pressurization algorithm allowed SWMM to represent highly dynamic unsteady flows in stormwater and sanitary sewer systems. The verification was evaluated over three articles, where the first used experimental field data, the second used well-known models (ROSSMAN, 2006) and the latter used analytical solutions of slow (PARMAKIAN, 1963; WATTERS, 1979) and fast transients (WYLIE et al., 1993) cases to verify potential improvements in SWMM by adopting artificial discretization, pressurization algorithms and alternatives of time steps. Even though these modeling conditions are strongly dependent and their influence in simulations are difficult to distinguish, some clear understanding on how they influence SWMM modeling were found.

In the first article, a field investigation was conducted to obtain data of rapid inflows in a collection system, comparing the SWMM modeling results to the water level measurements. The link-node approach used originally by SWMM was not capable to properly simulate the water level variation during the rapid filling situation. When artificial spatial discretization was adopted, significant improvements in terms of maximum peak level and water rise and decrease format were achieved. Among the researched approaches to add the spatial discretization, the diameter-based discretization was the recommended approach since it splits the links based on its characteristics. For instance, this discretization increases the calculation points where it is more needed (e.g. long and small conduits) and reduce extra calculation points where it is not required (e.g. short and large conduits). Furthermore, flow continuity errors presented a considerable reduction adopting artificial spatial discretization when compared to the original link-node. Since artificially discretized SWMM models have more calculation points to be solved during the simulation, additional computational effort was required to perform the simulations. However, this extra computational time spent is usual in more contemporary unsteady flow solvers and could be potentially avoided taking advantage of a parallelized SWMM code.

In the second article, SWMM models presented in Rossman (2006) were used to compare the discretized version against its original results. Besides that, comparisons between both available pressurization algorithms (EXTRAN & SLOT) were performed. Strong evidence showed that the SLOT method originally implemented in SWMM 5.1.013 reduced significantly the oscillations or fluctuations that were present in some simulations using the EXTRAN pressurization algorithm. This article also showed that small values of flow continuity error were produced when artificial spatial discretization is adopted, but it required a proper selection of routing time-steps. Running the discretized models simulations estimating the routing time-step following

the Vasconcelos, Eldayih et al. (2018) equation provided adequate routing time-steps. However, in some cases, a more restrict value of the head convergence tolerance was required to maintain the stability. Furthermore, numerical instabilities or oscillations were present in some of the original models that the additional spatial discretization was able to reduce significantly. Even though the computational time to perform the simulations was increased, it is believed that the gains in terms of model accuracy were more relevant. Also, this article showed that the newly implemented SLOT pressurization algorithm has potential to bring considerable improvements to the modeling of in modeling highly dynamic conditions in SWMM.

In the third and last work, classic cases of slow and fast transients were used to verify the SWMM capacity of modeling such situations. Since there are not many available data related to these phenomena, analytical solutions considering some simplifications were used. It is known that SWMM was not originally conceived to model these situations but the new SLOT method - with some modifications - can expand the SWMM applications to transient analysis. It was found that the EXTRAN pressurization algorithm is dependent of the temporal and spatial discretization, not being recommended for transient analysis in SWMM. The original SLOT implementation simulations showed some discrepancies when compared to the analytical solutions. Reducing the original slot width based on predetermined values of celerity leaded to more accurate results. Also, estimating routing time-steps based on the Courant condition produced more accurate simulations than those estimated by the EXTRAN based equations. The Courant condition seemed to estimate proper routing time-steps for situations such as pressurized flows or the transition from open-channel to pressurized flows. Moreover, the non-discretized models did not represent properly the analytical solutions but, when artificial spatial discretization is adopted along proper selection of routing time-step and pressurization algorithm, SWMM was able to represent slow and fast transients.

All things considered, the SWMM applications can be extended to more dynamic flows adapting its SLOT pressurization algorithm. Since the link-node approach used by SWMM is not suitable to represent these conditions, it is strongly recommended the use of artificial spatial discretization when dynamic flows are expected to occur in a simulation. Along the spatial discretization, a proper routing time-step should be selected but estimating it is not an easy task. It is difficult to recommend a specific value or equation for estimating routing time-steps that works properly for all situations since it depends directly on the system modeled and/or dynamics involved. However, based on previous works (ROESNER et al., 1988; VASCONCELOS; ELDAYIH et al., 2018) and in this thesis findings, an initial estimation of routing time-steps can be based on:

- Modeling without drastic changes in free flow conditions:

$$\Delta t = \frac{\Delta x}{\sqrt{gD}}, \quad (6.1)$$

- Modeling expecting rapid filling and/or mixed flows:

$$\Delta t = 0.1 \frac{\Delta x}{\sqrt{gD}}, \quad (6.2)$$

- Modeling transients in pressurized conduits:

$$\Delta t = 0.9 \frac{\Delta x}{a}. \quad (6.3)$$

It is important to highlight that this is a recommendation and not a rule. In some cases a more restrict routing time-step may be required.

Finally, these new modeling features explored in this thesis must be carefully considered by the user. In some cases, the simulation options, such as head convergence tolerance or inertial terms, must be adjusted to run a suitable simulation without any kind of numerical instability or continuity error. Even though reliable data were used in these articles, an analysis between SWMM and more robust models should be performed for comparison purposes.



## 7 CONCLUSIONS

This work assessed different SWMM approaches to simulate dynamic flows usually present in stormwater systems. Several simulation conditions were tested considering variations in spatial and temporal discretization along different pressurization algorithms. The findings of this work may be summarized as follows:

- SWMM is capable to simulate highly dynamic flows, such as slow and fast transients, with a correct selection of pressurization algorithm and spatial and temporal discretization;
- The traditional link-node approach used in SWMM does not properly simulate highly dynamic flows;
- The best technique to discretize SWMM is based on the link diameter;
- Extra computational effort is introduced by the artificial spatial discretization but it is comparable to other models that are able to represent transient flows;
- Flow continuity errors and numerical instability are significantly decreased when artificial spatial discretization is adopted along a proper selection of routing time-step;
- Spatially discretized models may have a more restrict head convergence tolerance or the inertial terms adjusted;
- SWMM is able to simulate transients in pressurized conduits using the SLOT pressurization algorithm with a narrower slot based on celerity values;
- The EXTRAN pressurization algorithm is not recommended to simulate transients in pressurized conduits because it is strongly dependent of the spatial and temporal discretization;
- Courant based equations estimate better routing time-steps for transients simulations;
- A software that introduces the artificial spatial discretization in SWMM input files was developed (Appendix A).

## REFERENCES

- ABDUL-AZIZ, O. I.; AL-AMIN, S. Climate, land use and hydrologic sensitivities of stormwater quantity and quality in a complex coastal-urban watershed. **Urban Water Journal**, v. 13, n. 3, p. 302–320, 2016. ISSN 17449006. DOI: 10.1080/1573062X.2014.991328.
- ARDUINO. 2018. Accessed in 16 January, 2018. Available at: <<http://www.arduino.cc/en/Guide/Introduction>>.
- ASCE. Criteria for Evaluation of Watershed Models. **Journal of Irrigation and Drainage Engineering**, v. 119, n. 3, p. 429–442, 1993.
- BATES, P. D.; LANE, S. N.; FERGUSON, R. I. **Computational fluid dynamics: applications in environmental hydraulics**. Chichester: John Wiley & Sons, 2005.
- BOUSSO, S.; DAYNOU, M.; FUAMBA, M. Numerical Modeling of Mixed Flows in Storm Water Systems : Critical Review of Literature. **Journal of Hydraulic Engineering**, v. 139, April, p. 385–396, 2013. DOI: 10.1061/(ASCE)HY.1943-7900.0000680.
- BRATER, E. F.; KING, H. W.; LINDELL, J. E.; WEI, C. Y. **Handbook of Hydraulics**. 7. ed. New York: McGraw-Hill, 1996.
- BUAHIN, C. A.; HORSBURGH, J. S. Advancing the Open Modeling Interface (OpenMI) for integrated water resources modeling. **Environmental Modelling and Software**, v. 108, April, p. 133–153, 2018. ISSN 13648152. DOI: 10.1016/j.envsoft.2018.07.015.
- BURGER, G.; SITZENFREI, R.; KLEIDORFER, M.; RAUCH, W. Parallel flow routing in SWMM 5. **Environmental Modelling and Software**, v. 53, p. 27–34, 2014. ISSN 13648152. DOI: 10.1016/j.envsoft.2013.11.002.
- CAMORANI, G.; CASTELLARIN, A.; BRATH, A. Effects of land-use changes on the hydrologic response of reclamation systems. **Physics and Chemistry of the Earth**, v. 30, p. 561–574, 2005. DOI: 10.1016/j.pce.2005.07.010.
- CAMPISANO, A.; CATANIA, F. V.; MODICA, C. Evaluating the SWMM LID Editor rain barrel option for the estimation of retention potential of rainwater harvesting systems. **Urban Water Journal**, Taylor & Francis, v. 14, n. 8, p. 876–881, 2017. ISSN 17449006. DOI: 10.1080/1573062X.2016.1254259. Available at: <<http://dx.doi.org/10.1080/1573062X.2016.1254259>>.
- CAMPISANO, A.; GULLOTTA, A.; MODICA, C. Using EPA-SWMM to simulate intermittent water distribution systems. **Urban Water Journal**, Taylor & Francis, v. 00, n. 00, p. 1–9, 2019. DOI: 10.1080/1573062X.2019.1597379. Available at: <<https://www.tandfonline.com/doi/full/10.1080/1573062X.2019.1597379>>.

CAPART, H.; SILLEN, X.; ZECH, Y. Numerical and experimental water transients in sewer pipes. **Journal of Hydraulic Research**, v. 1686, 1997. DOI: 10.1080/00221689709498400.

CHAUDHRY, M. H. **Open-channel flow**. New York: Springer Science & Business Media, 2007.

\_\_\_\_\_. **Applied hydraulic transients**. Third Edit. New York: Springer, 2013. v. 9781461485, p. 1–583. ISBN 9781461485384. DOI: 10.1007/978-1-4614-8538-4.

\_\_\_\_\_. **Open Channel Flow**. Springer Science & Business Media, 2008. P. 523. ISBN 9780387301747. DOI: 10.1007/978-0-387-68648-6.

CHO, J. H.; SEO, H. J. Parameter optimization of SWMM for runoff quantity and quality calculation in a eutrophic lake watershed using a genetic algorithm. **Water Science and Technology: Water Supply**, v. 7, n. 5-6, p. 35–41, 2007. ISSN 16069749. DOI: 10.2166/ws.2007.114.

CHOW, M. F.; YUSOP, Z.; TORIMAN, M. E. Modelling runoff quantity and quality in tropical urban catchments using Storm Water Management Model. **International Journal of Environmental Science and Technology**, p. 737–748, 2012. DOI: 10.1007/s13762-012-0092-0.

CUNGE, J. A.; HOLLY, F. M.; VERWEY, A. **Practical aspects of computational river hydraulics**. London: Pitman publishing, 1980.

DENAULT, C.; MILLAR, R. G.; LENCE, B. J. Assessment of possible impacts of climate change in an urban catchment. **Journal of the American Water Resources Association**, v. 42, n. 3, p. 685–697, 2006. ISSN 1093474X. DOI: 10.1111/j.1752-1688.2006.tb04485.x.

DHI. **Mouse Pipe Flow**. MIKE URBAN, 2017.

DI MODUGNO, M.; GIOIA, A.; GORGOGNONE, A.; IACOBELLIS, V.; FORGIA, G. la; PICCINNI, A. F.; RANIERI, E. Build-up/wash-off monitoring and assessment for sustainable management of first flush in an urban area. **Sustainability (Switzerland)**, v. 7, n. 5, p. 5050–5070, 2015. ISSN 20711050. DOI: 10.3390/su7055050.

DONGQUAN, Z.; JINING, C.; HAOZHENG, W.; QINGYUAN, T.; SHANGBING, C.; ZHENG, S. GIS-based urban rainfall-runoff modeling using an automatic catchment-discretization approach: A case study in Macau. **Environmental Earth Sciences**, v. 59, n. 2, p. 465–472, 2009. ISSN 18666280. DOI: 10.1007/s12665-009-0045-1.

FALCÃO DE CAMPOS, J. A.; FERREIRA DE SOUSA, P. J.; BOSSCHERS, J. A verification study on low-order three-dimensional potential-based panel codes. **Computers and Fluids**, v. 35, n. 1, p. 61–73, 2006. ISSN 00457930. DOI: 10.1016/j.compfluid.2004.08.002.

GHIDAOU, M. S.; ZHAO, M.; MCINNIS, D. A.; AXWORTHY, D. H. A Review of Water Hammer Theory and Practice. **Applied Mechanics Reviews**, v. 58, n. 1, p. 49, 2005. ISSN 00036900. DOI: 10.1115/1.1828050.

GHOSH, I.; HELLWEGER, F. L. Effects of Spatial Resolution in Urban Hydrologic Simulations. **Journal of Hydrologic Engineering**, v. 17, January, p. 129–137, 2012. ISSN 1084-0699. DOI: 10.1061/(ASCE)HE.1943-5584.0000405.

GIRONÁS, J.; ROESNER, L. A.; ROSSMAN, L. A.; DAVIS, J. A new applications manual for the Storm Water Management Model (SWMM). **Environmental Modelling & Software**, v. 25, n. 6, p. 813–814, 2010. ISSN 13648152. DOI: 10.1016/j.envsoft.2009.11.009. Available at: <<http://linkinghub.elsevier.com/retrieve/pii/S1364815209002989>>.

GUIZANI, M.; JOSE, G.; STEVEN, J.; KHLIFA, M. et al. Investigation of rapid filling of empty pipes. **The Journal of Water Management Modeling**, Computational Hydraulics International (CHI), v. 225, n. 20, p. 463–482, 2006.

GUO, L. L.; LIU, Z. G.; GENG, J.; LI, D.; DU, G. S. Numerical study of flow fluctuation attenuation performance of a surge tank. **Journal of Hydrodynamics**, Publishing House for Journal of Hydrodynamics, v. 25, n. 6, p. 938–943, 2013. ISSN 10016058. DOI: 10.1016/S1001-6058(13)60443-6. Available at: <[http://dx.doi.org/10.1016/S1001-6058\(13\)60443-6](http://dx.doi.org/10.1016/S1001-6058(13)60443-6)>.

GUO, Q.; SONG, C. C. S. Surging in urban storm drainage systems. v. 116, n. 12, p. 1523–1537, 1991.

HAMAM, M. A.; MCCORQUODALE, J. A. Transient conditions in the transition from gravity to surcharged sewer flow. **Canadian Journal of Civil Engineering**, v. 9, n. 2, p. 189–197, 1982. DOI: 10.1139/182-022.

HODGES, B. R.; LIU, F.; ROWNEY, A. C. **A New Saint-Venant Solver for SWMM**. Springer International Publishing, 2019. v. 1, p. 582–586. ISBN 9783319998671. DOI: 10.1007/978-3-319-99867-1. Available at: <[http://dx.doi.org/10.1007/978-3-319-99867-1%7B%5C\\_%7D100](http://dx.doi.org/10.1007/978-3-319-99867-1%7B%5C_%7D100)>.

HUBER, W.; ROESNER, L. The History and Evolution of the EPA SWMM" in "Fifty Years Of Watershed Modeling - Past, Present And Future. **Engineering Conferences International Symposium Series**. <http://dc.engconfintl.org/watershed/29>, 2012. Available at: <<http://dc.engconfintl.org/cgi/viewcontent.cgi?article=1001&context=watershed>>.

JOUKOWSKI, N. Water hammer. **Proceedings of American Water Works Association**, v. 24, p. 341–424, 1904.

JUNG, B. S.; KARNEY, B. A practical overview of unsteady pipe flow modeling: from physics to numerical solutions. **Urban Water Journal**, v. 14, n. 5, p. 502–508, 2017. ISSN 17449006. DOI: 10.1080/1573062X.2016.1223323.

KENDIR, T. E.; OZDAMAR, A. Numerical and experimental investigation of optimum surge tank forms in hydroelectric power plants. **Renewable Energy**, Elsevier Ltd, v. 60, p. 323–331, 2013. ISSN 09601481. DOI: 10.1016/j.renene.2013.05.016. Available at: <<http://dx.doi.org/10.1016/j.renene.2013.05.016>>.

KERGER, F.; ARCHAMBEAU, P.; ERPICUM, S.; DEWALS, B. J.; PIROTON, M. Journal of Computational and Applied An exact Riemann solver and a Godunov scheme for simulating highly transient mixed flows. **Journal of Computational and Applied Mathematics**, Elsevier B.V., v. 235, n. 8, p. 2030–2040, 2011. ISSN 0377-0427. DOI: 10.1016/j.cam.2010.09.026. Available at: <<http://dx.doi.org/10.1016/j.cam.2010.09.026>>.

KIM, S. H. Design of surge tank for water supply systems using the impulse response method with the GA algorithm. **Journal of Mechanical Science and Technology**, v. 24, n. 2, p. 629–636, 2010. ISSN 1738494X. DOI: 10.1007/s12206-010-0108-y.

KREBS, G.; KOKKONEN, T.; VALTANEN, M.; SETÄLÄ, H.; KOIVUSALO, H. Spatial resolution considerations for urban hydrological modelling. **Journal of Hydrology**, Elsevier B.V., v. 512, p. 482–497, 2014. ISSN 00221694. DOI: 10.1016/j.jhydrol.2014.03.013. Available at: <<http://dx.doi.org/10.1016/j.jhydrol.2014.03.013>>.

KULLER, M.; BACH, P. M.; RAMIREZ-LOVERING, D.; DELETIC, A. Framing water sensitive urban design as part of the urban form: A critical review of tools for best planning practice. **Environmental Modelling and Software**, Elsevier Ltd, v. 96, p. 265–282, 2017. ISSN 13648152. DOI: 10.1016/j.envsoft.2017.07.003. Available at: <<http://dx.doi.org/10.1016/j.envsoft.2017.07.003>>.

LEGATES, D. R.; JR., G. J. M. Evaluating the use of "goodness-of-fit" measures in hydrologic and hydroclimatic model validation. **WATER RESOURCES RESEARCH**, VOL., v. 35, n. 1, p. 233–241, 1999.

LI, J.; MCCORQUODALE, A. Modeling the Transition from Gravity to Pressurized Flows in Sewers. **Urban Drainage Modeling**, p. 134–145, 2001. DOI: doi:10.1061/40583(275)14.

LI, J.; MCCORQUODALE, A. Modeling Mixed Flow in Storm Sewers. **Journal of Hydraulic Engineering**, v. 125, n. 1983, p. 1170–1180, 1999.

MAIR, M.; SITZENFREI, R.; KLEIDORFER, M.; RAUCH, W. Performance improvement with parallel numerical model simulations in the field of urban water management. **Journal of Hydroinformatics**, v. 16, n. 2, p. 477–486, 2014. ISSN 1464-7141. DOI: 10.2166/hydro.2013.287.

- MALEKPOUR, A.; KARNEY, B. W. Spurious Numerical Oscillations in the Preissmann Slot Method: Origin and Suppression. **Journal of Hydraulic Engineering**, v. 142, n. 3, p. 04015060, 2015. ISSN 0733-9429. DOI: 10.1061/(asce)hy.1943-7900.0001106.
- MARCHI, C. H. Effect of P-Norms on the Accuracy Order of Numerical Solution Errors in Cfd. **Fluid Dynamics**, 2010.
- MATHEOU, G.; PANTANO, C.; DIMOTAKIS, P. E. Verification of a fluid-dynamics solver using correlations with linear stability results. **Journal of Computational Physics**, v. 227, n. 11, p. 5385–5396, 2008. ISSN 00219991. DOI: 10.1016/j.jcp.2008.01.055.
- MAYS, L. W. **Stormwater Collection Systems Design Handbook**. New York: McGraw-Hill Education, 2001. P. 1008.
- MEIERDIERCKS, K. L.; SMITH, J. A.; BAECK, M. L.; MILLER, A. J. Analyses of Urban Drainage Network Structure and Its Impact on Hydrologic Response. **Journal of the American Water Resources Association**, v. 46, n. 5, 2010.
- MEYERS, J.; GEURTS, B. J.; SAGAUT, P. A computational error-assessment of central finite-volume discretizations in large-eddy simulation using a Smagorinsky model. **Journal of Computational Physics**, v. 227, n. 1, p. 156–173, 2007. ISSN 00219991. DOI: 10.1016/j.jcp.2007.07.012.
- MOHAMED. YOSSEF. Flow Details near River Groynes: Experimental Investigation. **ASCE Journal of Hydraulic Engineering**, v. 138, July, p. 642–652, 2015. DOI: 10.1061/(ASCE)HY.1943-7900.
- MULETA, M. K.; PH, D.; NICKLOW, J. W.; PH, D.; BEKELE, E. G.; PH, D. Sensitivity of a Distributed Watershed Simulation Model. **Journal of Hydrologic Engineering**, v. 0699, March, 2007. DOI: 10.1061/(ASCE)1084-0699(2007)12.
- NASH, E.; SUTCLIFFE, V. River Flow Forecasting Through Conceptual Models Part I - A Discussion of Principles. **Journal of Hydrology**, v. 10, p. 282–290, 1970.
- NIAZI, M.; NIETCH, C.; MAGHREBI, M.; JACKSON, N.; BENNETT, B. R.; TRYBY, M.; MASSOUDIEH, A. Storm Water Management Model: Performance Review and Gap Analysis. **Journal of Sustainable Water Built Environment**, v. 3, n. 2, 2017. DOI: 10.1061/JSWBAY.0000817..
- NOVAK, P.; GUINOT, V.; ALAN, J.; E REEVE, D. **Hydraulic Modelling: an introduction, principles, methods and applications**. New York: Spon Press, 2010. v. 48, p. 599. ISBN 9780419250104. DOI: 10.1080/00221686.2010.492104.
- OBROPTA, C. C.; KARDOS, J. S. Review of Urban Stormwater Quality Models: Deterministic, Stochastic, and Hybrid Approaches. **Journal of the American Water Resources Association**, v. 43, n. 6, p. 1508–1523, 2007. DOI: 10.1111/j.1752-1688.2007.00124.x.

PACHALY, R. L.; VASCONCELOS, J. G.; ALLASIA, D. G. P. **ReSWMM v0.1**. GitHub, 2018. Available at: <<https://github.com/ecotecnologias/ReSWMM>>.

PACHALY, R. L.; VASCONCELOS, J. G.; ALLASIA, D. G. P.; MINETTO, B. Field evaluation of discretized model setups for the Storm Water Management Model. **Journal of Water Management Modeling**, p. 1–16, 2019. ISSN 2292-6062. DOI: 10.14796/JWMM.C465.

PARK, S.; LEE, K.; PARK, I.; HA, S. Effect of the aggregation level of surface runoff fields and sewer network for a SWMM simulation. **Desalination**, v. 226, n. 1, p. 328–337, 2008. 10th IWA International Specialized Conference on Diffuse Pollution and Sustainable Basin Management. ISSN 0011-9164. DOI: <https://doi.org/10.1016/j.desal.2007.02.115>. Available at: <<http://www.sciencedirect.com/science/article/pii/S0011916408001653>>.

PARMAKIAN, J. **Waterhammer analysis**. New York: Prentice-Hall, 1963. v. 9.

POLITANO, M.; ODGAARD, a. J.; KLECAN, W. Case Study: Numerical Evaluation of Hydraulic Transients in a Combined Sewer Overflow Tunnel System. **Journal of Hydraulic Engineering**, v. 133, 2007.

POPESCU, I. **Computational Hydraulics**. London: IWA Publishing, 2014. ISBN 9781780400440.

PREISSMANN, A. Propagation of translatory waves in channels and rivers. In: PROCEEDINGS of the 1st Congress of French Association for Computation, Grenoble, France. 1961. P. 432–443.

QIN, H.-p.; LI, Z.-x.; FU, G. The effects of low impact development on urban flooding under different rainfall characteristics. **Journal of Environmental Management**, Elsevier Ltd, v. 129, p. 577–585, 2013. ISSN 0301-4797. DOI: 10.1016/j.jenvman.2013.08.026. Available at: <<http://dx.doi.org/10.1016/j.jenvman.2013.08.026>>.

RIAÑO-BRICEÑO, G.; BARREIRO-GOMEZ, J.; RAMIREZ-JAIME, A.; QUIJANO, N.; OCAMPO-MARTINEZ, C. MatSWMM - An open-source toolbox for designing real-time control of urban drainage systems. **Environmental Modelling and Software**, v. 83, p. 143–154, 2016. ISSN 13648152. DOI: 10.1016/j.envsoft.2016.05.009.

RIDGWAY, K. E. Evaluating Force Main Transients with SWMM5 and Other Programs. v. 6062, p. 43–54, 2008. DOI: 10.14796/JWMM.R236-04..

RIDGWAY, K. E.; KUMPULA, G. Surge Modeling in Sewers using the Transient Analysis Program (TAP). **Journal of Water Management Modeling**, v. 6062, p. 155–164, 2007. DOI: 10.14796/JWMM.R228-10..

ROESNER, L. A.; ALDRICH, J. A.; DICKINSON, R. E.; BARNWELL, T. O. **Storm Water Management Model User's Manual, Version 4: EXTRAN Addendum**. Athens: Environmental Research Laboratory, Office of Research e Development, US Environmental Protection Agency, 1988.

ROSSMAN, L. A. Storm Water Management Model Quality Assurance Report: Dynamic Wave Flow Routing. **Storm Water Management Model Quality Assurance Report**, EPA/600/R-06/097, p. 1–115, 2006.

\_\_\_\_\_. Storm Water Management Model User's Manual Version 5.1. **U.S. Environmental Protection Agency**, EPA/600/R-14/413b, p. 1–353, 2015.

\_\_\_\_\_. Storm Water Management Model Reference Manual Volume II – Hydraulics. **U.S. Environmental Protection Agency**, Mayo, p. 190, 2017.

STURM, T. **Open channel hydraulics**. New York: Mc Graw Hill, 2001.

SUN, N.; HALL, M.; HONG, B.; ZHANG, L. Impact of SWMM Catchment Discretization: Case Study in Syracuse, New York. **Journal of Hydrologic Engineering**, v. 19, n. 1, p. 223–234, 2014. ISSN 1084-0699. DOI: 10.1061/(ASCE)HE.1943-5584.0000777. Available at: <<http://ascelibrary.org/doi/10.1061/%7B%5C%7D28ASCE%7B%5C%7D29HE.1943-5584.0000777>>.

TEMPRANO, J.; ARANGO, Ó.; CAGIAO, J.; SUÁREZ, J.; TEJERO, I. Stormwater quality calibration by SWMM: A case study in Northern Spain. **Water SA**, v. 32, Jan. 21, 2002, p. 5, 2006. ISSN 0959-3330. DOI: 10.1080/09593332308618381.

THORLEY, A. R. D. **Fluid transients in pipeline systems**. Herts: D. e L. George Ltd, 1991.

TRAJKOVIC, B.; IVETIC, M.; CALOMINO, F.; D'IPPOLITO, A. Investigation of transition from free surface to pressurized flow in a circular pipe. In: 9. WATER Science and Technology. Great Britain: Elsevier Science, 1999. v. 39, p. 105–112.

TRIPATHI, M. P.; RAGHUWANSHI, N. S.; RAO, G. P. Effect of watershed subdivision on simulation of water. **Hydrological Processes**, v. 1156, December 2005, p. 1137–1156, 2006. DOI: 10.1002/hyp.5927.

TSIHRINTZIS, V. A.; HAMID, R. Runoff quality prediction from small urban catchments using SWMM. **Hydrological Processes**, v. 12, June 1996, p. 311–329, 1998.

USEPA. **Storm Water Management Model (SWMM) ver. 5.0.13**. 2018. Available at: <<https://www.epa.gov/water-research/storm-water-management-model-swmm>>.

VASCONCELOS, J. G.; WRIGHT, S. J. Numerical modeling of the transition between free surface and pressurized flow in storm sewers. **Innovative modeling of urban water systems, Monograph 12**, v. 12, p. 189–214, 2004. DOI: 10.14796/JWMM.R220-10..



VASCONCELOS, J. G.; WRIGHT, S. J.; ROE, P. L. Improved Simulation of Flow Regime Transition in Sewers: Two-Component Pressure Approach. **Journal of Hydraulic Engineering**, v. 9429, JUNE 2006, p. 553–562, 2006.

VASCONCELOS, J. G.; ELDAYIH, Y.; JAMILY, J. A. Evaluating Storm Water Management Model accuracy in mixed flows conditions. **Journal of Water Management Modeling**, p. 1–21, 2018.

VASCONCELOS, J. G.; WRIGHT, S. J.; ROE, P. L. Current Issues on Modeling Extreme Inflows in Stormwater Systems. **Journal of Water Management Modeling**, v. 6062, p. 225–19, 2006. DOI: 10.14796/JWMM.R225-19.

WATTERS, G. Z. **Modern Analysis and Control of Unsteady Flow in Pipelines**. US: Ann Arbor Science Publishers, 1979. P. 92–97. ISBN 0-250-40492-3.

WOOD, D. J. Waterhammer Analysis — Essential and Easy (and Efficient). **Journal of Environmental Engineering**, v. 9372, August, p. 1123–1131, 2014. ISSN 07339372. DOI: 10.1061/(ASCE)0733-9372(2005)131.

WOOD, E. F.; SIVAPALAN, M.; BEVEN, K.; BAND, L. Effects of spatial variability and scale with implications to hydrologic modeling. **Journal of Hydrology**, v. 102, n. 1-4, p. 29–47, 1988. ISSN 00221694. DOI: 10.1016/0022-1694(88)90090-X.

WRIGHT, S. J.; VASCONCELOS, J. G.; CREECH, C. T.; LEWIS, J. W. Flow regime transition mechanisms in rapidly filling stormwater storage tunnels. **Environmental Fluid Mechanics**, v. 8, n. 5-6, p. 605–616, 2008.

WRIGHT, S. J.; VASCONCELOS, J. G.; RIDGWAY, K. E. Stormwater Storage Tunnels. **Journal of Water Management Modeling**, v. 6062, p. 357–372, 2003. DOI: 10.14796/JWMM.R215-18..

WYLIE, E. B.; STREETER, V. L.; SUO, L. **Fluid transients in systems**. Prentice Hall Englewood Cliffs, NJ, 1993. v. 1.

YEN, B. C. Hydraulics of sewers. In: **ADVANCES in hydroscience**. Orlando: Elsevier, 1986. v. 14. P. 1–122.

ZAGHLOUL, N. A. SWMM model and level of discretization. **Journal of the Hydraulics Division**, ASCE, v. 107, n. 11, p. 1535–1545, 1981.

ZAHMATKESH, Z.; BURIAN, S. J.; KARAMOUZ, M.; TAVAKOL-DAVANI, H.; GOHARIAN, E. Low-Impact Development Practices to Mitigate Climate Change Effects on Urban Stormwater Runoff : Case Study of New York City. **Journal of Irrigation and Drainage Engineering**, v. 141, n. 1, p. 1–13, 2015. DOI: 10.1061/(ASCE)IR.1943-4774.0000770..

ZÁRUBA, J. **Water hammer in pipe-line systems**. Elsevier, 1993. ISBN 0444987223.

ZHANG, X. X.; CHENG, Y. G. Simulation of hydraulic transients in hydropower systems using the 1-D-3-D coupling approach. **Journal of Hydrodynamics**, Publishing House for Journal of Hydrodynamics, v. 24, n. 4, p. 595–604, 2012. ISSN 10016058. DOI: 10.1016/S1001-6058(11)60282-5. Available at: <[http://dx.doi.org/10.1016/S1001-6058\(11\)60282-5](http://dx.doi.org/10.1016/S1001-6058(11)60282-5)>.

ZHOU, F. et al. Transient flow in a rapidly filling horizontal pipe containing trapped air. **Journal of Hydraulic Engineering**, American Society of Civil Engineers, v. 128, n. 6, p. 625–634, 2002.

ZOPPOU, C. Review of urban storm water models. **Environmental Modelling and Software**, v. 16, n. 3, p. 195–231, 2001. ISSN 13648152. DOI: 10.1016/S1364-8152(00)00084-0.

## APPENDIX A – RESWMM (V 0.1)

ReSWMM is an application for SWMM that introduces artificial spatial discretization in SWMM models. The routing algorithm used by SWMM does not employ intermediate calculation points between two adjacent nodes. In some highly dynamic situations, such as pressurization of conduits, entrapment of air pockets within the pipes, pressure surges, pipe-filling bores and even waterhammers, artificial spatial discretization along with the full form of the St. Venant equations brings significant improvements in SWMM results.

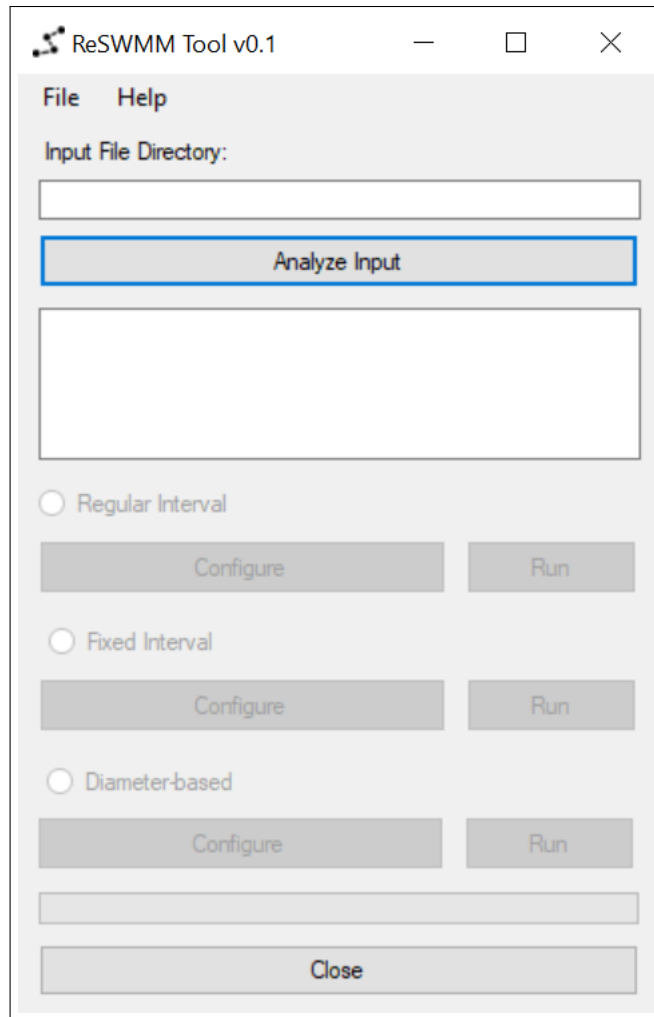
This software (Figure A.1) is able to read and edit the SWMM input file, recommend the routing time-step based on Roesner et al. (1988) and Vasconcelos et al. (2018), and create artificial spatial discretization by placing intermediate calculation points (dummy nodes) between actual nodes. Furthermore, the software analyses the input file to verify if discretization is required. This analysis is also based on the EXTRAN recommendation that the longest conduit in the system should not exceed four or five times the length of the shortest conduit.

Three types of discretization are available in its current version:

- Regular Interval Discretization: places a regular number of dummy nodes between actual nodes.
- Fixed Interval Discretization: limits the maximum and minimum space between dummy nodes by a maximum and minimum threshold.
- Diameter Based discretization: sets the number of dummy nodes in each link based on a ratio between the conduit length and diameter/max depth.

This application can be coupled within SWMM as an add-on or executed as a standalone application. The following sections will describe how to add this tool within SWMM and how to execute it as a standalone application. Also, an example showing the results of this tool is provided.

Figure A.1 – ReSWMM interface.

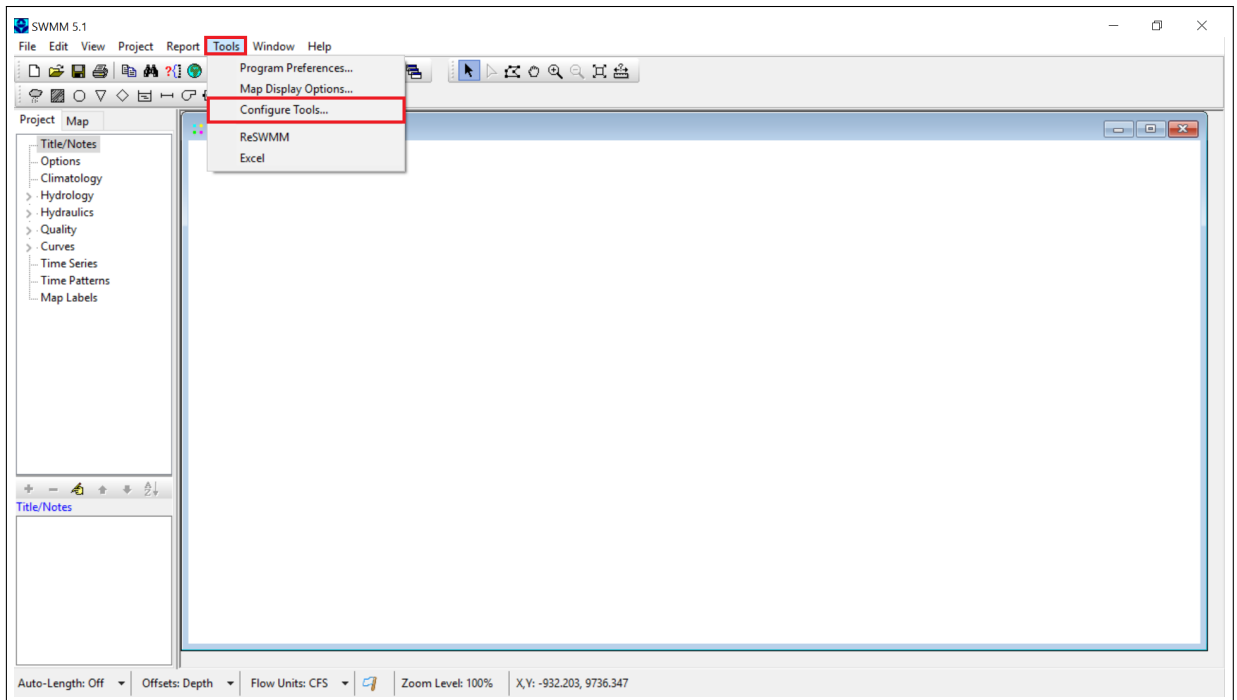


Source: The Author.

## A.1 SWMM ADD-ON

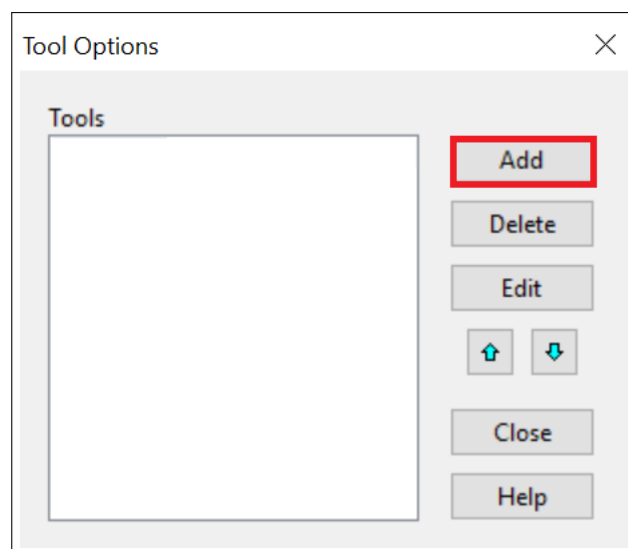
In order to use ReSWMM as an SWMM Add-on, the user must select Tool > Configure Tools (Figure A.2) in the SWMM interface and then click on Add (Figure A.3).

Figure A.2 – SWMM interface.



Source: USEPA (2018)

Figure A.3 – SWMM tool options.

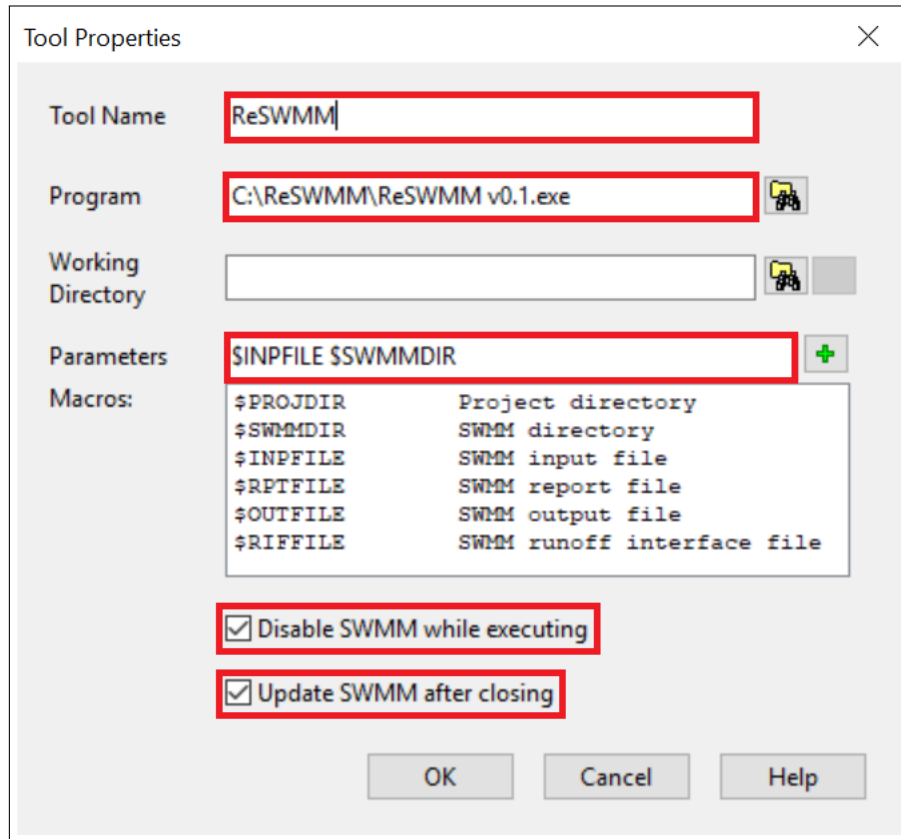


Source: USEPA (2018)

After, the user must fill the black spaces marked in red (Figure A.4). Tool Name should be filled with ReSWMM. In Program, the ReSWMM executable directory should be selected. In parameters, \$INPFILE and \$SWMMDIR should be selected. Finally,

the two options in the bottom should be marked.

Figure A.4 – SWMM add-on configuration.



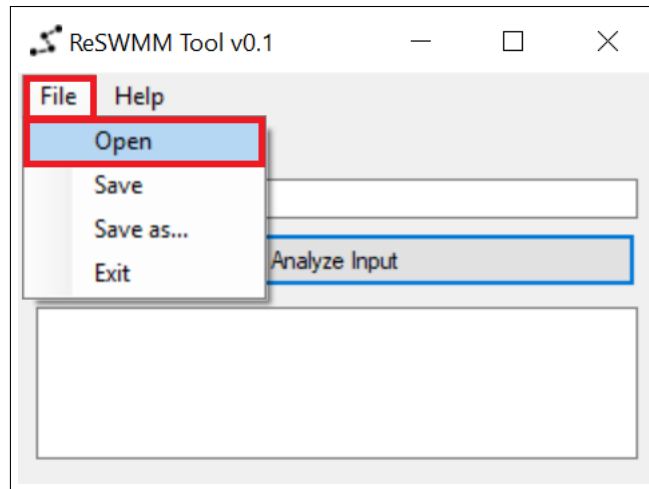
Source: USEPA (2018)

After this, the ReSWMM will appear at the Tool menu strip as shown in Figure A.2.

## A.2 STANDALONE APPLICATION

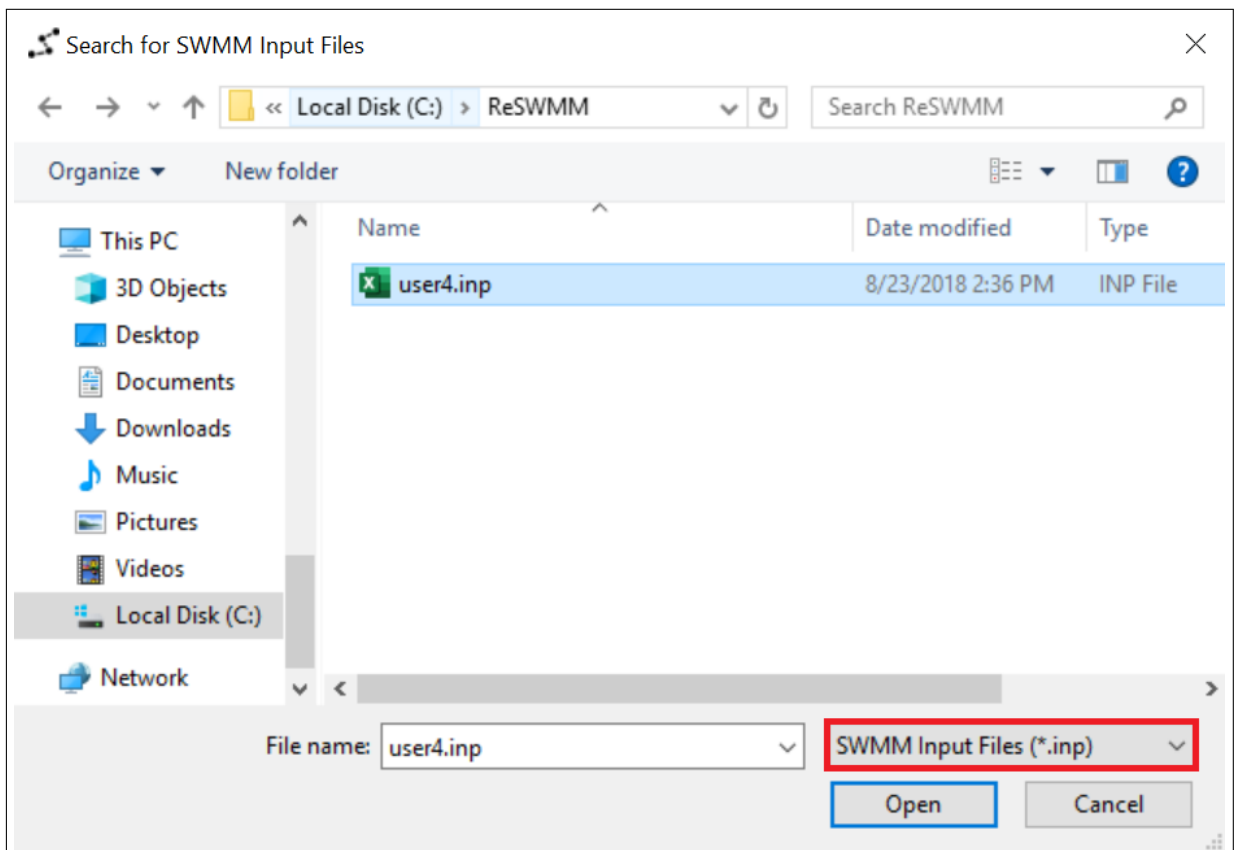
In order to work as a standalone application, the user only has to click on the ReSWMM executable (.exe) and select an SWMM input file (.inp) as shown in Figure A.5 and Figure A.6.

Figure A.5 – ReSWMM open input file.



Source: The Author.

Figure A.6 – ReSWMM select input file.

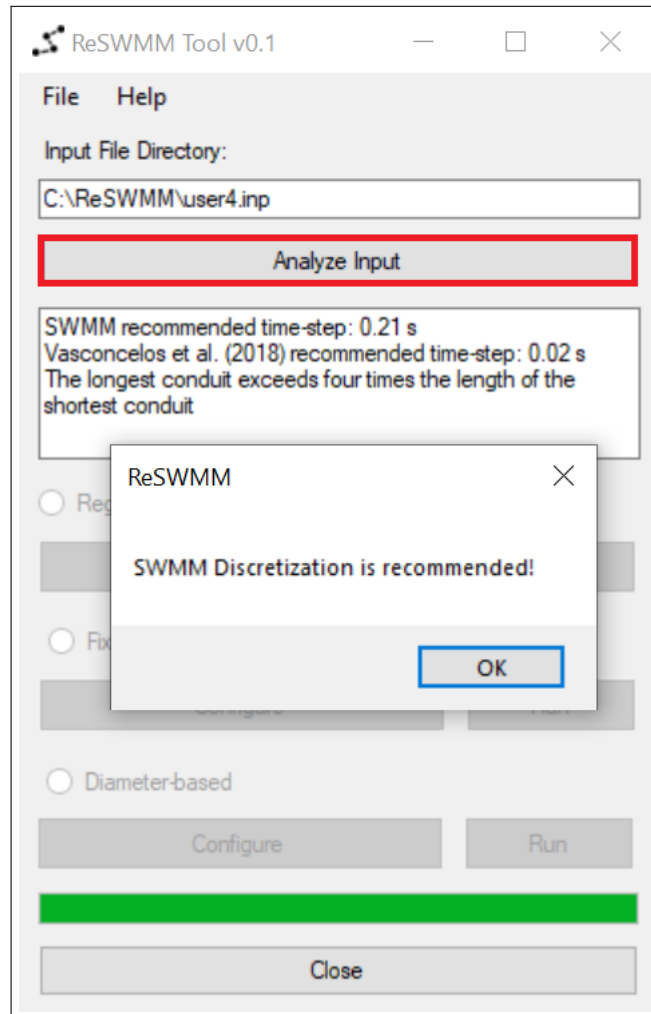


Source: The Author.

After this point, there is no difference in using ReSWMM as an add-on or as a standalone application.

With the SWMM input file selected, the user must analyze the input file clicking on Analyze Input as shown in Figure A.7. If the longest conduit in the system exceeds four times the length of the shortest conduit, ReSWMM will recommend to discretize the input file. If there is no need for discretization based on the Roesner et al. (1988) recommendation, the user can still discretize the model.

Figure A.7 – ReSWMM analyze input file.

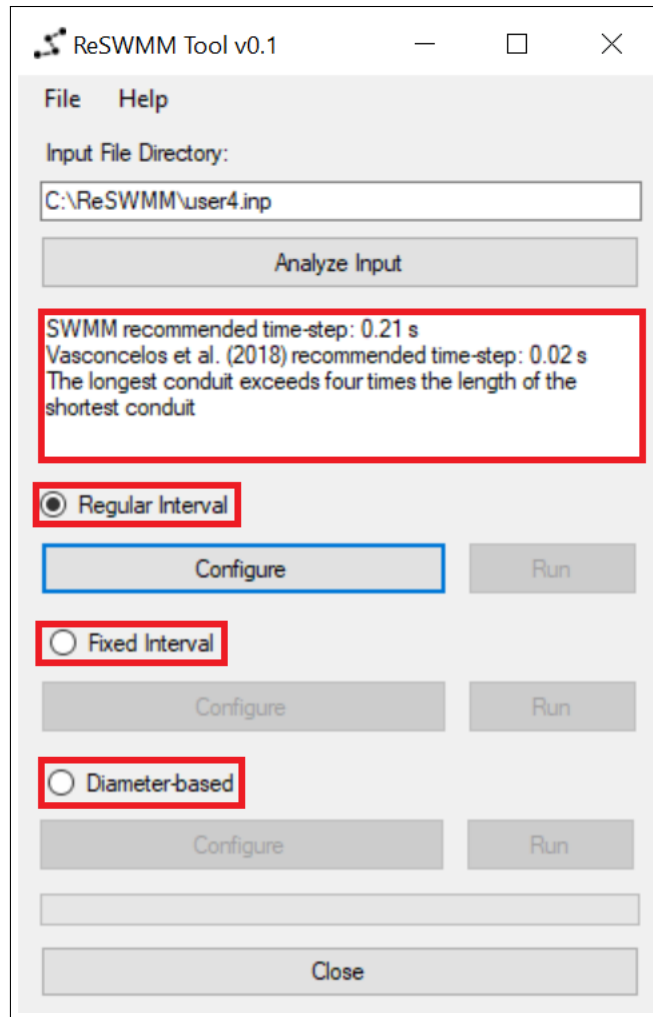


Source: The Author.

The two routing time-steps estimated by ReSWMM will appear at the text box as shown in Figure A.8. At this point, the user will be able to select which type of spatial discretization technique he will adopt to add the dummy nodes.



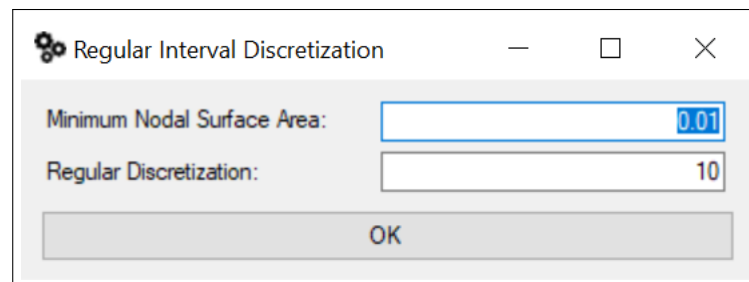
Figure A.8 – ReSWMM select discretization technique.



Source: The Author.

If the user selects the Regular Interval, a window as shown in Figure A.9 will appear. The user will be able to select a new value for the Minimum Nodal Surface Area (0.01 or less is recommended) and the quantity of dummy nodes that will be placed in-between the actual nodes.

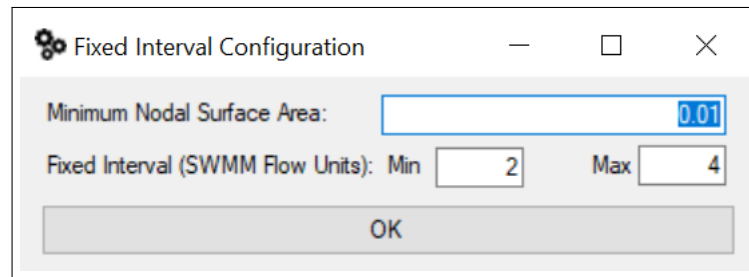
Figure A.9 – ReSWMM regular interval.



Source: The Author.

If the user selects the Fixed Interval, a window as shown in Figure A.10 will appear. The user will be able to select a new value for the Minimum Nodal Surface Area (0.01 or less is recommended) and the minimum and maximum threshold (in SWMM flow units) that will limit the minimum and maximum space between the dummy nodes.

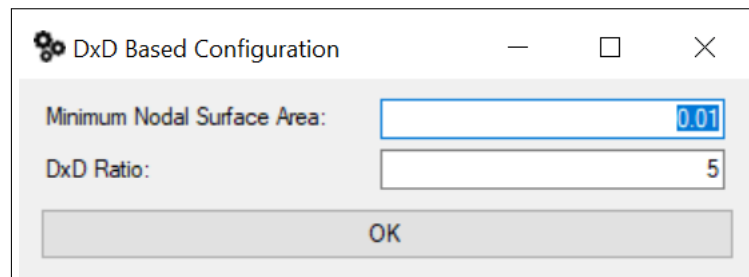
Figure A.10 – ReSWMM fixed interval.



Source: The Author.

If the user selects the Fixed Interval, a window as shown in Figure A.11 will appear. The user will be able to select a new value for the Minimum Nodal Surface Area (0.01 or less is recommended) and the ratio that will define the number of dummy nodes placed in each link.

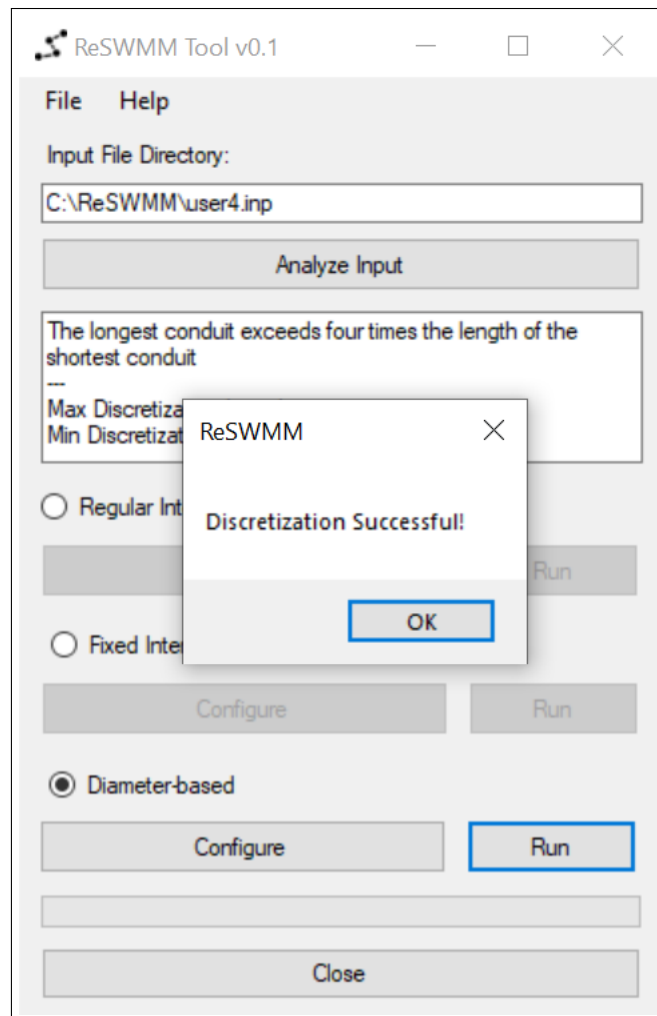
Figure A.11 – ReSWMM diameter-based.



Source: The Author.

If the discretization runs successfully a message as shown in Figure A.12 should appear. Clicking OK will update the SWMM project if used as Add-on or will save a new file if used as standalone application.

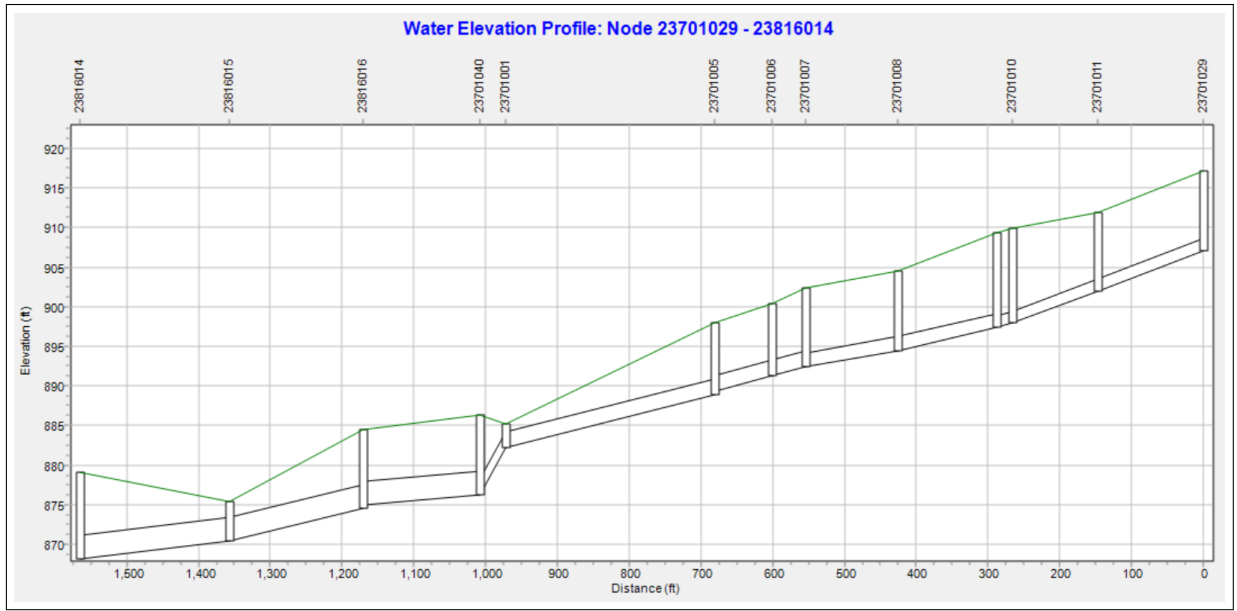
Figure A.12 – ReSWMM discretization successful.



Source: The Author.

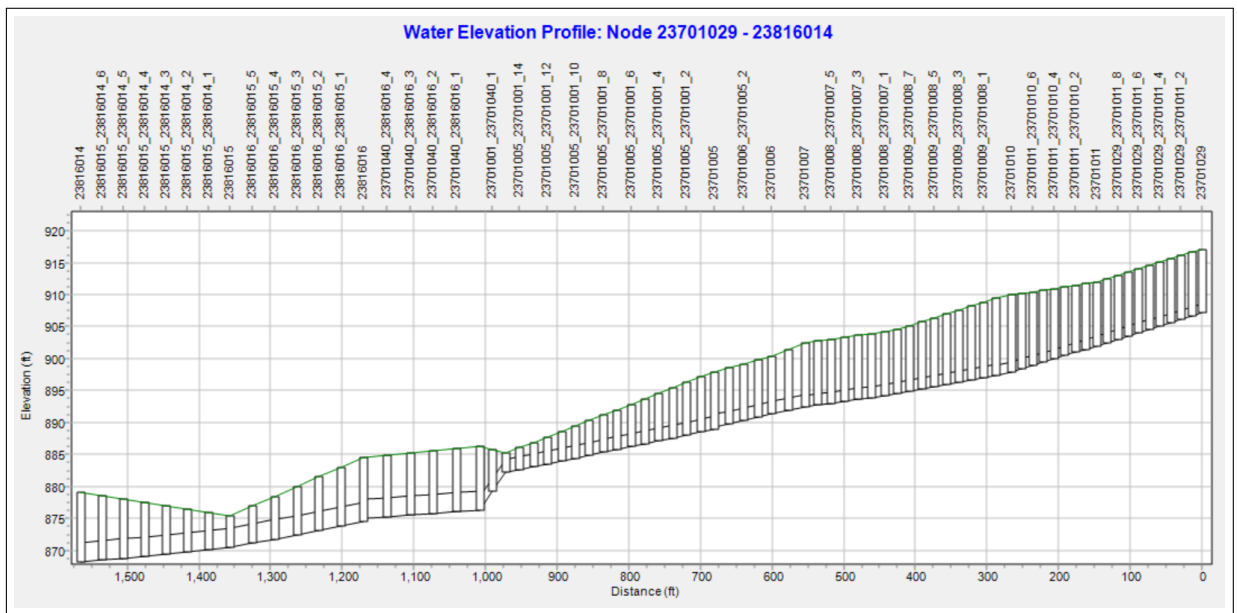
Figure A.13 shows a original link-node SWMM model and Figure A.14 shows the same model spatially discretized based on a DxD ratio of 10.

Figure A.13 – Link-node approach.



Source: The author

Figure A.14 – Diameter-based discretization.



Source: The Author.